

# UNIVERSITA' DEGLI STUDI DI VERONA

*DEPARTMENT OF*

*Neurosciences, Biomedicine and Movement Sciences*

*PhD SCHOOL OF*

*Life and Health Sciences*

*DOCTORAL PROGRAM IN*

*Biomolecular Medicine*

XXXVI Cycle / 2020-2023

---

***In Vitro* Prediction of Response to hCG Therapy in Patients with Cryptorchidism and Testicular Torsion in a Gubernaculum-based Model**

---

S.S.D. BIO/10

Coordinator: Prof. Lucia De Franceschi

Signature \_\_\_\_\_

Tutor: Prof. Ilaria Dando

Signature \_\_\_\_\_

Doctoral Student: Andrea Errico

Signature \_\_\_\_\_

## TABLE OF CONTENT

SOMMARIO.....	4
1. ABSTRACT.....	5
2. ABBREVIATIONS.....	6
3. INTRODUCTION.....	9
3.1 Male infertility.....	9
3.1.1 Definition and Prevalence.....	9
3.1.2 Etiology.....	9
3.1.3 Clinical approach.....	11
3.2 Andrological diseases that affect the fertility potential.....	14
3.2.1 Cryptorchidism: failure of testicular descent.....	14
3.2.2 Testicular torsion: urological emergency.....	19
3.3 Gubernaculum testis and testicular compartmentalization ensure male fertility .....	22
3.3.1 Gubernaculum testis: para/extra-testicular tissue.....	22
3.3.2 Testis: interstitial and tubular cells.....	24
3.3.3 Hypothalamic-pituitary-gonadal axis: endocrine regulation of testicular processes...26	
3.4 Human chorionic gonadotropin as hormonal therapy for male infertility.....	28
3.4.1 Luteneizing Hormone Receptor.....	28
3.4.2 LH and hCG: two ligands for a single receptor.....	29
3.4.3 Hormonal therapy with hCG.....	33
3.5 Testicular organoids.....	35
4. AIMS OF THE THESIS.....	39
5. MATERIALS AND METHODS.....	40
5.1 Patients.....	40
5.2 Inclusion criteria.....	40
5.3 Exclusion criteria.....	41
5.4 Gubernaculum surgical collection.....	42
5.5 Drugs and Chemicals.....	42
5.6 Tissue Processing and <i>In vitro</i> culture.....	42
5.7 RNA extraction and qPCR.....	43
5.8 Immunofluorescence analysis of LHCGR positive cells.....	44
5.9 Cell proliferation assay.....	44
5.10 Tubular structure formation assay.....	45

5.11	Oxygen Consumption Rate (OCR) and Extracellular Acidification Rate (ECAR) analysis..	45
5.12	Reactive Oxygen Species (ROS) levels analysis.....	46
5.13	Pyruvate kinase activity assay.....	46
5.14	L-lactic acid quantification in culture medium.....	46
5.15	Proteomic analysis.....	47
5.15.1	Protein extraction and tryptic digestion.....	47
5.15.2	Mass Spectrometry analysis.....	47
5.16	Statistical analysis.....	48
6.	RESULTS.....	49
6.1	Gubernacular tissue processing.....	49
	<i>Cryptorchidism</i>	
6.2	<i>In vitro</i> culture of gubernacular cells derived from cryptorchid patients.....	50
6.3	Gubernacular cells express receptors for gonadotropins and androgens.....	52
6.4	hCG stimulates cell proliferation and formation of tubular structures.....	54
6.5	Gubernacular cells express two different LHCGR variants.....	58
6.6	hCG decreases the oxygen consumption rate of gubernacular cells.....	59
6.7	hCG exhibits an anti-oxidative function.....	62
	<i>Testicular torsion</i>	
6.8	<i>In vitro</i> culture of gubernacular cells derived from patients with testicular torsion.....	64
6.9	Gubernacular cells express AR and LHCGR.....	65
6.10	Gubernacular cell proliferation is stimulated by hCG treatment.....	67
7.	DISCUSSION.....	68
8.	CONCLUSION.....	74
9.	BIBLIOGRAPHY.....	76

## SOMMARIO

Le malattie andrologiche che colpiscono i pazienti in età pediatrica rappresentano un importante fattore di rischio per l'alterazione del loro potenziale fertile in età adulta e, pertanto, la diagnosi ed il trattamento precoce, anche chirurgico e/o terapeutico, sono estremamente importanti. Il fattore di rischio meglio caratterizzato per l'infertilità in età adulta, così come per lo sviluppo del cancro testicolare, è rappresentato dal criptorchidismo, in cui si verifica l'assenza di uno o entrambi i testicoli nella sacca scrotale alla nascita. L'approccio più efficace per il trattamento del criptorchidismo è l'orchidopessi seguita dalla terapia con gonadotropina corionica umana (hCG); tuttavia, non tutti i pazienti mostrano un miglioramento significativo del volume e della vascolarizzazione dei testicoli dopo la terapia adiuvante. In questo studio, abbiamo generato un modello *in vitro* per prevedere la risposta del paziente all'hCG, attraverso la coltura e il trattamento di cellule primarie derivate da biopsie di gubernaculum testis - il legamento che collega il testicolo allo scroto - di quattro pazienti criptorchidi. Il gubernaculum condivide molte proprietà con le cellule testicolari, inclusa l'espressione del recettore dell'hCG (LHCGR), data la loro comune origine embrionale. In questo lavoro, mostriamo che l'hCG stimola le cellule gubernacolari a proliferare e a formare strutture simili a vasi con un'entità diversa tra le cellule derivate dai 4 pazienti, insieme ad una riduzione sia del consumo di ossigeno che di generazione delle specie reattive dell'ossigeno. Con queste osservazioni, mostriamo che la diversa risposta dei pazienti all'hCG può essere attribuibile alla loro età, poiché i pazienti più giovani rispondono meglio *in vitro* all'ormone. Oltre al criptorchidismo, anche la torsione testicolare rappresenta una condizione urgente che può influenzare negativamente il potenziale di fertilità. Questa patologia si manifesta in soggetti giovani generalmente prima dei 25 anni per i quali attualmente non è prevista alcuna terapia nella fase postoperatoria. In questo studio mostriamo anche che le cellule gubernacolari derivate da pazienti affetti da torsione testicolare possono essere coltivate e amplificate *in vitro* per testare l'efficacia della terapia con hCG, la cui applicazione è quindi adeguata anche in questa condizione patologica per recuperare la funzionalità testicolare. Infine, per comprendere meglio le proprietà del tessuto testicolare e le sue funzionalità, abbiamo generato e caratterizzato un sistema di coltura tridimensionale di organoidi testicolari umani, a partire da un pezzo di biopsia del tessuto testicolare. Nel complesso, i risultati di questa tesi aprono la strada alla futura applicazione del nostro modello di gubernaculum *in vitro* - preservando il prezioso tessuto testicolare - per prevedere la migliore terapia personalizzata per i pazienti criptorchidi e per supportare il recupero dei testicoli nei pazienti affetti da torsione testicolare.

## 1. ABSTRACT

Andrological diseases that affect patients in pediatric age represent important risk factors for alterations of their fertile potential in adulthood and, therefore, early diagnosis and treatment, even surgical and/or therapeutic treatments, are extremely important. The best-characterized risk factor for infertility in adulthood but also for testicular cancer development is represented by cryptorchidism, which is the absence of one or both testicles in the scrotal sac at birth. The most effective approach to treat cryptorchidism is orchidopexy followed by human chorionic gonadotropin (hCG) therapy; however, not all patients show a significant improvement of testis volume and vascularization after adjuvant therapy. In this study, we generated an *in vitro* model to predict the patient response to hCG by cultivating and treating primary cells derived from four cryptorchid patients' biopsies of gubernaculum testis, the ligament that connects the testicle to the scrotum. Gubernaculum shares many properties with testicular cells, including the expression of the hCG receptor (LHCGR), due to their common embryonic origin. Here, we show that hCG stimulates gubernacular cells to proliferate and to form vessel-like structures with a different extent among the four patients derived cells, together with a decrease of both oxygen consumption and reactive oxygen species generation. Hereby, we show that the diverse patient response to hCG may be ascribable to their age, as younger patients respond better *in vitro* to the hormone. In addition to cryptorchidism, testicular torsion also represents an urgent condition that may negatively influence the fertility potential. This pathology occurs in young men generally before the age of 25 for which a therapeutic approach is not currently considered in the postoperative phase. In this study, we also show that gubernacular cells derived from patients affected by testicular torsion can be cultured and amplified *in vitro* to test the efficacy of hCG therapy, which can also be used in this pathological condition to recover function of the testes. Finally, to better understand the properties of testicular tissue and its functionalities, we generated and characterized a three-dimensional human testicular organoid culture system, starting from a piece of testicular tissue biopsy. Altogether, the findings of this thesis pave the way to the future application of our *in vitro* gubernaculum model – preserving precious testicular tissue - to predict the best personalized therapy for cryptorchid patients and to support the testis recover in patients affected by testicular torsion.

## 2. ABBREVIATIONS

### 3

3-LGS: three-layer gradient system;  
3 $\beta$ -HSD: 3 $\beta$ -hydroxysteroid dehydrogenase;

### A

ABP: androgen binding protein;  
ACO1: cytoplasmic aconitate hydratase;  
ADP: adenosine diphosphate;  
AGC: automated gain control;  
AMH: Anti-Mullerian hormone;  
AP-1: Activator protein 1;  
AR: Androgen receptor;  
ARC: Arcuate nucleus;  
ART: assisted reproductive technology;

### B

*BCAT1*: branched-chain-amino acid aminotransferase;  
BSA: bovine serum albumin;  
BTB: blood testis barrier;

### C

C/EBPs: CCAAT/enhancer-binding proteins;  
cAMP: cyclic adenosine monophosphate;  
CAVD: congenital absence of vas deferens;  
CBAVD: congenital bilateral absence of vas deferens;  
CE-MRI: contrast-enhanced magnetic resonance imaging;  
CEUS: contrast-enhanced ultrasound;  
CGRP: calcitonin gene-related peptide;  
CREB: cAMP response element-binding protein;  
CREM: CRE modulator;  
CSL: cranial suspensory ligament;  
CUAVD: congenital unilateral absence of vas deferens;  
CYP11A1: P450 cholesterol side-chain cleavage enzyme;  
CYP17A1: 17-hydroxylase/C17-20-lyase;

### D

DCF-DA: diacetylated 2,7-dichlorofluorescein;  
DTT: dithiothreitol;

### E

ECAR: extracellular acidification rate;  
ECM: extracellular matrix;  
ESCs: embryonic stem cells;  
EXD2: exonuclease 3'-5' domain-containing protein 2;

## **F**

FBS: fetal bovine serum;  
FCCP: carbonyl cyanide 4-(trifluoromethoxy) phenylhydrazone;  
FDR: false discovery rate;  
FGF: fibroblast growth factor;  
FSH: follicle-stimulating hormone;  
FSHR: follicle-stimulating hormone receptor;

## **G**

GCLM: glutamate-cysteine ligase regulatory;  
GFN: genitofemoral nerve;  
GnRH: gonadotropin release hormone;  
GPCRs: guanine nucleotide-binding protein-coupled receptors;

## **H**

hCG: human Chorionic Gonadotropin;  
HH: hypogonadotropic hypogonadism;  
*HMGB2*: high-mobility group protein B2 protein;  
HPG: hypothalamic-pituitary-gonadal axis;  
hPSCs: human pluripotent stem cells;

## **I**

ICSI: intracytoplasmic sperm injection;  
INSL3: insulin-like 3;  
IRP1: the iron-regulatory protein;

## **K**

Kal- 1: Kallmann syndrome 1;  
Kal -2: Kallmann syndrome 2;

## **L**

LDH: lactate dehydrogenase;  
*LDHB*: lactate dehydrogenase B;  
LGR8: leucine-rich repeat-containing G-protein-coupled receptor 8;  
LH: luteneizing hormone;  
LHCGR: luteneizing hormone/chorionic gonadotropin receptor;  
LRRD: leucine-rich repeat domain;

## **M**

MBL: mean of branch length;  
MMS: mean meshes size;

## **N**

NADH: nicotinamide adenine dinucleotide;  
NIRS: near-infrared spectroscopy;  
NOA: non-obstructive azoospermia;  
NUDT2: bis(5'-nucleosyl)-tetraphosphatase;

## **O**

OA: obstructive azoospermia;  
OCR: oxygen consumption rate;

## **P**

P450scc: P450 cholesterol side-chain cleavage enzyme;  
PCT: perfusion computed tomography;  
PEP: phosphoenolpyruvate;  
PK: pyruvate kinase;  
PKA: protein kinase A;  
PRDX1: peroxiredoxin 1;  
PRDX3: peroxiredoxin 3;  
PROK2: prokineticin 2;  
PROK2R: prokineticin 2 receptor;

## **R**

ROS: reactive oxygen species;  
RP3V: rostral periventricular region of the third ventricle;  
RXFP2: relaxin family peptide receptor 2;

## **S**

SCLCs: sertoli cell-like cells;  
SDHA: succinate dehydrogenase A;  
SEM: standard error of the mean;  
SER: smooth endoplasmic reticulum;  
SF-1: steroidogenic factor 1;  
SL: scrotal ligament;  
SOD2: superoxide dismutase 2;  
SRXN1: sulfiredoxin-1;  
StAR: steroidogenic acute regulatory;  
STEAP3: metalloredutase six--transmembrane epithelial antigen of prostate 3;

## **T**

TCS: testicular cell suspension;  
TDS: testis-derived scaffold;  
TESA: testicular sperm aspiration;  
TESE: testicular sperm extraction  
TesLCs: testicular somatic cell-like cells;  
TO: testicular organoid;  
TRT: testosterone replacement therapy;  
TRUS: transrectal ultrasound;  
TXN: thioredoxin;  
TXNDC17: thioredoxin domain-containing protein 17;

## **U**

US: ultrasonography;

## **W**

WHO: World Health Organization.



### **3. INTRODUCTION**

#### **3.1 Male infertility**

##### **3.1.1 Definition and prevalence**

Clinical infertility is defined as the inability of a couple to conceive after 12 months of regular (at least twice weekly) unprotected intercourse<sup>1</sup>. World Health Organization (WHO) estimates that approximately 190 million people are struggling with infertility and the number of couples seeking assistance is progressively rising with more than 2.5 million Assisted Reproductive Technology (ART) procedures performed in 2019 worldwide. As male and female causes often co-exist, it is important that both partners are investigated for infertility and managed together. Male infertility is due to abnormal sperm parameters and contributes to 50% of all cases of infertility<sup>2</sup>. Although in recent years we have seen remarkable progresses in reproductive health, there is no clear knowledge regarding male infertility yet and the limited available data suggest that the prevalence of male infertility varies based on several sociodemographic factors, such as country and/or region, age, ethnicity, frequency of coitus, and fertility intentions. It has been reported that more than 30% of male infertility is due to testicular diseases, whereas in other 15-30% the cause is linked to endocrine defects, such as low levels of sex steroids and abnormal gonadotropin levels, indicating that there are several conditions and risk factors for this condition<sup>3</sup>. In about 60% of the cases, risk factors that could alter the fertility potential in males can be diagnosed and treated in pediatric/adolescent age<sup>4</sup>, opening the way to the importance of prevention and preservation of fertile potential in young patients.

##### **3.1.2 Etiology**

There are multiple reasons for male infertility to occur, including both reversible and irreversible conditions impairing sperm production and function, which can be related to different congenital or acquired factors acting at pre-testicular, post-testicular, or directly at the testicular level<sup>5</sup>.

Pre-testicular causes, which account for 10% of forms, are mainly represented by two types of pathological conditions: hypogonadotropic hypogonadism (HH) and coital disorders, such as retrograde ejaculation, anejaculation, genetic factors, chromosomal abnormalities.

HH is a condition in which male testes produce little or no sex hormones due to problems of the pituitary gland or hypothalamus<sup>5</sup>. Numerous pathologies may lead to primary testicular failure, such as cryptorchidism, orchitis, testis trauma, torsion and so on.

On the other side, post-testicular causes represent 15% of cases and include all obstructive/sub obstructive lesions of the seminal tract (distal or proximal), infections, and inflammatory diseases of accessory glands and autoimmune infertility<sup>5</sup>.

To date, due to general underreporting, cultural factors and regional variations, accurate statistics regarding male infertility are not available. Nevertheless, a partial summary of specific etiologies is listed below:

#### Congenital factors (about 30%)

- Anorchia: absence of both testes at birth. The prevalence of bilateral congenital anorchia is 1 in 20,000, and unilateral congenital anorchia is 1 in 5,000 males;
- Congenital urogenital abnormalities:
  - absent, dysfunctional, or obstructed epididymis,
  - Congenital Absence of Vas Deferens (CAVD): condition in which the *vasa deferentia* reproductive organs fail to form properly prior to birth. It may either be unilateral (CUAVD) or bilateral (CBAVD). Congenital bilateral absence of the vas deferens (CBAVD) is found in 1% to 2% of males with infertility and is present in 6% of obstructive azoospermia cases;
  - undescended testes or cryptorchidism, a condition in which one or both of the testes fail to descend from the abdomen into the scrotum, 3 % to 5 % of full-term boys at birth;
  - ejaculatory duct disorders (cysts).
- Genetic abnormalities: karyotype anomalies, including Klinefelter syndrome, Y chromosome microdeletions, congenital GnRH Deficiency (Kallmann syndrome), Sertoli cell-only syndrome, Kal- 1, Kal -2, FSH, LH, FGFs, GnRH1/GNRHR, PROK2/PROK2R gene deficiencies, Prader Willi syndrome, Laurence - Moon - Biedl syndrome, iron overload syndrome, familial cerebellar ataxia, mutations in genes involved in Hypothalamus–pituitary–gonadal axis, and Partial/Mild Androgen Insensitivity syndrome.

#### Acquired factors (about 20%)

- Testis trauma (1%);
- Surgeries that can damage vascularization of the testes (1%);
- Erectile and ejaculatory dysfunction (1%);
- Acquired hypogonadotropic hypogonadism or endocrine factors;

- Malignancies: sellar masses, pituitary macroadenomas, craniopharyngiomas, and surgical or radiation treatment to these conditions, testicular tumors, or adrenal tumors leading to an excess of androgens;
- Immunological causes: lymphocytic hypophysitis, hemosiderosis, hemochromatosis, sarcoidosis, histiocytosis, tuberculosis, fungal infections, etc;
- Testicular torsion (5%);
- Post-inflammatory forms (orchitis, epididymitis) (5%);
- Obstruction and sub obstruction of proximal and/or distal urogenital tract (5%);
- Recurrent urogenital infections, prostatitis, prostatovesiculitis (8%);
- Exogenous factors (10-15%): medications or drugs, such as cannabinoids, opioids, psychotropic drugs can cause inhibition of GnRH, exogenous testosterone or androgenic steroids supplementation and environmental toxins, among them insecticides, fungicides, pesticides;
- Systemic diseases, including liver cirrhosis, renal failure, etc. (20-25%);
- Varicocele, depending on the grade, is an enlargement of the veins within the loose bag of skin that holds the testicles (scrotum) (25-30%);
- Smoking, obesity, excess alcohol, aging, life style.

#### Idiopathic forms (about 50%)

- Unknown etiology: semen parameters are all normal, but the male remains infertile<sup>5</sup>.

### **3.1.3 Clinical approach**

The key purpose for evaluating male infertility is to identify factors contributing to it, offer treatment for those that are reversible, determine if he is a candidate for assisted reproductive techniques (ART) and offer counseling for irreversible and untreatable conditions<sup>6</sup>. Furthermore, male infertility is increasingly observed as a herald for future male health conditions<sup>3</sup>, with an association with cardiovascular disease, testicular cancer and increased all-cause mortality.

The diagnostic workup of the infertile male should include careful medical and reproductive history, physical examination, and semen analysis followed by second level exams, among which the most relevant are: hormonal measurement, genetic screening, DNA integrity tests, microbiological examination of semen and urine, urethral swab, scrotal and testicular ultrasound, scrotal color-doppler and transrectal ultrasound<sup>7</sup>.

## Semen analysis

Semen analysis is of fundamental importance to diagnose and define the severity of the male factor. Semen analysis should be performed according to the WHO manual in a standardized way. This analysis provides sperm density, total number, motility, morphology and semen parameters, such as semen volume, pH, viscosity, and liquefaction time<sup>8</sup>.

The nomenclature related to the pathological semen quality according to the WHO Laboratory Manual for the Examination and Processing of Human Semen (2010), is reported in table below<sup>9</sup>:

**Table 1**

<b>Normospermia</b>	all semen parameters within the acceptable Reference Limits
<b>Oligozoospermia</b>	sperm concentration $<15 \times 10^6/\text{ml}$ ; total sperm number $<39 \times 10^6/\text{ml}$
<b>Asthenozoospermia</b>	$<32\%$ progressively motile spermatozoa. Absolute asthenozoospermia is when no sperm moves at all, but they are not dead
<b>Teratozoospermia</b>	$<4\%$ morphologically normal spermatozoa
<b>Oligo-astheno-teratozoospermia</b>	disturbance of all three parameters
<b>Necrospermia or Necrozoospermia</b>	complete when all the sperm are dead on a fresh semen sample; incomplete if 5-45% are still viable.
<b>Leukospermia</b>	$>1 \times 10^6/\text{ml}$ leucocytes in the ejaculate (also called pyospermia and leukocytospermia).
<b>Cryptozoospermia</b>	spermatozoa absent from fresh preparation but observed in a centrifuged pellet.
<b>Azoospermia</b>	no spermatozoa in the ejaculate
<b>Aspermia</b>	no ejaculate at all

## Hormonal determinations

In men with testicular deficiency, hypergonadotropic hypogonadism is usually present, with high levels of follicle-stimulating hormone (FSH) and luteinizing hormone (LH), and with or without low levels of testosterone<sup>10</sup>. Generally, the levels of FSH correlate with the number of spermatogonia: when spermatogonia are absent or markedly diminished, FSH values are usually elevated; when the number of spermatogonia is normal, but maturation arrest exists at the spermatocyte or spermatid level, FSH values are within the normal range<sup>11</sup>. However, for an individual patient, FSH levels do not accurately predict the spermatogenesis status because men with maturation arrest histology could have normal FSH and testis volume and still be azoospermic<sup>12,13</sup>.

### Ultrasonography

In addition to physical examination, a scrotal ultrasonography (US) would be required to definitively identify pathologies such as spermatoceles, varicoceles, absence of the vas on physical examination, or the presence of testicular dysgenesis (e.g., non-homogeneous testicular architecture and microcalcifications) and testis tumor<sup>14</sup>. Scrotal ultrasound has been reported to identify abnormalities in 38% of infertile men. Of these, 30% had varicocele and 0.5% testicular cancer. In patients with low seminal volume and suspected distal obstruction, transrectal ultrasound (TRUS) is essential<sup>15</sup>.

### Testicular biopsy

Testicular biopsy is a focal part of the intracytoplasmic sperm injection (ICSI) treatment in patients with clinical evidence of non-obstructive azoospermia (NOA), for whom ICSI represents the only therapeutic option. In about 50% of these patients spermatozoa are found by a testicular sperm extraction (TESE) procedure and used for ICSI with fresh or cryopreserved spermatozoa. There is a good correlation between the histology found upon diagnostic biopsy and the likelihood of finding mature sperm cells during testicular sperm retrieval and ICSI<sup>16</sup>. However, no threshold value has been found for FSH, inhibin B, or testicular volume and successful sperm harvesting. Microsurgical TESE, preferred in severe cases of NOA, yields the highest sperm retrieval rates, and multibiopsy or multiple TESE - involving several tunical incisions (up to 15) with tissue extraction until sufficient sperm is obtained - is superior to conventional TESE<sup>17</sup>. ICSI shows worse results in NOA than in obstructive azoospermia (OA) according to retrieved sperm, but also birth rates are lower in NOA than in OA (19% vs. 28%). In longitudinal studies including patients with NOA as defined by testicular histopathology, only one out of seven NOA patients embarking for TESE and eventually ICSI will father their genetically own child<sup>18</sup>.

### Vasography

Vasography is used to evaluate the patency of the vas and identify the precise location of any vasal obstruction. It is most useful in azoospermic or severely oligozoospermic men with mature sperm on testicular biopsy and at least one identifiable vas. It can be done simultaneously with a testicular biopsy, as a separate open procedure, or percutaneously. Normal saline (with or without blue dye) or radiological contrast is injected into either end of the lumen of the vas. If the blue dye is seen in the

urine, no distal vasal obstruction is present. Radiologic contrast and X-rays can help identify the location of any proximal obstruction<sup>6</sup>.

### **3.2 Andrological diseases that affect the fertility potential**

Worldwide the incidence of andrological diseases is rising every year and, together with it, also the interest in them is increasing due to their strict association with disorders of the reproductive system, including impairment of male fertility, alterations of male hormones production, and/or sexual function<sup>19</sup>.

Many of the andrological diseases that occur in adulthood have their origins before the age of 18 years, within the first months of life and sometimes even in the period of gestation. In fact, the male gonad is extremely susceptible to external insults, a sensitivity persistent from the gestational period until puberty<sup>20</sup>. Due to the delays between diagnosis, treatment and reproductive age, it is challenging to predict the potential impact of congenital and acquired diseases - occurring in childhood - implicated in male infertility<sup>21</sup>. It is therefore essential to carry out andrological monitoring of the onset timing of pubertal and testicular development during childhood to observe abnormalities in the genital organs that occur very early, including alterations affecting the penis or abnormal positions of the testicle, and to identify risk factors for the subject's andrological and sexual health.

Prevention and early diagnosis of andrological dysfunctions have long been neglected, with the consequent increase in their incidence and prevalence: andrological diseases diagnosed in childhood are responsible for over 60% of adult male infertility. Such diseases would be easy to cure if diagnosed early and treated promptly, reducing the risks of infertility in adults. Among the andrological pathologies occurring in the pediatric age associated with a high impact on fertility are cryptorchidism and testicular torsion<sup>22</sup>.

#### **3.2.1 Cryptorchidism: failure of testicular descent**

##### Testicular descent

Testicular descent is a mandatory developmental process to ensure that the mature testis promotes normal spermatogenesis. It requires the interaction of both anatomical and hormonal factors and can be divided into two controlled phases: the transabdominal migration or translocation (between 8-15 weeks of gestation) and the inguinoscrotal phase (25-35 weeks of gestation)<sup>23</sup>. A schematic representation of testicular descent is showed in figure 1. The two major hormone/receptor systems that are involved in testicular descent are: i) INSL3/RXFP2 (former LGR8), Anti-müllerian

hormone (AMH) as well as testosterone that regulate the first phase and ii) testosterone with its receptor (androgen receptor-AR), genitofemoral nerve (GFN) and its neurotransmitter calcitonin gene-related peptide (CGRP) that influence the second phase<sup>24</sup>.

The process starts between 6 and 9 weeks as the metanephros enlarges and ascends from sacral to lumbar region below the suprarenal gland. The lateral displacement of gonad is believed to be caused by this movement<sup>25</sup>. In the early development, the anti-Müllerian hormone (AMH) produced by Sertoli cells causes regression of müllerian duct, meanwhile the testosterone produced by Leydig cells results in the masculinization of the external genitalia and persistence of Wolffian duct<sup>26</sup>. The two anatomical ligaments that are highlighted in this phase are the cranial suspensory ligament (CSL) and the caudal genitoinguinal ligament (or gubernaculum testis). The upper pole of testis is attached to the diaphragm by the cranial suspensory ligament, which degenerates in the male fetus under the influence of testosterone, resulting in the release of its cranial end<sup>25</sup>. In this phase, the thickening of gubernaculum, controlled by Leydig cell-produced hormone INSL3<sup>27</sup>, is a noticeable anatomical change that helps in positioning of the testes near the inguinal canal<sup>28</sup>. After the first phase of descent there is a pause before the commencement of the inguinoscrotal phase. The gubernaculum thickening and the increased abdominal pressure by the growth of the viscera results in the subsequent dilatation of the inguinal canal. This ensures the smooth passage of the testes and epididymis to the scrotum through the canal engulfed by the processus vaginalis which provides a peritoneal diverticulum to leave the abdomen. Once the descent is complete the processus vaginalis closes and later involutes. As the testes passes to the scrotum the collagen content of gubernaculum increases entailing its gradual involution<sup>29</sup>. To date it is extensively believed that the second phase of testicular descent is controlled indirectly and not directly by androgens. They act as paracrine factors and control the inguinoscrotal phase through the sensory branch of the genitofemoral nerve, the CGRP<sup>30</sup>, and induce the gubernaculum regression by increasing the collagen content and decreasing its extracellular matrix. The coherent explanation for why testes reach an extracorporeal location could be the hypothermic environment provide by the scrotum necessary for the physiological functioning of the male gonads – indeed the scrotal temperature, suitable for normal testicular spermatogenesis, is believed to be 2–3 °C lower than the core body temperature<sup>31</sup>.

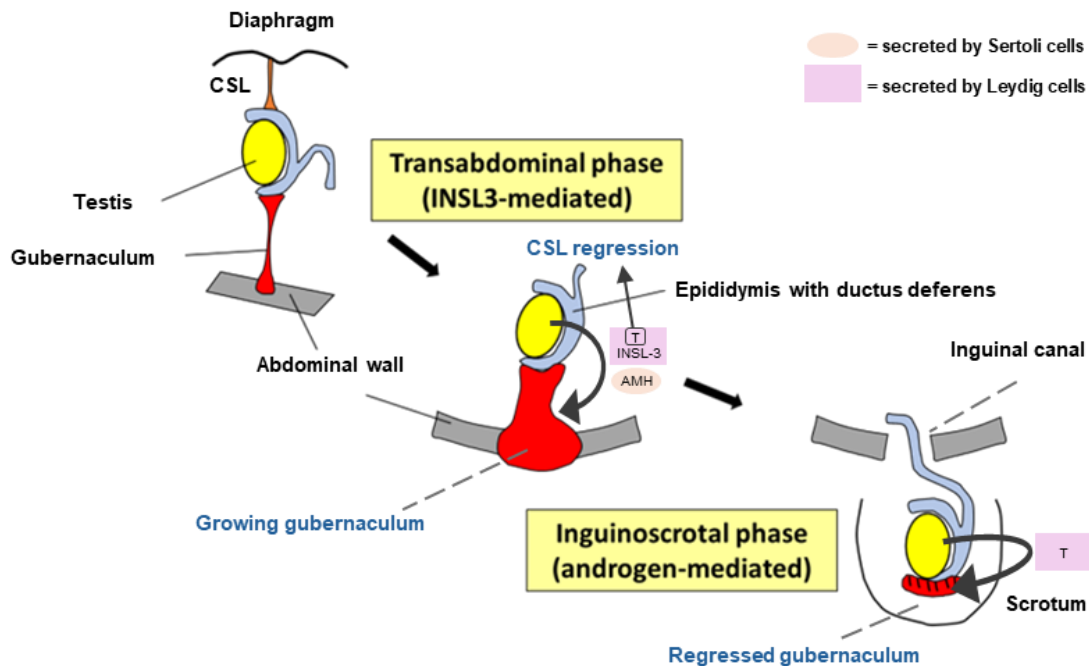


**Figure 1. Testicular descent**

Top, starting phase: the primitive testis is located near the kidney, held from one side – upper - by the cranial suspensory ligament (CSL) and from the opposite - bottom - side by gubernaculum testis.

Center, transabdominal phase: androgen-mediated dissolution of the CSL and insulin-like factor 3 (INSL3)-mediated gubernaculum swelling – both events are promoted by Leydig cells – allow the testis to enter the inguinal canal.

Bottom, inguino-scrotal migration: the testis passes through the inguinal canal into the scrotum, this phase is androgen-dependent.

### Undescended testis

The condition in which one or both the testes fail to properly descend from the abdomen into the scrotal sac is known as cryptorchidism. The name of this condition (from Greek *crypto-* ‘hidden’ + *orkhis*, *orkhid-* ‘testicle’) is derived from the improper position of the testes at the end of the gestational period. This pathology is one of the most common primary testicular dysfunction, being the most frequent congenital birth defect in male children occurring as an isolated disorder or in association with other congenital anomalies (syndromic cryptorchidism): approximately 4% of all males are born with at least one cryptorchid testis<sup>32</sup>. While about half of these cases spontaneously descend during the first three months of life, approximately 1% of all males remains cryptorchid at the end of their first year. Cryptorchidism occurs bilaterally in one third of cases and unilaterally in two thirds of cases, with a frequency of about 5% in full-term newborns and 30% in premature newborns<sup>33</sup>.



Undescended testis (UDT) can be classified as (a) unilateral or bilateral, (b) congenital and acquired, (c) palpable and non-palpable. The classification of the UDT on the basis of testicular location, may be anywhere along the normal course of descent (**Figure 2**) i.e. abdominal, inguinal canal, superficial inguinal ring, supra-scrotal, high scrotal or ectopic, when testes takes unusual way than the normal pathway of descent<sup>33</sup>.

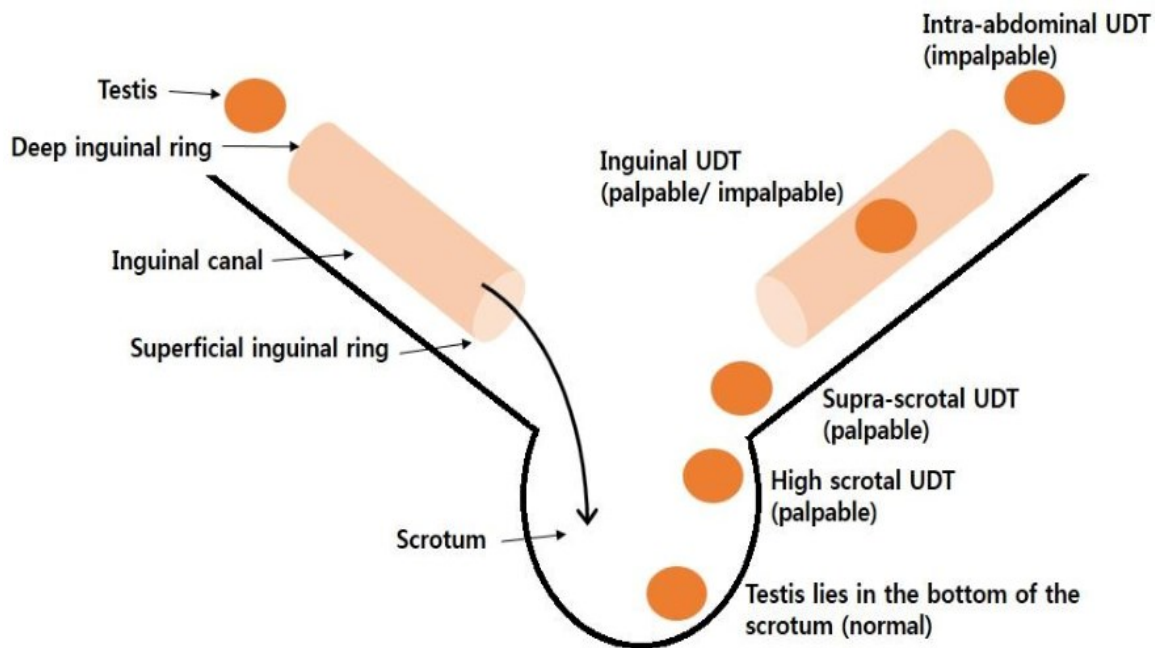


**Figure 2. Testicular position**

Testicular position is classified as intra-abdominal, inguinal, supra-scrotal, high scrotal, and scrotal according to the process of testicular descent. Intra-abdominal testes are not palpable. Inguinal testes are sometimes palpable. Supra-scrotal and high scrotal testis is palpable.

Scrotal testis is considered normal as it lies in the bottom of scrotum. UDT, undescended testis.

Figure provided by Shin, J. & Jeon, G. W. *Clin. Exp. Pediatr.* 63, 415–421 (2020)

### Etiology of Cryptorchidism

Although the exact cause of cryptorchidism is not known, different studies show that it could be due to the disruption of anatomical or hormonal factor or the combination of both<sup>34</sup>.

Regarding the two phases of testis descent, the most affected is the inguinoscrotal one, since many hormonal factors act during this phase, contributing to significant anatomical remodeling<sup>25</sup>. In addition to hormones, some environmental factors, including pesticides, phthalates, and bisphenol, can also aid to this pathological condition by interfering with normal androgen synthesis<sup>35</sup>. The abnormal action of the hypothalamic–pituitary–testicular axis, disruption of normal testicular differentiation, low production of placental gonadotropin, disruption of synthesis and action of

androgens, INSL3 factor and AMH or their receptors are few factors causing cryptorchidism<sup>25</sup>. Moreover, conditions like low birth weight, maternal exposure to estrogens during the first trimester, inherited X-chromosome-linked anomalies, aberrations of ipsilateral *GFN* regulation, increased GGN repeat length of the androgen receptor gene causing decreased androgen receptor function are all associated with high incidence of undescended testes<sup>36</sup>.

Studies have also reported maldevelopment to some extent in seminiferous tubules, including Sertoli cell only tubules and spermatogenic arrest associated with undescended testis<sup>37</sup>. Cryptorchidism is also observed in other complications during the developmental phase, such as inguinal hernia, hydrocele and ascending/retractile testes due to the incomplete disappearance of the processus vaginalis and even in microcephaly because of disruption in the hypothalamic–pituitary–testicular axis<sup>24</sup>. Therefore, although cryptorchidism is often considered a mild malformation, it represents the best-characterized risk factor for testicular cancer development and infertility in adulthood. Indeed, men with a history of cryptorchidism are frequently sub-fertile due to spermatogenic impairment, which is most frequently observed in bilateral forms<sup>38</sup>.

#### Therapeutic approach

Cryptorchidism occurs in up to 4–5% of males at birth and, if left untreated, it may lead to torsion, impaired fertility caused by the disrupted spermatogenesis, and a higher incidence of testicular cancer in later life<sup>36</sup>. In men with a history of cryptorchidism semen parameters are often altered: unlike cases of unilateral cryptorchidism in which paternity is almost equal (89.7%) to that in men without cryptorchidism (93.7%)<sup>39</sup>, in bilateral ones oligozoospermia can be found in 31% and azoospermia in 42% with a paternity rate of about 44%<sup>40</sup>.

Although multiple studies described the possible causes of undescended testes, it is not yet clear how the testicular descent process is regulated and what is the correct choice of first line of treatment and the most advantageous time for implementing the same<sup>25</sup>.

Nowadays, the surgical approach, called orchidopexy, is the treatment of choice in 95% of the cases, with a percentage of success of about 100%, representing the gold standard for cryptorchidism by minimizing germ cell loss and damage. Therefore, orchidopexy is recommended between 6 and 18 months of age to conserve spermatogenesis<sup>33</sup>, support hormone production, and decrease the risk of testicular tumors or other future complications<sup>41</sup>. In adolescence removal of intra-abdominal testis (with a normal contralateral testis) can be recommended, because of high risk of later malignancy<sup>42</sup>. Conversely, in adulthood, a palpable undescended testis should not be removed because it could still produce testosterone. Furthermore, as indicated above, correction of

bilateral cryptorchidism, even in adulthood, can lead to sperm production in previously azoospermic men<sup>43</sup>.

Vascular damage is the most severe complication of orchidopexy and can cause testicular atrophy in 1-2% of cases. In a study, post-operative atrophy in staged orchidopexy was reported in up to 40% of patients. Delayed orchidopexy for undescended testes has been associated with abnormal testicular histology, but the effect on subsequent fertility is unknown. Our group reported that testicular volume and hormonal function at 18 years old in patients diagnosed and treated for cryptorchidism during childhood are strongly conditioned by the age at which they underwent surgery<sup>44</sup> and whether the undescended testis was unilateral or bilateral<sup>45</sup>. In addition to surgery, it has been shown that post-operative hormonal treatment with hCG improves vascularization, testicular volume, and morphology, supporting the adjuvant use of hCG therapy for cryptorchid patients to sustain their fertility potential<sup>46</sup>. More details about hormonal treatment with hCG will be described below in the paragraph 3.4.3.

### **3.2.2 Testicular torsion: urological emergency**

Scrotal complaints are relatively common in the emergency department, comprising at least 0.5% of all emergency department visits. Testicular and spermatic cord torsion are a time-dependent diagnosis representing a true urologic emergency, occurring worldwide in about 1 out of 4,000 males younger than 25 years annually<sup>47</sup>. **Figure 3** shows a representative image of testicular torsion,<sup>48</sup> the most relevant cause of testis loss. In a report, cases of children with symptoms of acute scrotum - found in about 10% to 15% of patients with testicular torsion - it has been shown that torsion of the appendix testis was the most common pathology (45-57%), followed by torsion of the spermatic cord (26-27%), and epididymitis as a much less common condition (only 10-11%)<sup>49,50</sup> and among all these cases, orchiectomy rate is of 42%<sup>51</sup>. The mechanism of injury in testicular torsion is an ischemic event consisting of two phases: the first phase is characterized by the increase in venous pressure and congestion, followed by a second phase in which there is a decrease in arterial blood flow with ischemia. The consequent damage may then lead to loss of testicular function if blood flow is not restored in a timely manner<sup>49</sup>. Testis vascularization originates from the spermatic cord as well as from the cremasteric artery and gubernaculum. In fact, during testicular torsion, the third path of blood supply to the testis, i.e., the gubernaculum, is generally twisted and ischemic.

Torsion is classified as either intravaginal (the rotates within the tunica vaginalis) or extravaginal (the spermatic cord rotates with the tunica vaginalis)<sup>52</sup>. Testicular torsions diagnosed in the antenatally/early postnatal period are extravaginal and, despite intervention, generally result in loss of tissue viability<sup>51</sup>.

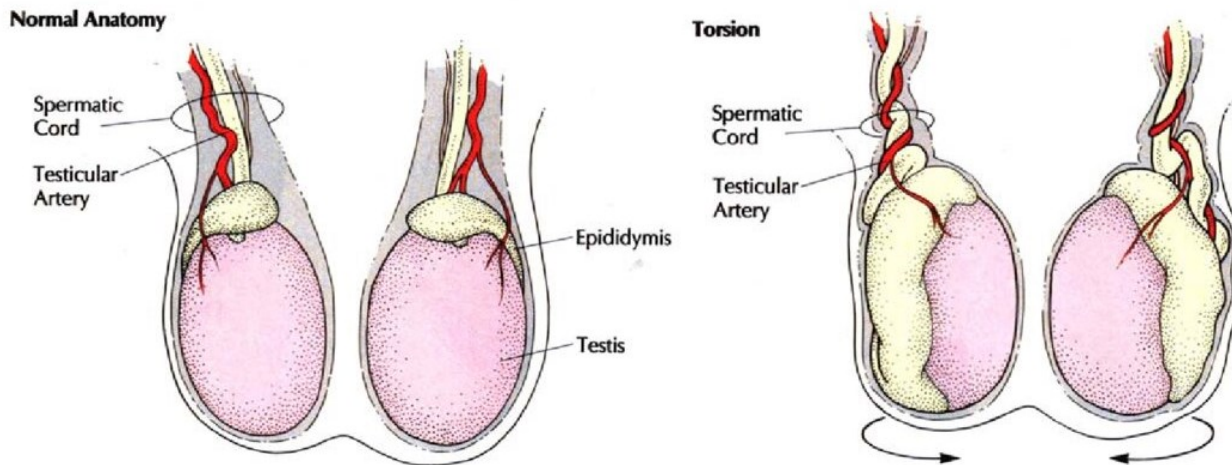


**Figure 3. Testicular torsion**

Torsion results when the testis rotates on its long axis within the tunica vaginalis, with consequent compromise of testicular blood supply.

Figure provided by Paola, A. S. & Khan, S. A. *Hosp. Pract.* **24**, 255–264 (1989)

### Sign and symptoms

Although many studies seem to indicate that testicular torsion is not associated with decreased fertility potential, conflicting conclusions make this an important area to try to understand, as well as to advise patients adequately at time of diagnosis<sup>21</sup>. The two most important factors determining testicular damage are the length of time from onset of symptoms to spermatic cord detorsion, and the degree of cord twist<sup>49</sup>. The characteristic signs and symptoms of testicular torsion include sudden, intense pain in the scrotum, swelling of the scrotum, blood in the semen, nausea and vomiting, pain in the abdomen, fever, lump in the scrotal sac, higher and unusual positioning of the testicle and frequent urination<sup>53</sup>. At onset, the only symptoms may be painful enlarged testicle and epididymis -found in 88% of patients; redness and edema of skin appear later, and sonographic appearance may be normal within the first hours. The testicle is placed more cranially due to the shortening of the spermatic cord. After several hours, the scrotal skin becomes red, the massive local swelling makes clinical examination difficult, sometimes nearly impossible<sup>49</sup>.

### Therapeutic approach

In most individuals, the testicle rotates between 90-180 degrees and compromised blood flow. Complete torsion is rare and quickly decreases the viability of the testes. It is commonly accepted that salvage of the human testis declines clearly with a symptom duration greater than 6 h. However, in the case of a high degree of twisting, necrosis can occur as early as within 4 hours<sup>54</sup>. Salvage rate of testes after detorsion is reported as 62-85% for descended testes and 29-40% for undescended testes<sup>55</sup>. Most authors report the testis as 'salvaged' if a palpable mass with Doppler signs of perfusion is preserved<sup>49</sup>.

The risk of testicular loss or unnecessary surgery calls for the necessity of novel diagnostic techniques; for instance, a recent study focused on the role of mean platelet volume in the diagnosis of testicular torsion<sup>47</sup>. The limited sensitivity of traditional ultrasound and its marked dependence on the radiologist's experience, especially in the case of small prepubertal testicles - 40% of neonatal testicles may have no apparent color flow doppler - has resulted in efforts to develop a new modality for highly sensitive quantitative evaluation that is less dependent on the expertise of the investigator<sup>49</sup>. New methods include contrast-enhanced ultrasound (CEUS), perfusion computed tomography (PCT), dynamic contrast-enhanced magnetic resonance imaging (CE-MRI), and near-infrared spectroscopy (NIRS)<sup>56</sup>.

By now, the only safe approach to resolve testicular torsion is surgery, which should be performed as soon as possible, and testicular viability is dependent to both the number of spermatic cord turns and the post-derotation recovery<sup>57</sup>. Real therapeutic doubt arises from the ability to predict which testes left in place after derotation will be viable and functional in the long term.

If the clinical concern is high, it is necessary to immediately seek a urological surgery consultation, which if early at presentation can be critical even in the absence of confirmatory testing<sup>58</sup>.

Manual detorsion should be attempted if urological intervention is not immediately available. The abnormal testicle should be rotated in a medial to lateral direction (open book) 180 degrees and then evaluated for pain relief. If the pain is increased, consider rotating the testicle in the opposite direction<sup>58</sup>. Manual detorsion of the spermatic cord is not a substitute for subsequent surgical exploration and bilateral orchidopexy. There is not enough evidence to use adjuvant measures in order to influence ischemic reperfusion injury after detorsion in humans<sup>59</sup>. Viable testis should be fixed with two or three nonabsorbable sutures to scrotal septum; however, partial resection or eversion of the tunica vaginalis is a more reliable method to prevent recurrent torsion<sup>60</sup>.

In neonates, bilateral scrotal exploration is done. Contralateral orchiopexy is always done to prevent future torsion. To date, adjuvant therapies for testicular torsion that improve testicular well-being are not indicated and patients who require an orchiectomy for a non-viable testis usually have a testicular prosthesis inserted 4-6 months after the initial surgery to allow the inflammation to subside<sup>58</sup>.

### **3.3 Gubernaculum testis and testicular compartmentalization ensure male fertility**

#### **3.3.1 Gubernaculum testis: para/extra-testicular tissue**

The gubernaculum testis was first described by the Scottish surgeon John Hunter in 1762 as caudal genitoinguinal ligament developing during the sixth week of gestation. It arises from the caudal pole of the gonads and extends in the space between the mesonephric and the paramesonephric - Mullerian duct destined to disappear - associating only with the former<sup>61</sup>. During the developmental stages, the gubernaculum is involved in the formation of the vaginal process, whose growth results in the division of the gubernaculum into three parts: the main gubernaculum, vaginal and infra-vaginal gubernaculum<sup>62</sup>. The gubernaculum is an elongated conical structure composed by an abundant loose extracellular matrix rich in glycosaminoglycans and mesenchymal cells, mainly including fibroblasts and smooth muscle cells. Gubernaculum, as the name suggests (from Latin gubernāculum “a helm, rudder”) has a guide role in testicular descent - it pulls the testes through the abdomen and the inguinal canal down into the scrotum. From a histological examination, it has been reported that gubernaculum consists of moderately vascular, fibrofatty tissue with a core of essentially longitudinally oriented collagenous fibers surrounded by mature fatty tissue<sup>63</sup>. As previously described, testicular descent is regulated by gubernaculum through the cross-talk with testicular Leydig cells.

During testicular migration, the gubernaculum undergoes extensive remodeling, which contributes to the testicular descent toward the scrotum. The gelatinous and bulky nature of gubernaculum is due to the hydrophilic nature of hyaluronic acid<sup>64</sup>. During 10–15 weeks in male fetuses the caudal end of the gubernaculum undergoes thickening and anchors the developing testis to the inguinal region<sup>25</sup>. This thickening known as gubernaculum/swelling reaction is believed to be caused by the increase in glycosaminoglycans and hyaluronic acid. A study showed that during 15 to 16 weeks of gestation, collagen fibers composing gubernaculum were sparser and more embedded in a loose extracellular matrix; then, at 28 weeks of gestation, the number of fibers gradually increased, making the gubernaculum mostly collagenous.

Fibroblasts largely predominate over other cell types and decrease in number with gestational age, whereas smooth muscle cells are restricted to the walls of blood vessels. Striated muscle cells are generally detected at the scrotal end of the gubernaculum, decreasing in number with age<sup>64</sup>.

During transabdominal migration, INSL3 produced by Leydig cells binds specifically to the relaxin family peptide receptor 2 (RXFP2), a G protein-coupled receptor (GPCR), which is located on the gubernacular cell membrane to form the INSL3/RXFP2 complex. The activation of this complex stimulates cAMP production and gubernacular cell division, thus regulating growth and development of gubernaculum<sup>65</sup>. INSL3/RXFP2 axis has an essential role in the development of the gubernaculum for the initial transabdominal descent of the testis and also in the maintenance of reproductive health in men<sup>66</sup>. Many genes are reported to regulate this first phase by their action on gubernaculum. A study in rodents has reported that Wnt-5a and its receptor Ror2 were strongly expressed within the mesenchyme of the gubernaculum early during its development, and their mutation resulted in undescended testes<sup>24</sup>.

During inguinoscrotal phase, the androgens indirectly control the migration of gubernaculum by means of CGRP released from the sensory branch rather than the motor nerve of GFN<sup>25</sup>. The CGRP provides a chemotactic signal to the gubernaculum and induces rhythmic contractions that are more pronounced by the increased intra-abdominal pressure to assist gubernaculum – whose size is not enough for taking a longer route- for aiding the testicular descent<sup>67</sup>. Interestingly, as the observed contractions are highly vigorous, these studies suggest the possibility of an embryonic cardiac muscle in gubernaculum testis<sup>68</sup>. Despite the inguinoscrotal phase being directly or indirectly mediated by androgens, some studies have also shown the involvement of INSL3/RXFP2 complex<sup>69</sup>. In addition, it has been shown that rat gubernacular cells show an increased production of cAMP upon stimulation with INSL3 and that bilateral cryptorchidism in INSL3- and RXFP2-deficient mice is linked with the impaired development of the gubernaculum<sup>69</sup>.

In animal models, it has been reported that, during this remodeling, gubernaculum becomes enriched in vessels under the effect of testosterone, which increases the expression of the androgen receptor (AR) in fibroblasts, with secondary contraction of the gubernacular muscle. This means that the post-operative gubernacular stimulation can improve the testicular growth by enhancing the vascularization of the testes<sup>70,71</sup>, although up to now it has not been demonstrated whether there is also a relation with an increased testicular function.

During the process of descent, the proximal end of gubernaculum appears short. The shortening of the gubernacular cord with subsequent regression of cranial suspensory ligament, facilitates the positioning of testes over the inguinal ring<sup>25</sup>. This also results in the enlargement of inguinal canal and scrotum allowing testicular movement to its destination.

Interestingly, steroid hormone estradiol was shown have a role in gubernacular growth: it was proposed to have an inhibitory effect by causing the gubernacular reduction in volume and size of extracellular matrix<sup>25</sup>.

Usually, after birth, the muscles and connective tissues obliterate any opening and the gubernaculum testis becomes the scrotal ligament (SL), persisting in adults as a fibrous residual structure only individualized as microscopic connective fiber. The SL is typically described as a “Y-shape” ligament with the testis and epididymis as proximal insertions and the scrotum as a distal attachment. However, in some cases, authors have shown the absence of attachment to the adult scrotum, supporting the involution of the gubernaculum after birth and therefore the possible absence of SL<sup>72</sup>.

To date, most studies on gubernaculum testis have focused on animal models, describing its peculiar and unique role in testicular descent, but so much remains to be known about the properties of this ligament whose development is closely connected to the gonadal one.

### **3.3.2 Testis: a compartmentalized system**

Male fertility is dependent on the continual production of sperm, starting at puberty and continuing throughout adult life. This is only possible if the architecture and functionality of the testes - the male reproductive organs - is conserved<sup>73</sup>.

The testicle is a compartmentalized system, within which occur two crucial processes: spermatogenesis and steroidogenesis. Testis is surrounded by two distinct layers of protective connective tissue: an outermost serous membrane called the tunica vaginalis and a white and dense connective tissue layer - the tunica albuginea - which invaginates to form from 300 to 400 septa called lobules. In each lobule, two basic compartments can be distinguished: the interstitial (intertubular) compartment and the seminiferous tubule one<sup>74</sup>.



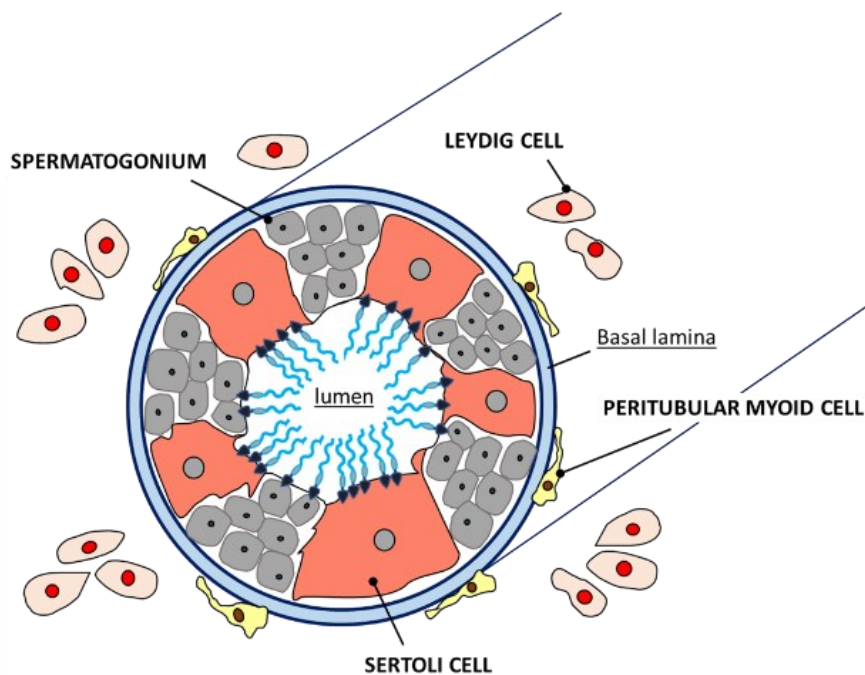


**Figure 4. Testicular compartmentalization**

Two distinguishable compartments in the testis lobules: 1) interstitial compartment composed mainly of peritubular myoid cells and Leydig cells and 2) seminiferous tubule compartment composed by Sertoli cells and germ cells.

### Interstitial compartment

The interstitial compartment of the testis, which constitutes the area of the organ outside of the seminiferous tubules, is highly vascularized and contains several cell types, such as peritubular cells, vascular endothelial cells, vascular smooth muscle and other perivascular cells, Leydig cells and their undifferentiated mesenchymal progenitors, and immune cells that under normal conditions mainly include testicular macrophages<sup>73</sup>. Among all these different cell types, a pivotal role in testicular functionality is played by Leydig cells.

Leydig cells. Leydig cells are responsive to luteinizing hormone (LH) and through secretion of hormones and growth factors, are responsible for steroidogenesis, thus supporting both developing/maintaining of secondary sexual characteristics and spermatogenesis progression.

The Leydig cell has abundant smooth endoplasmic reticulum (SER) and mitochondria, both of which contain the enzymes associated with steroid biosynthesis (**figure 4**).

### Tubular compartment

The tubular compartment is maintained separately from the interstitial one by peritubular cells (often called peritubular myoid cells) covering a collagen- and laminin-containing basement membrane. This organization allows the two compartments to be physically separated.

The tightly coiled seminiferous tubules form the bulk of each testis (60-80% of total testicular volume). Inside the seminiferous tubules there are six different cell types: sustentacular or Sertoli cells, as well as five types of developing sperm cells called germ cells. The correct architecture of the tubules is sustained by Sertoli cells, which trace the circular perimeter of the tubules, arranging close to the basement membrane and thus supporting the development progression of germ cells starting from the basement membrane—at the perimeter of the tubule—toward the lumen, where finally formed sperm are released into the duct system of the testis.

**Sertoli Cells.** Sertoli cells, represented in **figure 4**, are a type of supporting cell known also as sustentocyte, that are typically found in epithelial tissue. Sertoli cells secrete signaling molecules that promote sperm production and can control whether germ cells live or die. As above described, they extend physically around the germ cells from the peripheral basement membrane of the seminiferous tubules to the lumen. Tight junctions between these sustentacular cells create the blood–testis barrier, which on the one hand protects the germ cells by preventing bloodborne substances from reaching them and, at the other hand, keeps surface antigens on developing germ cells from leaking into the bloodstream and triggering an autoimmune response.

### **3.3.3 Hypothalamic-pituitary- gonadal axis: endocrine regulation of testicular processes**

The production and maintenance of spermatozoa by functional testes requires a highly complex endocrine regulation. Hypothalamic-pituitary-gonadal (HPG) axis plays a fundamental role in the reproductive function as it provides a privileged and well-regulated path of communication between these different organs. Along this axis, the signaling network is triggered by the neuropeptide Kisspeptin, produced by hypothalamic neurons as the rostral periventricular region of the third ventricle (RP3V) and arcuate nucleus (ARC). Kisspeptin stimulates the secretion of gonadotropin-releasing hormone (GnRH) – a short peptide hormone - by neurons scattered in the anterior hypothalamus directly into the hypophyseal circulation where it then binds to GnRH receptors located on pituitary gonadotropic cells. Here, GnRH pulsatively stimulates the anterior pituitary gland to secrete two hormones vital for reproduction, follicle-stimulating hormone (FSH) and LH<sup>75</sup>. The binding, also pulsatory, of the two gonadotropins LH and FSH to the G protein-coupled receptors LHCGR and FSHR, respectively, induces a conformational change in the receptor and triggers an intracellular signaling pathway that ultimately results in increased testosterone synthesis by Leydig cells. On the other side, FSH stimulation supports the synthesis of proteins as P-450 aromatase, androgen binding protein (ABP), inhibin, growth factors, and other molecules that

support sperm cells and spermatogenesis by Sertoli cells<sup>76</sup>. Kisspeptin seems to have a central role in the onset of puberty, which is a phenomenon that is activated by increasing pulsatility of GnRH secretion from the hypothalamus. The HPG axis is controlled by a classic negative feedback loop where inhibin B secreted by Sertoli cells continuously feeds back to the pituitary to regulate FSH release, while circulating testosterone secreted by Leydig cells feeds back to both hypothalamus and pituitary to adjust Kisspeptin, GnRH and LH output respectively. Despite the simplicity of the pathway promoted by HPG axis (**figure 5**), disruption of any of these steps can have a huge impact on male fertility.

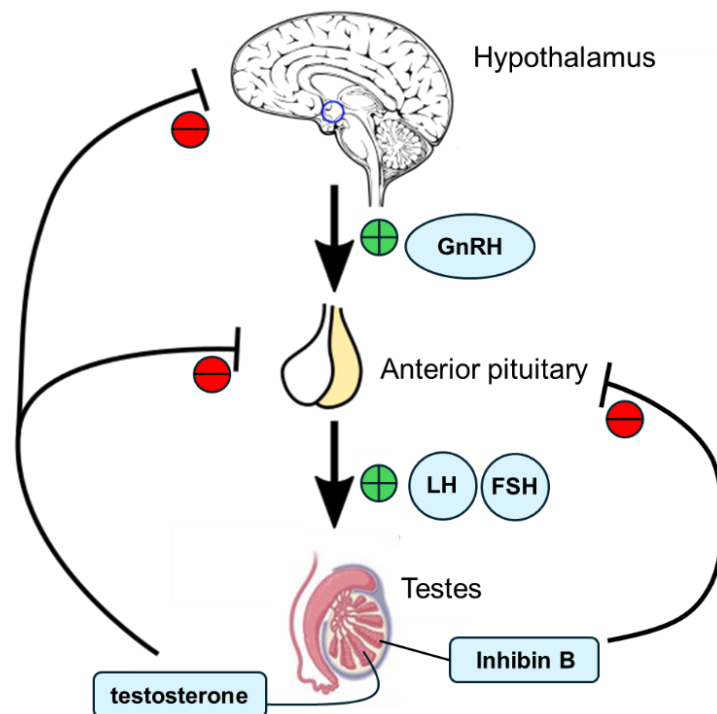


**Figure 5. Hypothalamic Pituitary Gonadal axis**

Endocrine regulation of testicular functionality by HPG. Negative feedback loop mediated through inhibin B secreted by Sertoli cells and testosterone secreted by Leydig cells.

### 3.4 Human chorionic gonadotropin as hormonal therapy for male infertility

Many andrological diseases affecting male fertility are closely linked to the function of complex organs, such as the pituitary gland and gonads, which produce and secrete hormones. Since hormonal supply is essential for the normal development of male characteristics and subsequent fertility, currently preclinical and clinical efforts to treat andrological diseases are mainly directed towards hormonal therapies.

#### 3.4.1 Luteneizing Hormone Receptor

Proper functionality of the luteinizing hormone receptor is crucial in the case of hormonal therapy with hCG, mostly because it activates specific signal transduction pathways that support the function of Leydig cells.

LHCGR is a member of the class A guanine nucleotide-binding protein-coupled receptors (GPCRs). The overall organization of the LHCGR gene is highly conserved between species, consisting of 11 exons and 10 introns. In humans, as well as in primates, this conserved genomic organization is complemented by an additional primate-specific exon, the exon 6A, which lies in intron 6, thus resulting in a gene composed of 12 exons and 11 introns<sup>77</sup>(Figure 6).

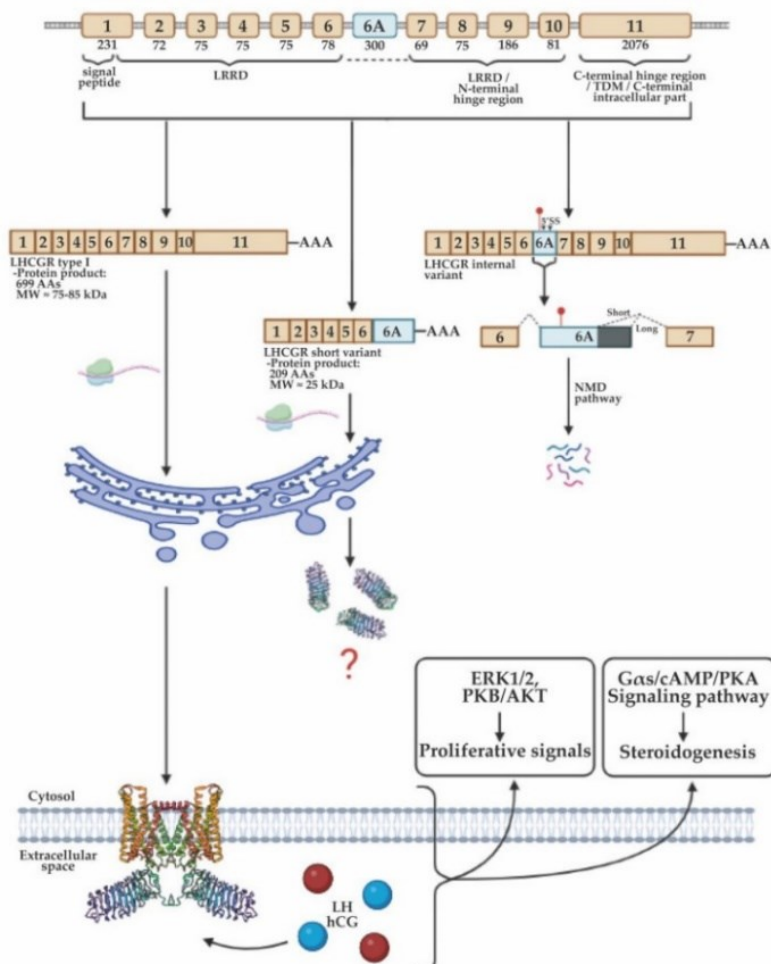


**Figure 6**

Transcription and translation of LHCGR variants. From top to bottom, we graphically report the complete *LHCGR* gene assembly, the putative transcriptional model, and the receptor structure/signaling pathways activated by LHCGR. In the schematic representation of the internal variant, the red spot indicates the translational stop codon, while 5' SS indicates the two 5' splicing sites that give rise to the internal-short and internal-long variants, both degraded by nonsense-mediated mRNA decay (NMD) pathway. The 3D monomeric LHCGR structural models, here reported as dimer on the cellular surface, have been uploaded from Protein Data Bank (protein #7FIJ).

Human LHCGR (hLHCGR) is located on the short arm of chromosome 2 (2p21), where exons 1–10 contain the code for the transcription of the signal peptide, N-terminal Cys-rich region, the leucine-rich repeat domain (LRRD), and the N-terminus of the hinge region that connects the LRRD to the serpentine-like transmembrane domain. The C-terminal segment of the hinge region, the seven transmembrane helices, the connecting loops, and the C-terminal intracellular part are encoded by exon 11<sup>78</sup>. The full-length hLHCGR (named also type I variant), which contains exons from 1 to 11 including exon 6 (and not exon 6A), is composed of 699 amino acids, with a total mass of 85–95 kDa when is mature and fully glycosylated<sup>78</sup>. Functionally, the full-length hLHCGR exploits its central role in a physiological aspect of gonadal maturation by binding both hCG and LH mainly on the cell membrane of the ovarian theca, granulosa, luteal, and Leydig cells<sup>78</sup>. Another important function of the full-length LHCGR is the capability to form homo- and hetero-dimers<sup>79,80</sup> or homo-oligomers, introducing the possibility of cis- and trans- activation mechanisms<sup>81</sup>, as well as constitutive and agonist-dependent self-association mechanism<sup>82</sup>.

On the other hand, variants containing exon 6A result in the expression of three diverse types of transcripts that are reported in Figure 6. These three mRNAs can be divided into two untranslated internal transcripts and one terminal transcript, which results in a truncated protein (called short-length variant) containing 209 amino acids. (**Figure 6**). The short LHCGR variant is highly expressed, with values comparable or higher to the full-length LHCGR transcript<sup>83</sup>. The functional role of the LHCGR short variant is not fully understood, it may be capable of hormone binding, considering that this shorter gene segment can encode 8 out of 10 LRRD repeats of the putative extracellular domain present in the full-length receptor, but without showing any signaling activity due to the lack of the transmembrane and intracellular domains<sup>83</sup>. Some authors reported that the full- and the short-length variants of hLHCGR can co-exist in the same cells and that the truncated protein may be secreted acting as a “hormone scavenger” capable of modulating the availability of hCG and LH by binding to them<sup>84</sup>. Conversely, other authors reported that the short variant of hLHCGR, co-expressed with the full-length receptor in transfected 293T cells, shows almost no hormone-binding activity and that its expression is mainly limited to the cytoplasm<sup>85</sup>.

### **3.4.2 LH and hCG: two ligands for a single receptor**

LH and hCG are hormones crucial for sexual development and reproduction. They work by binding to the same receptor, LHCGR, which mediates ligand-specific intracellular signals modulated to support the physiological functions of the two hormones. Since LH and hCG are used as drugs for

the treatment of infertility, it is very useful to explore their mechanism of action in detail for interpreting gonadotropin-related pathological conditions and optimizing their clinical treatment.

**Luteinizing Hormone.** LH is a glycoprotein hormone that belongs to the family of gonadotropins, which includes FSH and hCG. Gonadotropins are coded by similar genes, and, thus, they share similar properties, including the expression of alpha and beta subunits, linked by a non-covalent bond. The alpha subunit is common between FSH, LH, and hCG, whereas the beta subunit is different and gives each hormone a kind of biological specificity<sup>86</sup>. Particularly, the alpha subunit of LH is made up of 92 amino acids and the beta is made up of 120 amino acids and, thus, the combination of these two subunits has a total mass of 28 kDa<sup>87</sup>. As described above (**par 3.3.3**), LH is released by pituitary under GnRH stimulation and moves into the testicle, where it binds to LHCGR, which is expressed by Leydig cells. LHCGR belongs to the G-protein-coupled receptor family and once triggered by LH, it activates adenylyl cyclase, an enzyme that increases intracellular cAMP concentration, which then activates a kinase molecule called protein kinase A (PKA). PKA is the main kinase responsible for the phosphorylation of specific transcription factors, including steroidogenic factor 1 (SF-1), cAMP response element-binding protein (CREB), CRE modulator (CREM), CCAAT/enhancer-binding proteins (C/EBPs), and activator protein 1 (AP-1), that are implicated in regulating the expression of the genes encoding for steroidogenic acute regulatory (StAR) proteins and steroidogenic enzymes<sup>88</sup>. In the end, the generation of cAMP by LH results in the synthesis of testosterone. Indeed, the cAMP promotes the transfer of cholesterol to the inner mitochondrial membrane where it is metabolized into pregnenolone via the P450 cholesterol side-chain cleavage enzyme (P450scc or CYP11A1) and, further, is converted to progesterone by 3 $\beta$ -hydroxysteroid dehydrogenase (3 $\beta$ -HSD). In Leydig cells, the maturation of progesterone to androstenedione is catalyzed by 17-hydroxylase/C17-20-lyase (CYP17A1). Finally, androstenedione is converted into testosterone by type 3 17 $\beta$ -hydroxysteroid dehydrogenase (17 $\beta$ -HSD3)<sup>89</sup>. In the serum, LH levels change along the male's life (**Table 2**); indeed, during the first postnatal hours, the circulating levels of LH are very low. Subsequently, they increase during the first weeks of life until 3 to 6 months of life, which is typically known as “mini-puberty”. Afterwards, serum LH drops to non-detectable levels, remaining stable until puberal onset. Over puberty, from the ages of 9 to 14, LH levels increase and stimulate the proliferation of Leydig cells and the production of androgens even during adulthood<sup>90</sup>. As reported in **Table 2**, the normal range for men over the age of 18 is approximately 1.8–8.6 IU/L, at 50 years, it is 2.1/10.4 IU/L, and over 70 years, it is 2.2/11.2 IU/L<sup>91</sup>.

**Table 2.** Serum LH levels in men, from fetal life to adulthood.

Period of life	LH serum levels (UI/L)	References
<b>Gestation</b>	0-1 weeks	no detectable
	1-2 weeks	
	3-4 weeks	
	1-2 months	20
	2-3 months	
	second trimester	
	third trimester	
<b>Birth</b>		
<b>Infancy “mini-puberty”</b>	after 2 days of birth	0.21
	after 7 days of birth	3.94
	after 10 days of birth	4.81
	after 20 days of birth	2.67
<b>Childhood</b>	1-10 years of life	no detectable
<b>Puberty</b>	Tanner stage I	0.02-0.42
	Tanner stage II	0.26-4.84
	Tanner stage III	0.64-3.74
	Tanner stage IV	0.55-7.15
	Tanner stage V	1.7-8.6
<b>Adulthood</b>	18-30 years of life	1.8-8.6
	50 years of life	2.1-10.4
	70 years of life	2.22-11.2

**Human chorionic gonadotropin (hCG).** HCG is one of the most recently studied hormones in the context of andrological pathologies. The name of this glycoprotein hormone derives from Ancient Greek  $\chi\acute{o}\rho\iota\omicron\nu$ , meaning “membrane surrounding the fetus”, “afterbirth”, since it is produced mainly by differentiated syncytiotrophoblasts<sup>97</sup>. It is involved in embryonic signaling and is a key element of gestations development during pregnancy<sup>98</sup>. The molecular weight of hCG ranges from 36 up to even 41 kDa according to the glycosylation of its various forms. As already mentioned above, hCG binds to LHCGR as the “sister” gonadotropin LH. Indeed, the two gonadotropins are encoded by a common gene cluster and their protein structures are more than 80% homologous<sup>97</sup>. Aside from the aminoacidic sequences, carbohydrates bound to both hormones are crucial for their biological functions and the hepatic clearance of them from the body.

In a recent study, it has been demonstrated that the removal of carbohydrates from hCG generates its de-glycosylated forms, which bind LHCGRs with the same high affinity as the parental molecule, but with partial or complete impairment of function. Interestingly, these de-glycosylated “antagonist” variants of the hormone have been detected in the sera of patients with chronic renal failure disease associated with hypogonadism<sup>99</sup>. Serum levels of hCG change during the fetal life, essentially the presence of hCG is detectable only throughout the gestation period, with a peak between the second and the third month (**Table 3**). Afterwards, hCG level decreases until birth and becomes undetectable for the rest of the male’s life<sup>100</sup>. The absence of hCG in the serum of children and adults makes its detection a valuable marker not only for pregnancy but also for some neoplasms, including testicular germ cell tumors that produce and secrete this hormone<sup>101</sup>, seemingly due to the epigenetic regulation of its expression in cancer cells.

**Table 3.** Serum hCG levels during gestation.

Period of life	hGC serum levels (UI/L)	References
	0-1 weeks	0-50
	1-2 weeks	40-300
	3-4 weeks	500-600
<b>Gestation</b>	1-2 months	5000-200.000 <sup>100</sup>
	2-3 months	10.000-100.000
	second trimester	3000-50.000
	third trimester	1000-50.000

The effects of LHCGR activation due to hormone binding are sex-specific and depend on the intracellular enzymatic apparatus of the target cells and, apparently, on the receptor expression levels. Although both two gonadotropins share multiple features, the hCG effect is different from that of LH based on their different interactions with the receptor at the extracellular hinge region: the diverse binding with the same receptor causes the LH and hCG activation of different signaling pathways<sup>102</sup>. In the male gonads, the activation of LHCGR by both LH and hCG conclusively results in the production of testosterone, thanks to the activation of the cAMP/PKA pathway described above. However, in the last decade, several *in vitro* studies demonstrated that hCG activates the steroidogenic cAMP/PKA pathway to a greater extent than human LH, which, instead, preferentially stimulates the proliferative and anti-apoptotic pathways of extracellular signal-regulated kinases and protein kinase B.



Interestingly, the steroidogenic efficiency of this intracellular pathway seems to decrease with age, as an assumed effect of cumulative exposure to oxidative stress occurring during the individual's life<sup>103</sup>. Furthermore, hCG also induces a more rapid and effective recruitment of the  $\beta$ -arrestin 2 compared to LH, suggesting that hCG exerts more efficiently the receptor desensitization<sup>104</sup>. Despite the remarkable progress in recent years, further studies on the molecular mechanisms triggered by LHCGR activation are needed; moreover, the intrinsic pro-apoptotic potential of these hormones, the existence of receptors assembled as heteromers, and their expression in extragonadal tissues need to be investigated.

### **3.4.3 Hormonal Therapy with hCG**

Male infertility is a frequent medical condition and is increasingly observed as a reliable sensor of future male health conditions. The challenge for reproductive modern medicine is represented by early diagnosis and proper management of infertile men.

To evaluate testicular functionality, it is necessary to check principally serum gonadotropins and testosterone levels together with spermatogenesis, functions that are mainly regulated by the HPG axis. Therefore, in most cases, patients should receive therapies aimed at improving the function of this complex hormonal axis, rather than treating their downstream problems.

#### Hormonal therapy for cryptorchid patients

Since the 1930s, in Europe, the most supported and used therapeutic approach for testicular descent failure was the administration of hormonal therapy, given the belief that gonadotropin and androgen deficiencies were one of the etiological factors at the basis of undescended testicle causes<sup>105</sup>. Despite the fact that the most frequently used hormonal therapy was hCG because of its capacity to mimic the effects of LH in Leydig cells, this method has been mostly abandoned because of a success rate percentage of less than 20%<sup>106</sup>. Indeed, without surgical correction, an undescended testicle would likely descend during the first three months of life; if it remains undescended, to reduce the risk of increased testicular germ cell tumors outcome, testicular torsion, inguinal hernias and to minimize the risk of infertility (especially bilateral cases), the testicles should be brought into the scrotum with surgery, i.e., orchiopexy<sup>107</sup>. This surgical procedure takes place between 6 and 18 months of age, since within this time window there is a lower risk of future complications. Nevertheless, the hCG role in support of testicle wellbeing is widely described and, thus, even though it is not even used as a first-line treatment anymore, it could be administered after surgery.

Indeed, hCG adjuvant therapy has been shown to improve testicular vascularization, volume, and morphology safely<sup>44</sup>. Currently in cryptorchid patients, hCG is administered subcutaneously once or twice a week for six weeks. Each injection consists of 250 IU for children under 1 year; 500 IU for children between 2 to 6 years and 1,000 IU from 6 to 11 years. Early corrective surgery is therefore necessary, recommended, and based on an observational and follow-up study that analyzed various metrics in adulthood that have yielded favorable results regarding early orchidopexy and reproductive function<sup>108</sup>.

#### Hormonal therapy for infertile patients

HCG has also found a leading role in treating endocrine failure of the testicle in patients with infertility associated with hypogonadotropic and/or anabolic steroid induced hypogonadism - lost ability to produce their own testosterone - and hCG therapy has showed helping recover endogenous testosterone production, thus restoring spermatogenesis or steroid induced impairment of spermatogenesis<sup>109</sup>. In addition, other studies have also observed a decrease in triglyceride levels and an increase in lean body mass and muscle tissue in patients with hypogonadism after treatment with hCG. Finally, hCG has also been used to reduce some of the side effects of testosterone replacement therapy (TRT), mainly preventing testicular atrophy and helping maintain response to TRT by “cycling off” TRT with a periodic replacement of therapy with hCG.

As the age of men with hypogonadism continues to decrease and the age of paternity continues to increase more men will need to treatment for hypogonadism while maintaining fertility. hCG is a safe and efficacious alternative or adjunct to TRT in men desiring to preserve fertility while treating their hypogonadism<sup>109</sup>.

Based on the clinical application, there is a specific differential approach for hCG administration. As regards infertile adults, hCG may be administered together with FSH, since quantitatively and qualitatively normal spermatogenesis requires the synergistic action of FSH and LH, which are both essential for initiation and maintenance of spermatogenesis. In adults, hCG is given at 1,000 IU three times a week for three months, or 5,000 IU once a week for three months. Whereas, for FSH the starting dose is 75 IU twice a week for three months, or 125 IU if FSH levels are under range. It has been reported that hCG therapy for males with NOA and spermatogenic failure seems to be a valuable strategy to overcome infertility<sup>110</sup>. In this study, 8 NOA males received long-term treatment with hCG twice a week to stimulate spermatogenesis and 6 of them received additional recombinant FSH supplementation at 150-225 IU twice weekly. After therapy, viable spermatozoa were retrieved from the ejaculate in 2 patients and by testicular sperm aspiration (TESA) in another 2 subjects.

Singleton spermatozoon retrieved from the testes of these 4 subjects were frozen: 2 live births were obtained after intracytoplasmic sperm injection with ejaculated spermatozoa, 1 live birth was achieved, and a pregnancy using thawed spermatozoa from TESA was ongoing<sup>110</sup>.

Therefore, the application of already existing hormonal therapies or new ones could be considered in the clinical practice, prior validation in *in vitro* and *in vivo* models, in order to support a prompt recovery of the testicle in case of damages or pathologies, always keeping in mind that it would help the patient to avoid fertility problems.

### 3.5 Testicular organoid

Over the years many studies explored the andrological diseases affecting male fertility. Although to date it is possible to describe the etiology of some of them, there is still much to investigate regarding the morphogenesis, physiology, and pathophysiology of the male gonads. The need to understand more deeply what happens in the testicular tissue following the dysfunction of processes crucial to reproductive health, such as steroidogenesis and spermatogenesis, has therefore become increasingly pressing. The first effort forward in this direction is represented by generation of testicular organoids.

**Concept.** The terms “organoid” derives from Greek and means “organ-like”; indeed, it is a 3D *in vitro* model based on stem or differentiated cells capable of self-organizing and mimicking many aspects of the complex structure and function of the corresponding tissue *in vivo*. The history of organoids is relatively recent: several years of attempts were aimed at improving cell culture conditions to simulate the *in vivo* microenvironment and thus moving from a 2D to 3D culture system. Only in 2009 was the first report – by Sato et al.<sup>111</sup> - on establishing 3D organoid culture derived from a single adult stem cell. This study set the scene for many subsequent organoid works in other systems, including mesendoderm (e.g., stomach, liver, pancreas, lung, and kidney)<sup>112–114</sup> and neuroectoderm (brain and retina)<sup>115,116</sup> using either adult stem cells or pluripotent stem cells. If the history of organoids can be defined as recent, the approach to testicular organoids can be considered newly born but advanced. Testicular organoids (TOs) represent the highest level of *in vitro* culture of spermatogenic cells in a simulated testicular environment and recapitulate the processes of self-organization during development, implying the following features: (1) multiple organ-specific cell types; (2) ability to mimic some specific functions of the organ; (3) grouping and spatial organization of cells similar to that in an organ.

**History.** The first authors to introduce the term “testicular organoid” were Baert and colleagues<sup>117</sup>, who studied the culture of human pubertal testicular cell suspensions (TCSs) on adult decellularized testicular tissue slices. The study<sup>117</sup> showed that primary human testicular cells were capable of self-organizing into human TOs, either with or without the support of a biological scaffold, opening up to the possibility of *in vitro* reengineering of a human testicular microenvironment from primary cells. Despite the lack of a correct testis-specific organization, these minitissues nurtured spermatogonia and their important niche cells, which retained specific functionalities during long-term culture. Furthermore, the Alves-Lopes and Stukenborg group<sup>118</sup> developed and characterized a novel 3D multilayer model, the three-layer gradient system (3-LGS), which allows the generation of rat TOs with a functional blood-testis barrier (BTB) and germ cell establishment and proliferation. Then, their study was extended to human first-trimester embryonic gonadal tissue and they<sup>119</sup> showed that testicular cell suspensions reorganized into testis-like organoids with distinct seminiferous-like cords located within an interstitial environment after 7 days. Later, Wyns and colleagues<sup>120</sup> created TO using hydrogels developed by solubilizing the extracellular matrix of decellularized porcine immature testicular tissue (ITT) and compared cell numbers, organization, and function to those of TOs generated in collagen-only hydrogels. In both models of TOs, Sertoli cells and germ cells assembled into seminiferous tubule-like structures delimited by a basement membrane, while Leydig cells and peritubular cells were localized on the outside; TOs were maintained for 45 days in culture and secreted inhibin B and testosterone, demonstrating the functionality of both Sertoli and Leydig cells, respectively<sup>120</sup>. However, this study showed better preservation of growth factors within TOs developed from decellularized ITT and, thus, better potential to restore reproductive capacity. Other TO culture systems were developed by Sadri-Ardekani and Bishop group, who presented the 3D human TO system as a novel testicular toxicity screening tool and *in vitro* model for human spermatogenesis<sup>121</sup>, and by Baharvand group who demonstrates the importance of a novel platform for testicular tissue engineering and *in vitro* spermatogenesis consisting of macroporous testis-derived scaffolds (TDS)<sup>122</sup>. Further contribution to characterization of TOs was by Dobrinski group, who presented a microwell aggregation approach to establish multicellular 3D TOs from pigs, mice, macaques, and humans. Their study indicated the utility of organoids for toxicity screening and their application in screening for factors affecting testicular morphogenesis<sup>123</sup>. They also found that organoids could be generated from cryopreserved testis cells and preserved by vitrification. A relevant role in TOs could be also played by culture microenvironment: Woodruff group directly tested whether the culture microenvironment was the prime factor promoting TO self-assembly. Using Matrigel as a representative ECM, they compared multiple culture conditions, 2D and 3D, ECM-free and ECM<sup>124</sup>.

Collectively, the different studies<sup>123,124</sup>, in which cellular self-assembly and organoid formation were achieved independently of the culture microenvironment, suggested that self-assembly was an innate property of immature testicular cells and was not dependent on but was capable of being promoted by the culture environment. Subsequently, Sekido and colleagues reported the generation of testicular somatic cell-like cells (TesLCs), including Sertoli cell-like cells (SCLCs), from mouse embryonic stem cells (ESCs) in a xeno-free culture; finally, their study proved the capability to achieve the *in vitro* reconstitution of a testicular environment from ESCs and provided further insights into the generation of sperm in a xeno-free culture<sup>125</sup>.

However, because adult testicular cells have a limited self-organization capacity and lifespan, the Jordan group investigated an optimal model of the human testis, which was created through the use of human pluripotent stem cells (hPSCs) and testicular cells in combination<sup>126</sup>.

**Applications.** The development of testicular organoid culture system is promising and can be applied to different types of investigations and analyses. TOs represent a new tool for testicular toxicity screening and a first-level drug screening tool. Furthermore, several TOs approaches aim to test spermatogenesis *in vitro* and study the mechanisms of testicular development and spermatogenesis via gene editing. Also, it is useful for understanding the effects of environmental factors on male reproductive health, and potentially even providing insights into infertility treatments. Finally, an advanced approach to TOs is the organ-on-a-chip multi-tissue co-culture platform through which can be evaluated the systemic interaction between different organs *in vitro*.

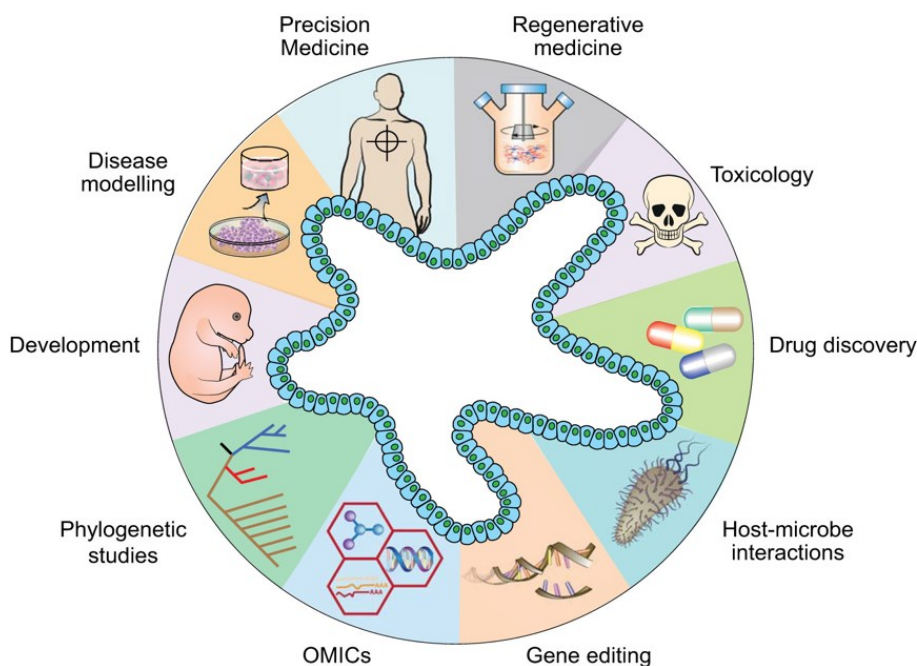


**Figure 7.** Diverse applications of organoid technology. Schematic diagram summarizing various applications of organoids in many areas, including developmental biology, disease modeling, precision medicine, regenerative medicine, toxicology, drug discovery studies, host-microbiome interactions, gene editing, multiomics, and phylogenetic studies. Image provided by Corò et al., *Am J Physiol - Cell Physiol*. 2020

The 3D organization of organoids confers advantage over the conventional 2D conditions because cell-to-cell and cell-to-ECM relationships are better modulated. Following this approach, testicular organoids could also be applied to explore testicular development by tracking the reorganization process and the interactions between different cell populations in a 3D environment mimicking the *in vivo* situation better than 2D culture conditions. Furthermore, the easy manipulation of cell suspensions, the relatively fast reorganization of these structures, and the controlled *in vitro* conditions make testicular organoids a culture system of choice and very useful for researchers to answer scientific questions in a simple and efficient way<sup>127</sup>. However, the generation of TOs is still evolving, and there is still much room for improvement in dealing with the many challenges and prospects to achieve the goal of TOs able to simulate the testicular microenvironment *in vitro* or even reconstruct the process of spermatogenesis without the need to reconstruct seminiferous tubules.

#### 4. AIMS OF THE THESIS

Andrological diseases affecting pediatric patients represent important risk factors for alterations of their fertile potential in adulthood; hence, early diagnosis and treatment, even surgical and/or therapeutical, are of primary importance. In this context, the discovery of the biological cues connected with alterations in the andrological sphere both in the pediatric age and adulthood could offer new insights into the identification of altered fertility potential markers or new therapeutic approaches. In this thesis, we cultured *in vitro* biopsies of gubernaculum testis, a para-testicular ligament that shares many properties with testicular cells due to their common embryonic origin. The advantage of using gubernaculum testis biopsies is that the surgeon leaves the testis surgically untouched, thus preserving it as much as possible. The tissues are derived from patients with andrological diseases with the aim of developing a personalized cellular model. To generate the gubernacular *in vitro* model for each patient, we first optimized the procedure to culture *in vitro* primary gubernacular cells, leading us to define a standardized protocol that has been applied to cells derived from different patients with diverse andrological pathologies, in particular cryptorchidism and testicular torsion.

Cryptorchidism: since about 40% of cryptorchid patients treated with hCG adjuvant therapy don't show beneficial effects, including improvement of testis volume and vascularization, we aimed to set the basis for the development of an *in vitro* model that could predict the response to post-surgical hCG therapy. For this aim, we developed *in vitro* cultures of cells derived from the biopsy of gubernaculum testis of different cryptorchid patients, then we treated these cells with hCG and analyzed the effect on cell proliferation. The advantage of generating this *in vitro* model is that it can predict the response to therapy for each patient in the future to define the best therapeutic approach or dosage before clinical administration. In addition, we characterized the effect of hCG on the cells *in vitro*, including the analysis of reactive oxygen species production and the metabolic arrangement given by this hormone.

Testicular torsion: since up to now no adjuvant therapies are considered after testicle derotation, our aim was first to evaluate the testicular health status after surgery by culturing *in vitro* gubernacular cells derived from different patients and, secondly, to test *in vitro* whether hCG may improve cell proliferation. The potential clinical application of our study has a major impact on disease-related definition of appropriate dosage and treatment types for each patient. Specifically, this study aims to add further information and indications to support observations on the effectiveness of hCG therapy, which is already described in the literature for cryptorchid patients, and to propose a pharmacological treatment - which has not yet been provided in the post-operative phase - also for patients with testicular torsion.

## 5. MATERIALS AND METHODS

### 5.1. Patients

This study was approved by the Pediatric and Fertility Lab Internal Review Board and by the Institutional Ethics Committee of Azienda Ospedaliera Universitaria Integrata” (AOUI) of Verona, Italy (“ANDRO-PRO”, protocol code N. 4206 CESC). Informed consent was obtained from all the parents/patients. At our Institution, we collect samples of patients with primary azoospermia, genetic syndromes associated with azoospermia, undescended testis, testicular torsion, testicular trauma, and testicular neoplasms. We catalogue each patient with a progressive identification number. At present, the tissue collection is composed by biopsies of different tissues (gubernaculum, testis, fat) and serum obtained from 108 patients aged between 1 and 35 years.

### 5.2. Inclusion criteria

#### Cryptorchidism

We considered all patients with unilateral undescended testes, without any other disease nor genital malformations. Only patients treated by the same surgeon were considered in this specific study. Also, patients with no previous hormonal therapy nor previous inguinal surgical procedures were considered. All patients had testicular hypotrophy at surgery.

Among these patients we selected the following:

Patient #2: 8-year-old patient with cryptorchidism and testicle retained in the medial third of the inguinal canal.

Patient #3: 14-month-old patient with cryptorchidism and testicle retained in the upper third of the inguinal canal.

Patient #7: 5-year-old patient with retractile testicle in the lower third of inguinal canal.

Patient #20: 22-month-old patient with cryptorchidism and testicle retained in the medial third of the inguinal canal.



### Testicular torsion

We considered all patients with testicular torsion that were clinically diagnosed and treated within 24 h of symptom onset and surgically treated within 2 h after hospital arrival in order to avoid bias related to hospital coordination.

The patients included in this study are:

Patient #4: 12-year-old male with testicular torsion with an onset of symptoms less than 8 h before surgery. Spermatic cord torsion: two loops (720°). Testis left in place.

Patient #12: 14-year-old male with testicular torsion with an onset of symptoms less than 14 h before surgery. Spermatic cord torsion: one loop and half. Testis removed.

Patient #15: 14-year-old patient with torsion of the hydatid of Morgagni and epididymitis (not torsion of the testicle), with an onset of symptoms less than 10 h before surgery. Rotation of 540 degrees, Testis left in place.

Patient #55: 13-year-old patient with testicular torsion. Testis left in place.

### Other andrological diseases

Patient #40: 30-year-old patient with azoospermia underwent the testicular sperm extraction (TESE).

## **5.3. Exclusion criteria**

### Cryptorchidism

We excluded patients with non-palpable testes during the pre-operative visit and patients who required intraabdominal approach.

### Testicular torsion

We excluded patients treated for torsion that had definitely occurred at least 24 h before symptom onset, either reported in history or showing an absence of pain on palpation. Moreover, patients reporting testicular trauma immediately before a suspected torsion being considered as the main cause of their torsion were excluded.

#### **5.4. Gubernaculum surgical collection**

##### *Cryptorchidism*

During surgery all patients underwent standard inguinal approach (orchidopexy); after surgical dissection all testes were fixed into the scrotum. During this phase, the surgical biopsy of the gubernaculum (at least 5 mm from the lower pole of the testes) was collected together with a small fat biopsy; this procedure did not remove important tissue nor vascularization to the testes.

##### *Testicular torsion*

All patients underwent surgery by the same operator under general anaesthesia. All procedures were performed with a trans-scrotal incision. All testes were delivered, the torsion was resolved, and then 3 micro-biopsies were performed to verify the vitality. If necessary and in absence of bleeding, the testes were removed. In cases with partial testicular viability (bleeding and/or good parenchymal color), the testes were left in place. All patients underwent gubernaculum biopsies to deduce more information about vascularization. No other procedures were performed on the contralateral testes.

#### **5.5. Drugs and Chemicals**

Highly purified human chorionic gonadotropin (hCG) extracted from pregnant women urine was kindly provided by IBSA Italia.

#### **5.6. Tissue Processing and *In vitro* culture**

Gubernacula were processed by firstly cutting the piece of tissue (about 10–20 mm<sup>3</sup>) with a scalpel in 500 µL of phosphate-buffered saline (PBS) on a Petri dish in sterility under the biological hood. Then, the fragmented tissues were enzymatically disaggregated with 1X collagenase type I and hyaluronidase (both from Sigma-Aldrich, St. Louis, MO, USA, Merck) resuspended in 200 µL of a complete cell culture medium and incubated at 37 °C until complete homogenization of the tissue. Cell viability was assessed with a trypan blue assay and was variably around 20–40%. Finally, the cell suspension was grown in DMEM-Glutamax supplemented with 10% fetal bovine serum (FBS), 4.5 g/L glucose, and 50 µg/mL gentamicin sulfate (all from Gibco/Life Technologies, Waltham, MA, USA) and maintained at 37 °C with 5% CO<sub>2</sub> in Corning Primaria cell culture flasks (Corning, New York, NY, USA).

Before hCG treatment, cells were maintained for 16 h in the same medium but without FBS, which contains two gonadotropins (FSH and LH) at different concentration depending on lot-to-lot, as reported by manufacturers' sheet. Then cells were treated at the indicated doses and times in the medium without FBS. Bright field cell images were acquired with inverted microscope (Axio Vert. A1, Zeiss, Oberkochen, Germany).

For the adult azoospermic patient, we only had the availability of testicular biopsy. In this case, we disaggregated the testicular tissue by using an enzymatic mix composed by DNase, collagenase, hyaluronidase, and incubated by shaking for about 15 min at 37°C, in order to obtain single cell suspension. Then, cells were grown in DMEM-Glutamax implemented with 10% FBS and 50µg/ml gentamicin sulfate and were maintained at 37°C with 5% CO<sub>2</sub> in Corning Primaria cell culture flasks. The treatment with hCG has been performed in the same conditions of gubernacular cells.

## 5.7. RNA extraction and qPCR

Total RNA was extracted from  $1 \times 10^5$  cells using Single Cell RNA purification Kit (Norgen Biotek), according to the manufacturer's instructions and 1 µg of RNA was reverse transcribed using first-strand cDNA synthesis. qPCR was performed in triplicate samples by SYBR-Green detection chemistry with GoTaq qPCR Master Mix (Promega, USA) on a QuantStudio 3 Real-Time PCR System (Thermo Fisher Scientific, USA). RNA integrity was determined by electrophoresis on an agarose gel. Total RNA (1 µg) was used to synthesize first-strand cDNA by RT-PCR.

The primers used in this study were: LHCGR forward, 5'-GCTGCGATTAAGACATGCCA-3', LHCGR reverse, 5'-AGAAGGCCACCACATTGAGA-3'; LHCGR short-variant forward: AGGCAATAAAGGAGCTCACCC; LHCGR short-variant reverse: AAAGGCAGTGCACCAAGGAT; FSHR forward, 5'-GGCCATGCTCATCTTCACTG-3', FSHR reverse, 5'-ATAGAGGAAGGGTGGCAC-3'; AR forward, 5'-CCCACTTGTGTCAAAGCGA-3', AR reverse, 5'-GCAGCTTCCACATGTGAGAG-3'; succinate dehydrogenase A (SDHA) forward 5'-GGACCTGGTTGTCTTTGGTC-3', SDHA reverse 5'-CCAGCGTTTGGTTTAATTGG-3'. The cycling conditions used were: 95°C for 10 min, 40 cycles at 95°C for 15 s, 60°C for 1 min, 95°C for 15 s, and 60°C for 15 s. The average of cycle threshold of each triplicate was analyzed according to the  $2^{-\Delta\Delta C_t}$  method using SDHA as an endogenous control. Real-time PCR data were calculated as fold change relative to the positive control MCF7, a breast cancer cell line previously described in Dando et al.<sup>128</sup>.

### 5.8. Immunofluorescence analysis of LHCGR positive cells

Gubernacular cells were fixed on Ibidi Imaging Chambers with 4% paraformaldehyde for 8 min and washed 3 times with PBS for 5 min each. To saturate unspecific binding sites, the cells were incubated for 45 min at room temperature (RT) with a blocking solution containing 5% bovine serum albumin (BSA) in PBS. Samples were then incubated overnight at 4°C with anti-LHCGR primary antibody (1:200; Thermo Fisher #8G9A2) diluted in blocking solution. After 3 washes with PBS of 10 min each, cells were incubated for 1 hour at RT in the dark with anti-mouse specific secondary antibody (1 µg/ml) conjugated with Alexa Fluor-488 (Molecular Probes). Samples were mounted in anti-bleaching medium (Dako Fluorescent Mounting Medium), then examined by confocal microscope (Leica TCS SP5 AOBS).

### 5.9. Cell proliferation assay

To analyze the cell proliferation rate, gubernacular cells were plated in 24-well cell culture plates ( $25 \times 10^3$  cells/well) in DMEM-Glutamax supplemented with 10% FBS, 4.5 g/L glucose, and 50 µg/mL gentamicin sulfate (all from Gibco/Life Technologies, Waltham, MA, USA) and incubated at 37°C with 5% CO<sub>2</sub>. Viable cells were counted by Trypan Blue dye exclusion after 2, 4, 7, and 10 days of culture. The doubling time was calculated using the formula  $T = (T_2 - T_1) \times \log_2 / \log(Q_2/Q_1)$ , where: T<sub>1</sub>, day 2; T<sub>2</sub>, day 7; Q<sub>1</sub>, cell number at day 2; and Q<sub>2</sub>, cell number at day 7.

To test the effect of hCG on cell proliferation, gubernacular cells were plated in 96-well cell culture plates ( $6 \times 10^3$  cells/well) and incubated at 37°C with 5% CO<sub>2</sub>. Cells were treated with 100 IU/ml of hCG once a week for four weeks and cell viability was measured by Crystal Violet assay (Merck Millipore) according to the manufacturer's protocol and absorbance was measured by spectrophotometric analysis (A595<sub>nm</sub>). The Crystal Violet assay is designed to work with adherent cells and, when cells die, they detach from the surface of the plate. Thus, this assay is suitable for *in vitro* cell proliferation and cell cytotoxicity studies, as reported in several manufacturer's sheets.

### 5.10. Tubular structure formation assay

Formation of tubular structure was analyzed by seeding gubernacular cells ( $10^5$  cells/well) on the top of Matrigel® (50  $\mu$ l/well) into a 96-well plate at 37°C with 5% CO<sub>2</sub>. To evaluate the hCG effect on the formation of tubular structures, cells were suspended in serum-free DMEM:F12 complemented with 100 IU/ml of hCG. Five pictures per well (center of the well and four cardinal points) were taken every 3 hours up to 24 h using Evos imaging system (Thermo Fisher). Two wells per conditions were seeded. Image analysis was performed using a specific program developed by ImageJ that is “Angiogenesis Analyzer”, a precise tool built in the ImageJ setting<sup>129</sup>.

### 5.11. Oxygen Consumption Rate (OCR) and Extracellular Acidification Rate (ECAR) analysis

OCR and ECAR were measured in gubernacular cells derived from patient #20 by using a Seahorse XFe24 Extracellular Flux Analyzer (Agilent Technologies, Milan, Italy). Cells were seeded at the density of  $1 \times 10^4$  cells/well in a V7 XFe24-well cell-culture microplate and treated with hCG 100 IU/ml once a week for 4 weeks. On the day of the analysis, cells were incubated in Mitostress assay medium consisting of Seahorse XF DMEM Medium (Seahorse Bioscience, cat. No. 103575-100) supplemented with 10 mM glucose, 0.5 mM Sodium Pyruvate, and 2 mM glutamine, pH 7.4, or alternatively in Glycostress assay medium consisting of Seahorse XF DMEM Medium (Seahorse Bioscience, cat. No. 103575-100) supplemented with 2 mM glutamine, pH 7.4, and incubated at 37°C in a non-CO<sub>2</sub> incubator for 1 h. A Mitostress test was performed recording OCR, at the baseline and after sequentially adding 1  $\mu$ M oligomycin A (port A), 3  $\mu$ M of carbonyl cyanide 4-(trifluoromethoxy) phenylhydrazone (FCCP, port B), and 0.5  $\mu$ M each of Rotenone and Antimycin A (port C). A Glycostress test was performed recording ECAR at the baseline and after sequentially adding 10 mM glucose, 1  $\mu$ M oligomycin A and 50 mM of 2-deoxyglucose. OCR and ECAR raw data were normalized to the DNA content per well, which was quantified with the CyQUANT Cell proliferation assay kit (Thermo Fisher Scientific, cat. No. C35007) following the instructions of the manufacturer. Data related to mitochondrial respiration were calculated as described<sup>130</sup>. Data related to glycolysis were calculated as follows: Basal glycolysis:  $ECAR_{\text{BASAL}} - ECAR_{2\text{-DG}}$ ; glycolytic capacity:  $ECAR_{\text{OLIGO}} - ECAR_{2\text{-DG}}$ ; glycolytic reserve:  $ECAR_{\text{OLIGO}} - ECAR_{\text{BASAL}}$ .

### **5.12. Reactive oxygen species (ROS) levels analysis**

The non-fluorescent diacetylated 2,7-dichlorofluorescein (DCF-DA) probe (Sigma-Aldrich), which becomes highly fluorescent upon oxidation, was used to evaluate intracellular ROS production. Briefly, gubernacular cells derived from patient #20 were plated in 96-well plates ( $1 \times 10^4$  cells/well) in 10% FBS medium. The day after the culture medium was replaced with a serum-free medium and the cells were treated with hCG at 100 IU/ml. To analyze the levels of ROS produced daily for up to 7 days after hCG treatment, the cells were incubated in culture medium with 10  $\mu$ M DCF-DA for 15 min at 37 °C. The cells were washed with Hanks' solution and the DCF fluorescence was measured by using a multimode plate reader (Ex485 nm and Em535 nm) (Tecan Infinite 200 PRO). The values were normalized by Crystal Violet assay.

### **5.13. Pyruvate kinase activity assay**

One  $\mu$ g of total protein extracts obtained from gubernacular cells derived from patient #20 untreated or treated with 100 IU/ml of hCG once a week for 4 weeks were used to analyze pyruvate kinase (PK) activity, as previously reported<sup>131</sup>. Briefly, PK activity was measured according to published methods by a continuous assay coupled to lactate dehydrogenase (LDH). The change in absorbance at 340 nm owing to oxidation of NADH was measured using a Tecan Infinite 200 PRO. Kinetic assays for activity determinations contained recombinant pyruvate kinase (20–100 ng) or cell lysate (1–2  $\mu$ g), Tris pH 7.5 (50 mM), KCl (100 mM),  $MgCl_2$  (5 mM), ADP (0.6 mM), PEP (0.5 mM), NADH (180  $\mu$ M), and LDH (80 units), Brij (0.015%), and DTT (1mM).

### **5.14. L-lactic acid quantification in culture medium**

The culture media of gubernacular cells derived from patient #20 untreated or treated with 100 IU/ml of hCG once a week for 4 weeks have been collected and diluted 30-fold in H<sub>2</sub>O. For each sample 5  $\mu$ l has been analyzed in a final reaction volume of 112 $\mu$ l (Megazyme, #K-LATE 07/14). Absorbance at 340 nm has been read after 10 min the activation of the reaction and L-lactic acid concentration (g/L) has been calculated according to the manufacturer's instructions.

## 5.15. Proteomic analysis

For proteomics analysis, the data indicated in this work are extrapolated from an ongoing study on the untargeted proteomics study of the effect of hCG on gubernacular cells.

### 5.15.1 Protein extraction and tryptic digestion

Gubernacular cells derived from pt #20 untreated or treated with 100IU/ml hCG once a week for 4 weeks were processed for protein extraction and peptide cleaned up using EasyPEP™ Mini MS Sample Prep Kit. Extracted proteins were quantified using the Pierce™ BCA Protein Assay Kit and 50 µg of protein sample was digested after incubation in a tryptic solution (furnished by Kit) with shaking at 37°C for 3 hours. Then, collected clean peptide samples were quantified using Pierce Quantitative Fluorimetric Peptide Assay.

### 5.15.2 Mass Spectrometry analysis

LC-ESI-MS/MS analysis was performed using an Ultimate 3000 nanoUPLC system (Thermo Fisher Scientific) coupled to an Orbitrap Fusion Lumos Tribrid mass spectrometer (Thermo Fisher Scientific). For reversed phase UPLC separation of peptides, 2 µl of solution (corresponding to 1 µg of the peptide mixture) were loaded onto the analytical column (Easy-Spray PepMap RSLC C18, 2 µm, 500 × 0.075 mm, Thermo Fisher Scientific) and separated applying a gradient from 4% to 50% ACN over 90 min. The eluant was ionized using a nanoESI source, operating in positive ion mode. MS<sup>1</sup> spectra were acquired using the Orbitrap analyzer operating in data dependent, ranging from 375 m/z to 1500 m/z, at a resolution of 120,000 (at 200 m/z), with standard automated gain control (AGC), and a maximum injection time of 50 ms. The MS<sup>2</sup> spectra were acquired using the Orbitrap analyzer at a resolution of 50,000 (at 200 m/z). Precursors were selected based on their intensity from all signals with a charge state from 2<sup>+</sup> to 5<sup>+</sup>, isolated in a 2.0 Da window, and fragmented in HCD mode using a dynamic exclusion of 60 s. For each condition, the experiments were performed in quadruplicate. LC-ESI-MS/MS data analysis was performed using Proteome Discoverer (v2.5). Identification was conducted using the Sequest HT search engine and the following parameters: stable modification carbamidomethyl (C), oxidation (M) and acetylation (protein N terminus) as variable modifications, the Uniprot database, trypsin as a specific protease, and a maximum of two missed cleavages. The “match between runs” option enabled transfer of identifications across samples within a time window of 2 min of the aligned retention times. The level of confidence for peptide identifications was estimated using the Percolator algorithm with decoy database searching. Identifications were filtered by FDR validation based on q value, the strict FDR was set to 0.01 and relaxed FDR to 0.05. Label free quantification of identified proteins

was referred to unique peptides, required a minimum ratio count of two and were calculated based on the raw spectral protein intensity. For each condition, raw intensities were logarithmized and then normalized to the calculated average and used for downstream analyses. Student's t test was performed on the normalized protein intensities, and proteins with  $p < 0.05$  and a fold change  $> 1.3$  were considered significantly altered in abundance between the samples.

### **5.16. Statistical analysis**

Results are presented as mean  $\pm$  standard error of the mean (SEM) of at least three different biological replicates. Statistical differences were determined by Student's t-test two-sided and one-way analysis of variance (ANOVA) for multiple comparisons. Data were analyzed using GraphPad Prism software (version 7.0) and statistical significance was defined as  $p < 0.05$ .



## 6. RESULTS

### 6.1 Gubernacular Tissue Processing

Gubernaculum testis biopsies obtained from patients were generally about 10–20 mm<sup>3</sup> in volume. Gubernacula of patients were processed as fresh or thawed tissue; the latter was previously stored at –80°C for one week and then stored in liquid nitrogen. As reported in **Figure 8**, the gubernacular tissue was disaggregated by using an enzymatic mix composed of 1X collagenase-I and hyaluronidase and was incubated at 37 °C until the tissue appeared as a homogenous solution. Then, the cells obtained from the processed tissue were counted; cell number was estimated to be at least more than 300,000 for each patient. Then, the complete cell suspensions were grown in a T25 primary cell culture flask.

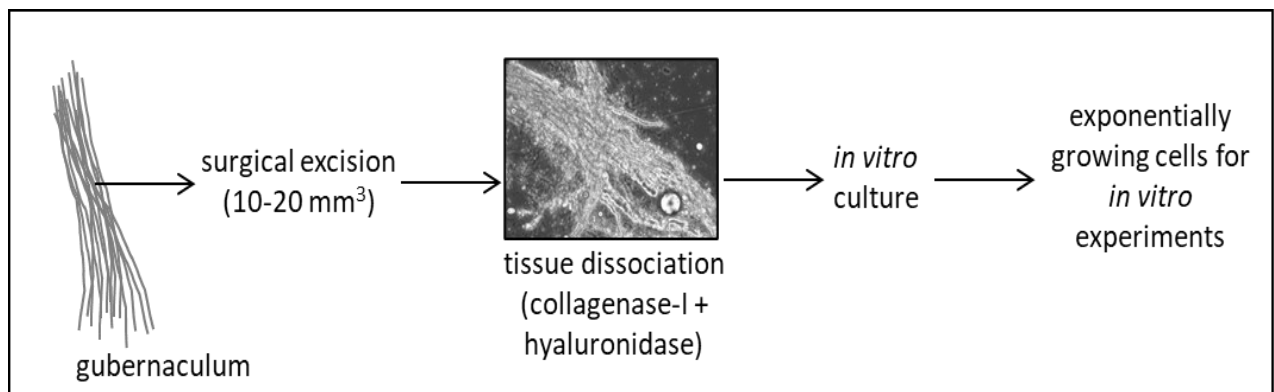


**Figure 8**

Gubernacular tissue in vitro culture. (A) Schematic representation of the protocol that we optimized to isolate and in vitro cultivate gubernacular cells. Scale bar: 100 μm

## Cryptorchidism

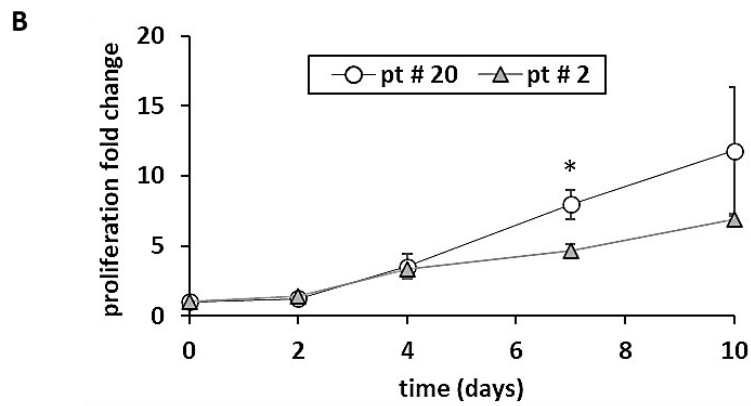
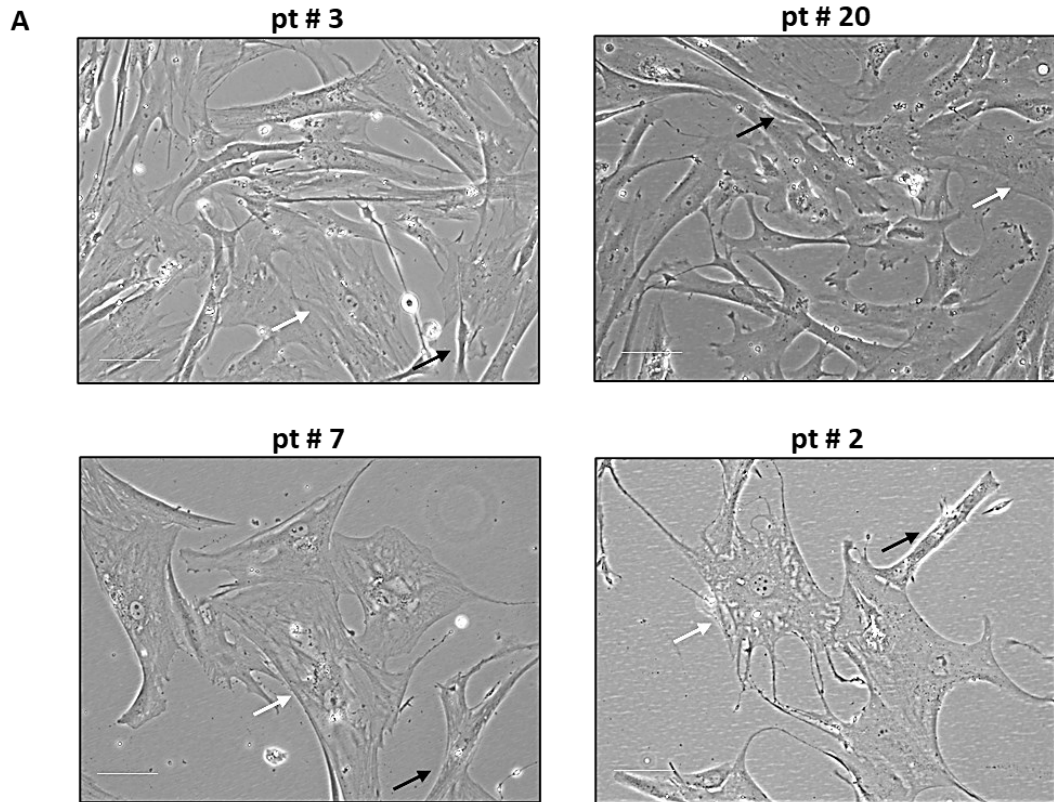
### 6.2 *In vitro* culture of gubernacular cells derived from cryptorchid patients

In this study, we aimed at the generation of an *in vitro* model to predict the response of cryptorchid patients to hCG therapy by exploiting the culture of gubernaculum testis. Firstly, we collected gubernacular biopsies from 4 cryptorchid patients (pt #3, #20, #7, and #2) that exhibited the inclusion criteria (**Table 4**). It is noteworthy that this patient set covers a wide range of ages, from 1 to 8 years old. In addition to case study patients, we also analyzed 3 control cases: gubernacular biopsies from 2 patients affected by testicular torsion (pt #55 and #15) and a testicular biopsy from one adult azoospermic patient (pt #40) (**Table 4**).

**Table 4.** Clinical details of the patients.

Patient number	Age (years)	Pathology	Tissue biopsy	Patient type
pt # 3	1	Cryptorchidism – intra-abdominal testicle	gubernaculum	Case study
pt # 20	2	Cryptorchidism – inguinal testicle	gubernaculum	Case study
pt # 7	5	Retractile testicle	gubernaculum	Case study
pt # 2	8	Cryptorchidism – inguinal testicle	gubernaculum	Case study
pt # 55	13	Testicular torsion	gubernaculum	control
pt # 15	14	Morgagni hydatid torsion and epididymitis	gubernaculum	control
pt # 40	30	Azoospermia	testis	control

After tissue dissociation, cells from all the patients were able to grow *in vitro* and the different cell types composing gubernaculum can be identified from a morphological point of view (**Figure 9A**). Indeed, white arrows indicate cells with the typical morphology of myofibroblasts or smooth muscle cells, whereas black arrows indicate fibroblasts (**Fig. 9A**). Despite all the 4 gubernacular samples were maintained in culture for at least three months, cells derived from two patients showed a significantly different proliferation capacity. Indeed, at 7 days of culture gubernacular cells from patient 20 (pt #20), who is 2 years old, Furthermore, the doubling time for pt #20 is of about 2 days, whereas 3 days is for cells derived from pt #2, with a statistical difference between the two patients are more proliferative in comparison to those from patient 2 (pt #2), who is 8 years old (**Figure 9B**).



Patient	Doubling time (days)	Significance
pt # 2	$2.99 \pm 0.53$	* $p < 0.05$
pt # 20	$1.94 \pm 0.26$	

**Figure 9: Gubernacular cells derived from cryptorchid patients grow in vitro.**

A) Representative bright field images of gubernacular cells of patients #3, #2, #7, and #20. White arrows indicate cells with the typical morphology of muscle cells, black arrows indicate fibroblastic cells. Scale bar: 10 mm. B) Proliferation rate of gubernacular cells derived from patient #2 and #20, as representative cases of infant and child patients. Values are reported as fold change relative to the beginning of the experiment (T0) and are the means ( $\pm$  SEM) of four independent biological replicates. Statistical legend:  $p < 0.5$  (\*) for pt #2 versus pt #20. Based on these curves, we also report the values of doubling time (days) of both patients.

Finally, as for case study patients, also cells derived from controls were able to grow and proliferate *in vitro* (Figure 9C).

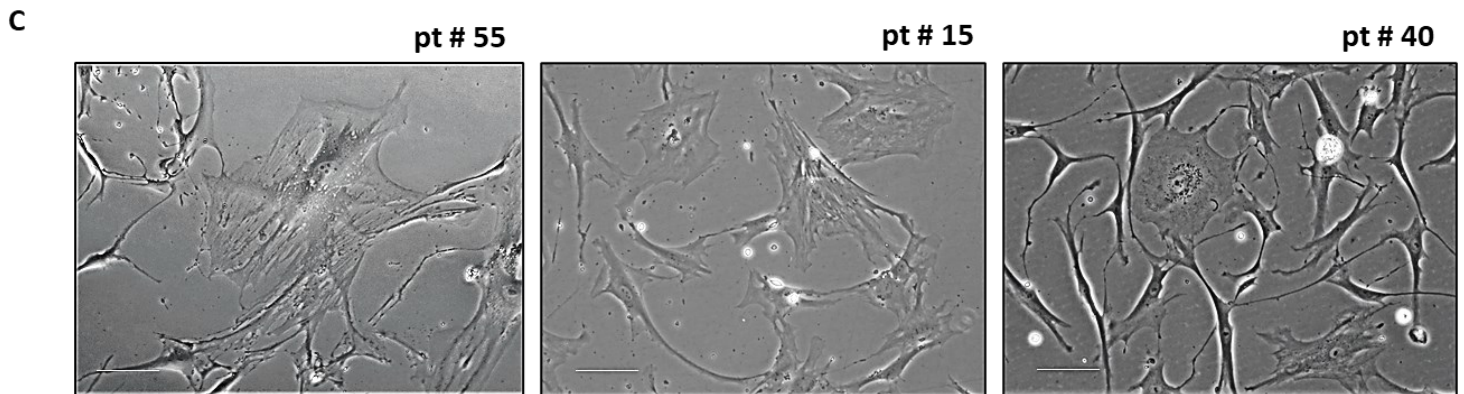


**Figure 9C**

Representative bright field images of gubernacular cells of control patients #55, #15, and #40. Scale bar: 10 mm.

### 6.3 Gubernacular cells express receptors for gonadotropins and androgens

In order to analyze the effect of hCG on gubernacular cells cultured *in vitro*, we firstly verified the expression of the full-length form of luteinizing hormone/choriogonadotropin receptor (LHCGR) at mRNA and protein levels in case study patients. Our data show that all the patients, also including a control patient chosen for a different pathology (pt #15), express high mRNA levels of LHCGR full-length (Figure 10A). In addition, all cryptorchid patient derived tissues express LHCGR at protein level, as observable in the immunofluorescent images in which the green spots correspond to the receptor (Figure 10B). In addition to LHCGR, we also checked the mRNA expression of another gonadotropin receptor, i.e. follicle stimulating hormone receptor (FSHR), and of AR, which has been described to have a role in gubernaculum regression during the fetal period, regulating the testicular descent<sup>132</sup>. Our data show that FSHR is almost equally expressed by all the patients, whereas AR is significantly overexpressed in patient #3 and #2 in comparison to patients #20, #7, and control (pt #15) (Figure 2 A). Our results confirm that LHCGR is not only expressed by testicular Leydig cells, as widely reported in the literature<sup>133</sup>, leading us to exploit the *in vitro* analysis of hCG effects on these cells.

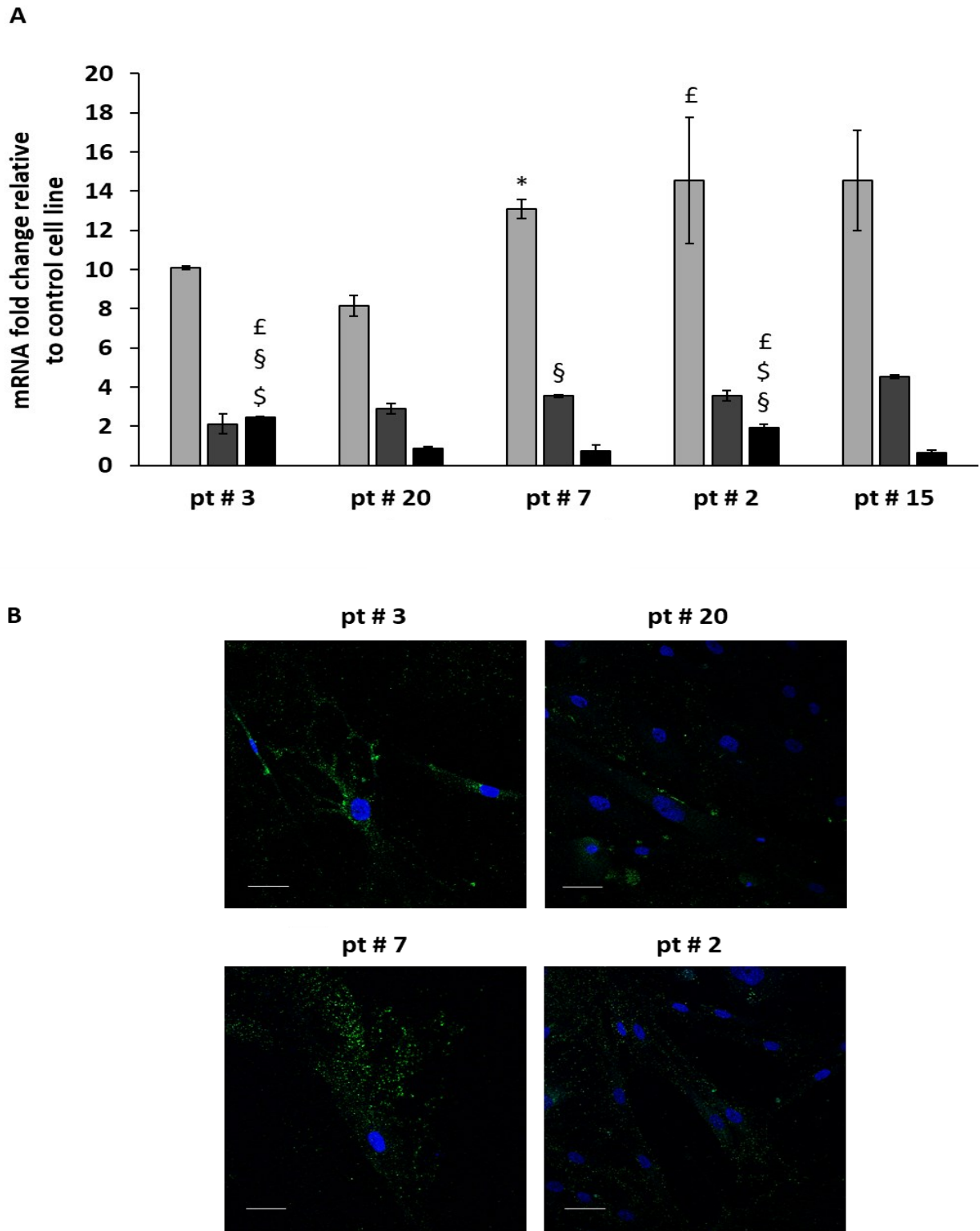


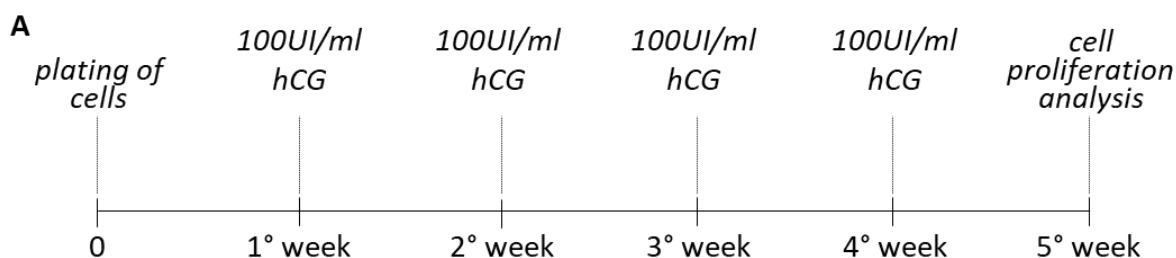
**Figure 10: Analysis of gonadotropin and androgen receptor expression in gubernacular cells cultured *in vitro*.**

A) LHCGR (light grey histograms), FSHR (dark grey histograms), and AR (black histograms) mRNA expression levels in four cryptorchid patients (#3, #20, #7, and #2) and one control patient (#15). The mRNA levels of the receptors have been normalized on the housekeeping gene succinate dehydrogenase (SDHA) expression and reported as fold change relative to the levels of expression in the breast cancer cell line MCF7 used as reference. Values are the means ( $\pm$  SEM) of four independent biological replicates. Statistical legend: (\*)  $p < 0.05$  versus pt #3; (§)  $p < 0.05$  versus pt #20; (£)  $p < 0.05$  versus pt #7, and (§)  $p < 0.05$  versus pt #15. B) Representative immunofluorescent images of LHCGR expression (green) in gubernacular cells derived from patients #3, #20, #7, and #2. Nuclei are marked with DAPI in blue. Sale bar: 50 mM

## 6.4 hCG stimulates cell proliferation and formation of tubular structures

To study the *in vitro* effect of hCG treatment on cell proliferation and vascularization induction, we seeded each patient derived cells in absence of fetal bovine serum (FBS), as we previously described <sup>128</sup>, in order to avoid interferences due to the presence of gonadotropins in this medium supplement. Subsequently, we treated cells with 100 IU/ml of hCG once a week for 4 weeks and evaluated the effect of the treatments at the end of the fifth week (**Figure 11A**). We chose this treatment scheme in order to mimic as much as possible the clinical posology.

Concerning the effect of hCG on cell proliferation, which is comparable to the enhancement of testicular volume evaluated in clinic <sup>134</sup>, our data show that gubernacular cells derived from cryptorchid patients significantly respond to the hormonal stimulation in comparison to untreated cells derived from the same patient (represented as dashed line in **Figure 11B**). Interestingly, after hCG treatment, cryptorchid patients show a significant increase of cell proliferation in correlation with the age: indeed, the oldest case study patient (pt #2) has the lowest proliferative induction (140%) in comparison to the two youngest case study patients pt #20 and #3 (215% and 234%, respectively) (**Fig. 11B**). In line with this evidence, cells derived from the oldest control patient (pt #40) don't respond to hCG, having a slightly non-significant increase of proliferation in comparison to the relative untreated cells. The two other controls (pt #15 and #55) present an increase of proliferation after hCG treatment of 125% and 132%, respectively. These data suggest that younger patients could respond better to hCG proliferative stimulation.



**B**

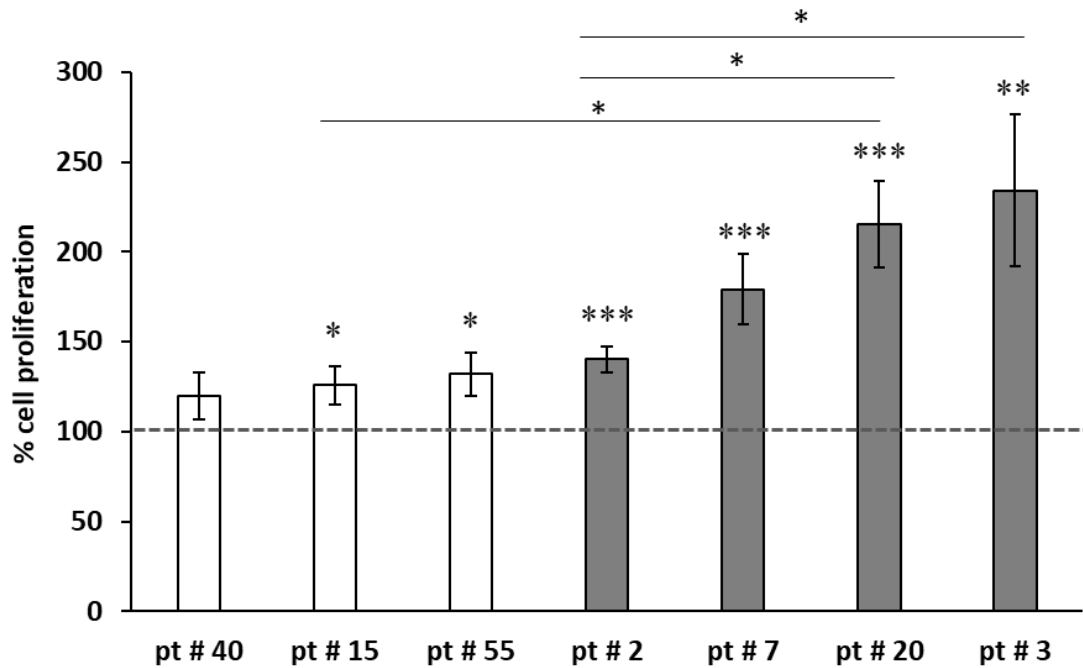


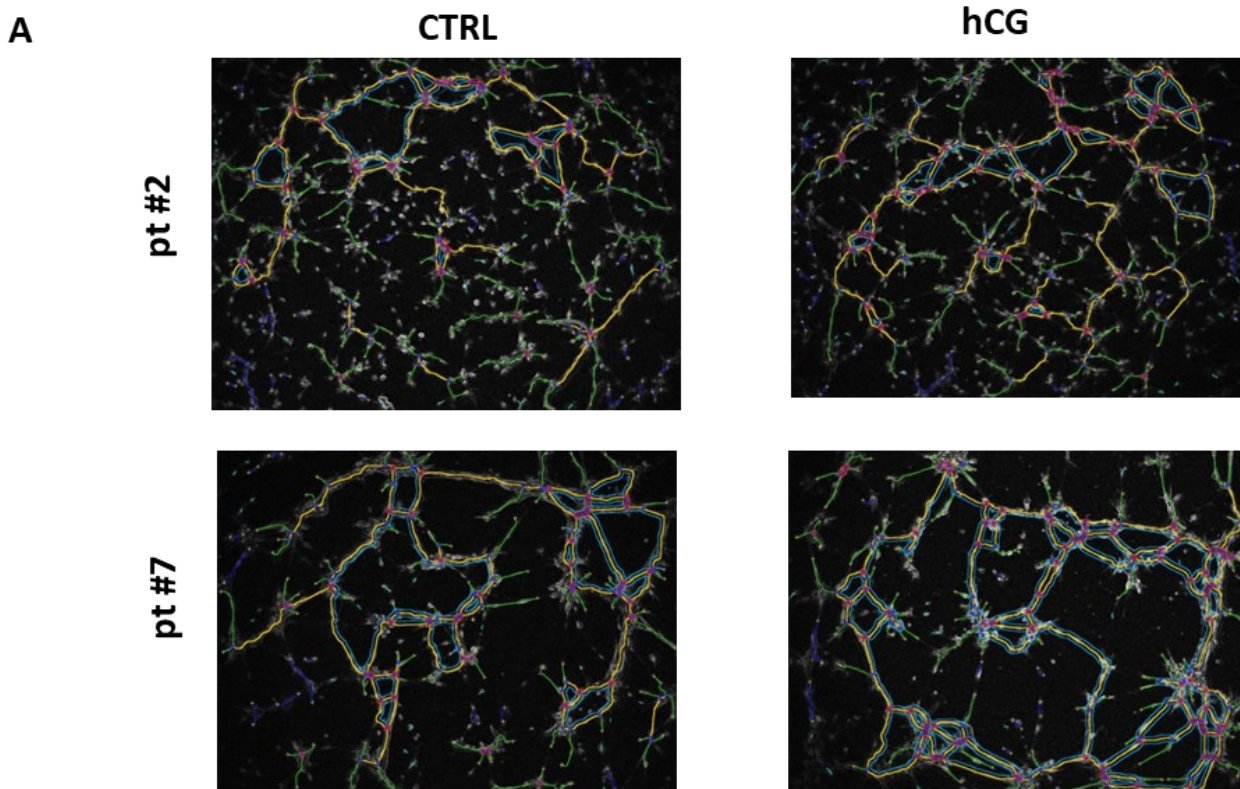
**Figure 11: Effect of hCG on gubernacular cell proliferation.**

A) Schematic representation of the treatment protocol adopted to analyze the effect of hCG on cell proliferation. B) Cell proliferation of gubernacular cells cultured at 37°C with 5% CO<sub>2</sub> in the FBS-deprived medium treated with 100 IU/ml hCG once a week for 4 weeks. White histograms represent control patients (#40, #15, #55), whereas grey histograms represent cryptorchid patients (#2, #7, #20, #3). The percentage of cell proliferation has been evaluated by analyzing the data of hCG treated cells (corresponding to the histograms) with those of untreated cells (dashed line), whose proliferation correspond to 100%, for the same patient. Cell proliferation was measured by Crystal Violet assay and absorbance was measured by spectrophotometric analysis (A<sub>595nm</sub>). Values are the means (± SEM) of four independent biological replicates. Statistical legend: p<0.05 (\*), p<0.01 (\*\*), and p<0.001 (\*\*\*) for treated cells versus untreated cells of the same patient, or for the comparison among different patients.

The other aspect that we evaluated in our *in vitro* model was the stimulation of tubular structures formation after hCG stimuli, a phenomenon comparable to the increased vascularization clinically demonstrated in patients treated with hCG<sup>134</sup>. Representative images of cells untreated and treated with hCG elaborated with a dedicated software (as described in methods section) are reported in **Figure 12A**. Through this analysis, we compared the effect of hCG on all cryptorchid patients at five time points (T1, T2, T3, T4, and T5). As shown in **Figure 12B**, we evaluated different parameters, such as the number of junctions, segments, meshes, the mean branch/segments length,

and the mean meshes size, which describe the generation and maintenance over the time of the tubular structures (see method section for details).

HCG treated cells derived from the youngest cryptorchid patient (pt #3) present a constant maintenance during the time of the number of junctions, segments, and meshes, suggesting a strong capability to generate and conserve vessel-like structures. Oppositely, the cells derived from the oldest cryptorchid patient (pt #2) show fewer segments and meshes over the time, supporting a low vasculogenic propensity of these cells after hCG treatment, particularly in comparison to the two youngest patients (pt #3 and pt# 20). Accordingly, the mean of branch length (MBL) is significant lower in patient #2 in comparison with all the other patients. Finally, it is noteworthy that the mean meshes size (MMS) is higher in patient #2, indicating that these cells generate less and longer tubular structures.





B

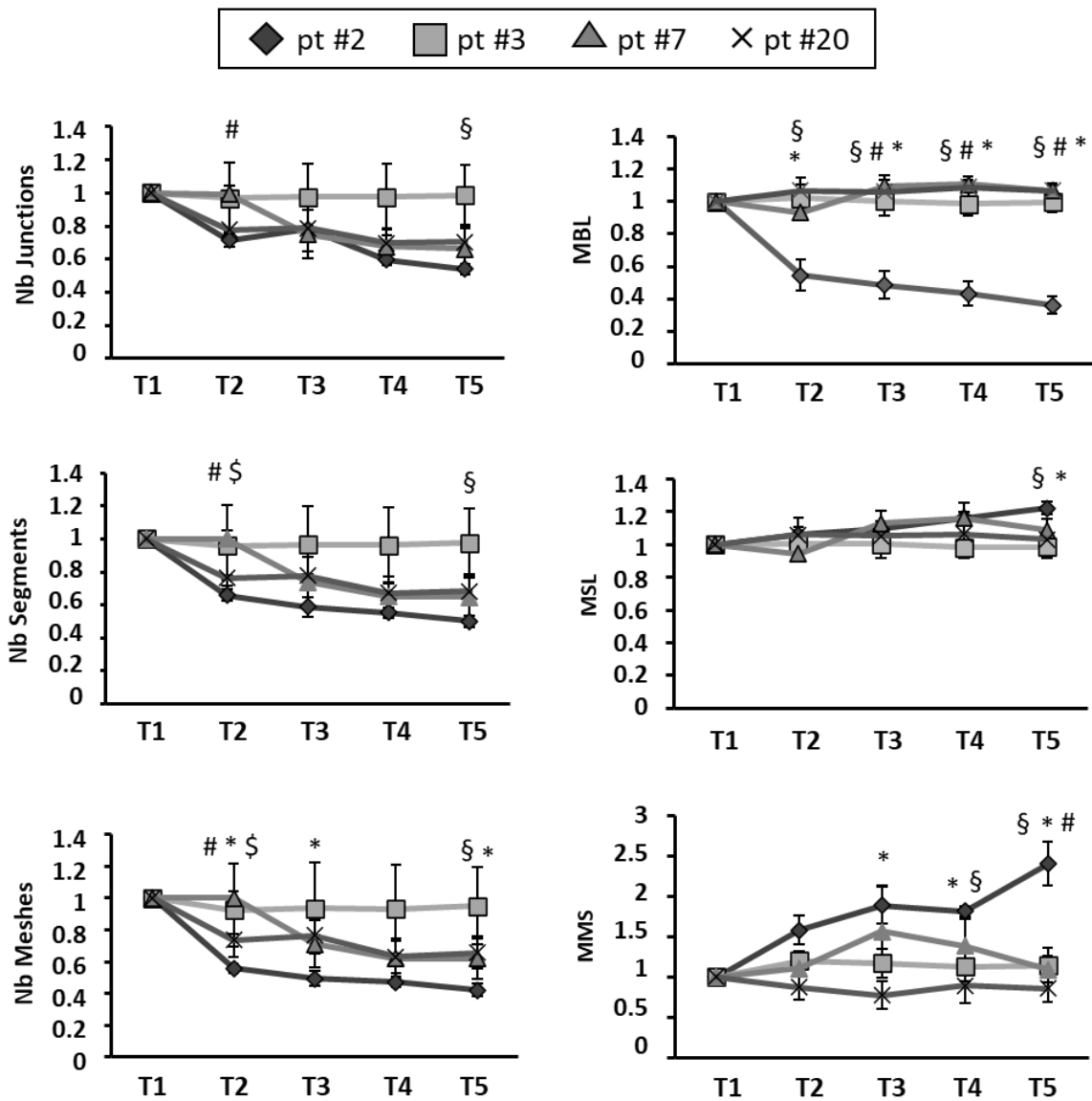


**Figure 12: Effect of hCG on tubular structure formation of gubernacular cells.**

A) Representative images of tubular structures and relative analysis with Angiogenesis Analyzer tool of ImageJ software<sup>19</sup>. B) Analysis of the number of junctions, segments, meshes, the mean branch/segments length, and the mean meshes size relative to hCG-treated gubernacular cells derived from cryptorchid patients (#2, #7, #20, #3) at five different time points: after 3 (T1), 6 (T2), 9 (T3), 12 (T4), and 15 (T5) hours from the seeding. Statistical legend: (§)  $p < 0.05$  pt #2 vs pt #3; (#)  $p < 0.05$  pt #2 vs pt #7; (\*)  $p < 0.05$  pt #2 vs pt #20; (§)  $p < 0.05$  pt #7 vs pt #20.

## 6.5 Gubernacular cells express two different LHCGR variants

LHCGR is a highly conserved gene among species, however in humans and primates its genomic organization has an additional exon, *i.e.* exon 6A, that could be included through alternative splicing<sup>135</sup>. The exclusion or inclusion of exon 6A determines two different protein variants of the receptor that are generally expressed at the same levels: the full length, which has a complete structure and is fully functional, and the short length, which contains exon 6A and, structurally, it lacks the transmembrane and intracellular domains<sup>136</sup>. The functional role of the short variant is still under investigation, however some preliminary studies show that it is soluble and capable to bind the ligands (*i.e.* hCG and luteinizing hormone- LH) presumably by sequestering them in the microenvironment and, thus, limiting its interaction and activation of the full length LHCGR<sup>137</sup>. To better understand whether the different effect of hCG on patient #2 and #20 could be not only linked to the different age of the patients but also to the presence of the short LHCGR variant, we analyze its expression through real-time PCR. Our results show that patient #2 expresses significant more LHCGR short variant in comparison to patient #20, whereas on the other side the levels of LHCGR full-length are similar between the two patients (**Figure 13 and Figure 10A**). This data require more strengthens by the literature, however open the way to the future consideration of LHCGR short variant expression levels to predict the response to the hormonal therapy.

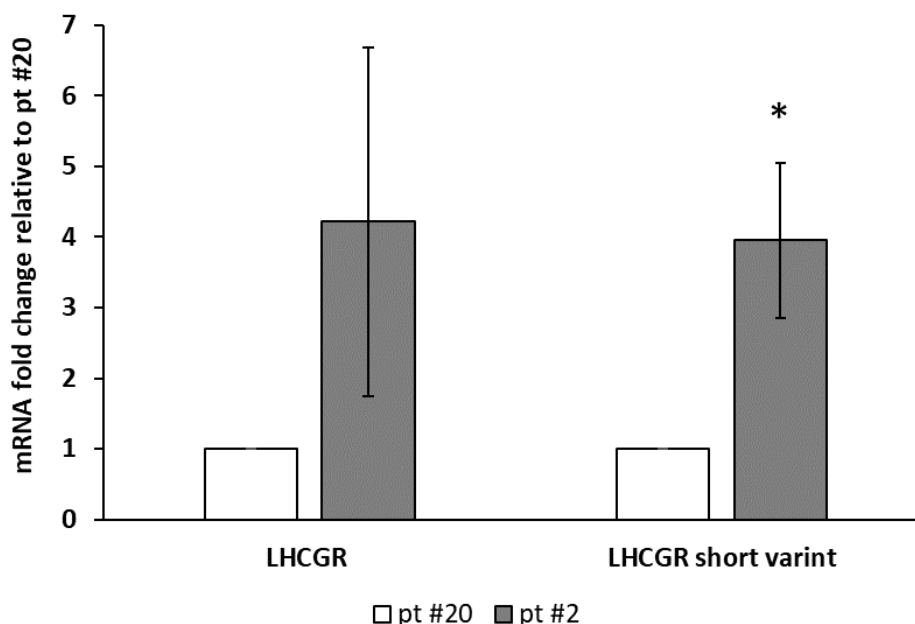
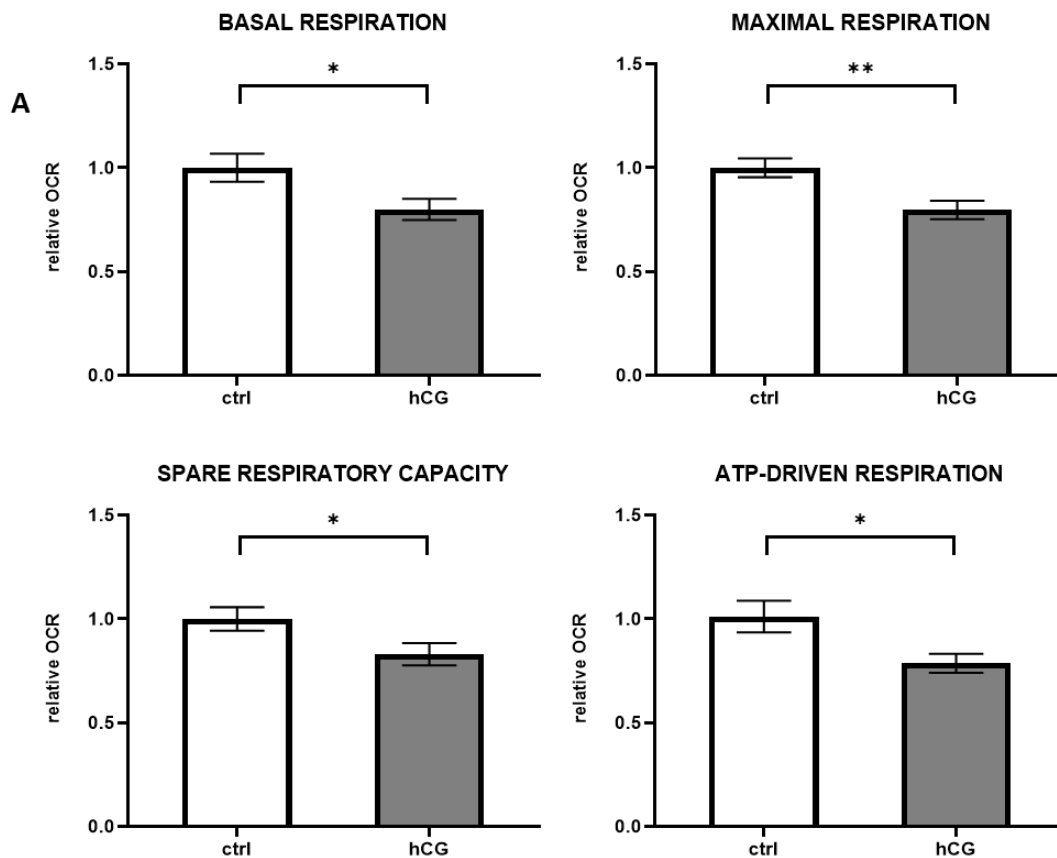


**Figure 13: Analysis of the expression of LHCGR variants in gubernacular cells cultured *in vitro*.**

LHCGR full length variant (on the left) and LHCGR short length variant (on the right) in two cryptorchid patients (pt #20 in white and pt #2 in grey). The mRNA levels of the receptors have been normalized on the housekeeping gene (SDHA) expression and reported as fold change relative to the levels in pt #20. Values are the means ( $\pm$  SEM) of four independent biological replicates. Statistical legend: (\*)  $p < 0.05$ .

## 6.6 hCG decreases the oxygen consumption rate of gubernacular cells

The induction of cell proliferation by hCG led us to investigate whether this hormone could alter the energetic metabolism of cells. For this aim, we performed the analysis of oxygen consumption rate (OCR - **Figure 14A**) and extracellular acidification rate (ECAR - **Figure 14B**) through Seahorse Technology of gubernacular cells derived from patient #20 untreated (control) and treated with hCG once a week for 4 weeks. We chose this patient since his cells well respond to hCG stimulation *in vitro* and, from a technical point of view, the relative cell proliferation rate is compliant. Concerning OCR results, our data show that the basal and maximal respirations are significantly decreased after hCG effect, together with low levels of the spare respiratory capacity and the ATP-driven respiration (**Figure 14A**). These data suggest that, after hCG treatment, gubernacular cell proliferation is connected with a decreased respiratory rate of the cells. Surprisingly, the decreased oxidative metabolism is not associated with a concomitant increase of glycolysis (ECAR) after hCG exposition, as reported by our data in **Figure 14B**. In order to exclude that the effect of hCG on the metabolism could be due to an adaptation of cells to the long exposure (i.e. 4 weeks), we also analyzed OCR and ECAR after 1 week of hCG treatment and a similar -not significant- trend of modulation has been detected (data not shown).



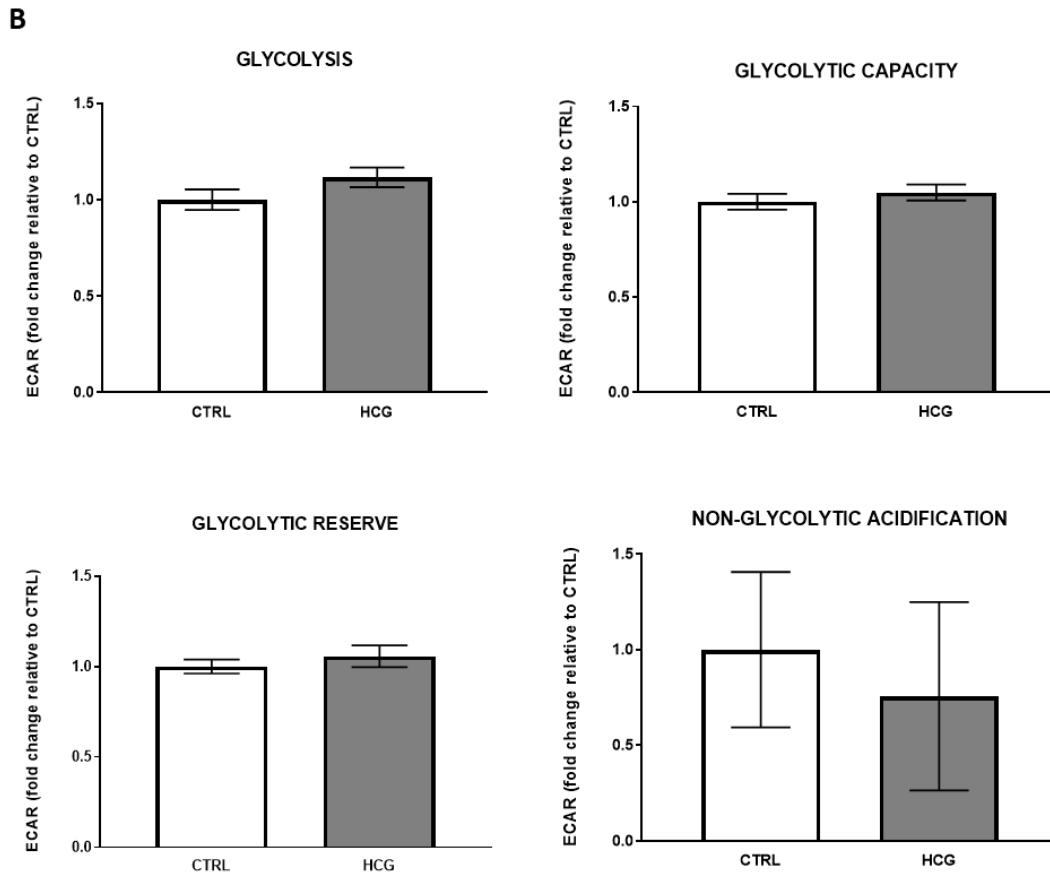


**Figure 14: hCG treatment impairs oxygen consumption parameters and no effect on glycolytic metabolism.**

A) Seahorse analysis of Oxygen Consumption Rate (OCR) of gubernacular cells derived from pt #20 untreated (control) and treated with hCG; extrapolated data include basal, maximal respiration, spare respiratory capacity and ATP-driven respiration B) Seahorse analysis of Extracellular Acidification Rate (ECAR) of gubernacular cells derived from pt #20 untreated (control) and treated with hCG.

Histograms legend: white: untreated (CTRL) cells; grey: hCG-treated (HCG) cells.

Moreover, we also analyzed the activity of the pyruvate kinase enzyme (PK) (**Figure 15A**), a key protein involved in the last step of glycolysis, and the level of lactate secreted in the cell medium (**Figure 15B**), connected with enhanced glycolysis. Our data demonstrate that hCG treatment (once a week for 4 weeks) does not significantly alter PK activity and lactate levels in comparison with control cells, supporting the evidence that the hormone does not target glycolysis *in vitro*.

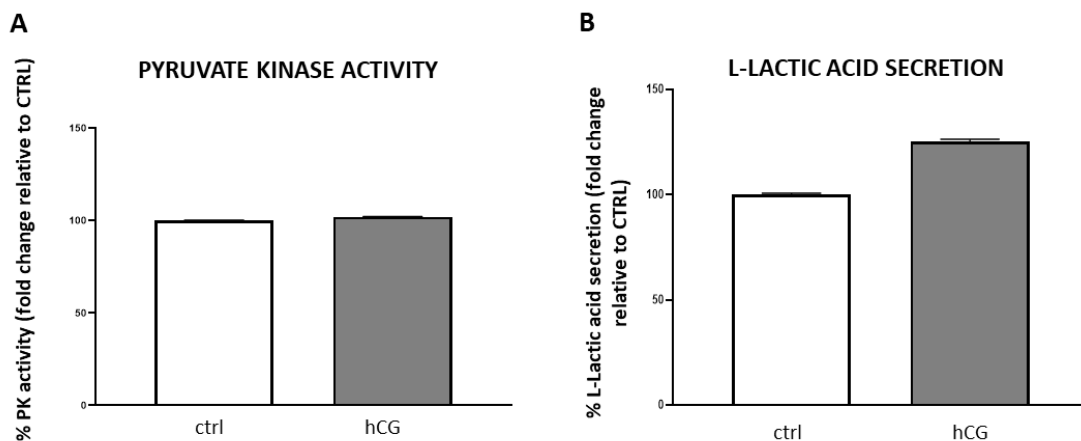


**Figure 15: hCG does not affect PK activity and Lactate secretion**

A) Analysis of pyruvate kinase activity and B) L-Lactic acid secretion by gubernacular cells derived from pt #20 untreated (control) and treated with hCG. Histograms legend: white: untreated (CTRL) cells; grey: hCG-treated (HCG) cells.

To further deepen the metabolic alterations by hCG, we also investigated the expression levels of enzymes that control the energetic metabolism through an untargeted proteomic approach with Orbitrap mass spectrometer on gubernacular cells derived from patient #20 untreated (control) and treated with hCG. From the output, we identified 2 proteins that are implicated in the regulation of energetic metabolism and that resulted significantly modulated by hCG treatment (**Table 5**). Specifically, the high-mobility group protein B2 protein (*HMGB2*), whose expression is increased of about 2-fold after hCG treatment, has been reported to deliver cells towards a more glycolytic metabolism respect to a more oxidative one by increasing glucose uptake and by activating lactate dehydrogenase (*LDHB*) transcription and lactate production<sup>138</sup>. Conversely, it has been identified as down-regulated in hCG-treated cells the branched-chain-amino acid aminotransferase (*BCAT1*), which has been shown to promote mitochondrial biogenesis and to repress mitochondrial ROS in breast cancer cells<sup>139</sup>. *BCAT1* is connected both directly or indirectly with the functionality and biogenesis of mitochondria, thus its low levels further corroborate the diminished respiratory capacity of the cells, in line with the high expression levels of *HMGB2*, a protein that supports glycolysis instead of oxidative metabolism.

**Table 5:** List and abundance ratio (hCG-treated cells *versus* control cells) of up- and down-regulated proteins involved in the regulation of energetic and antioxidant metabolism ( $p < 0.05$ ). Up arrows and down arrows indicate up- and down-regulation, respectively.

Protein	Gene symbol	Abundance ratio (hCG / control)	Reference
<b>Proteins involved in energetic metabolism regulation</b>			
High mobility group protein B2	HMGB2	↑ 2.18	140
Branched-chain-amino-acid aminotransferase, cytosolic	BCAT1	↓ 0.69	141
<b>Proteins involved in antioxidant response</b>			
Exonuclease 3'-5' domain-containing protein 2	EXD2	↓ 0.47	142
Glutamate-cysteine ligase regulatory subunit	GCLM	↓ 0.54	143
Cytoplasmic aconitate hydratase	ACO1	↓ 0.56	144,145
Thioredoxin	TXN	↓ 0.65	146
Thioredoxin domain-containing protein 17	TXNDC17		
Bis(5'-nucleosyl)-tetraphosphatase	NUDT2	↓ 0.68	147
Metalloreductase STEAP3	STEAP3	↓ 0.69	148

## 6.7 hCG exhibits an anti-oxidative function

To further confirm that hCG affects oxidative phosphorylation, we also analyzed the levels of reactive oxygen species (ROS) through a fluorescent assay. Indeed, it is known that mitochondria generate approximately 90% of cellular ROS and that this production is strictly connected with alterations of electron transport complex activity<sup>149</sup>. Based on this concept, we show that hCG significantly decreases ROS levels in comparison to control cells and maintains this antioxidant effect even after 7 days from the hormone exposition (**Figure 16**).

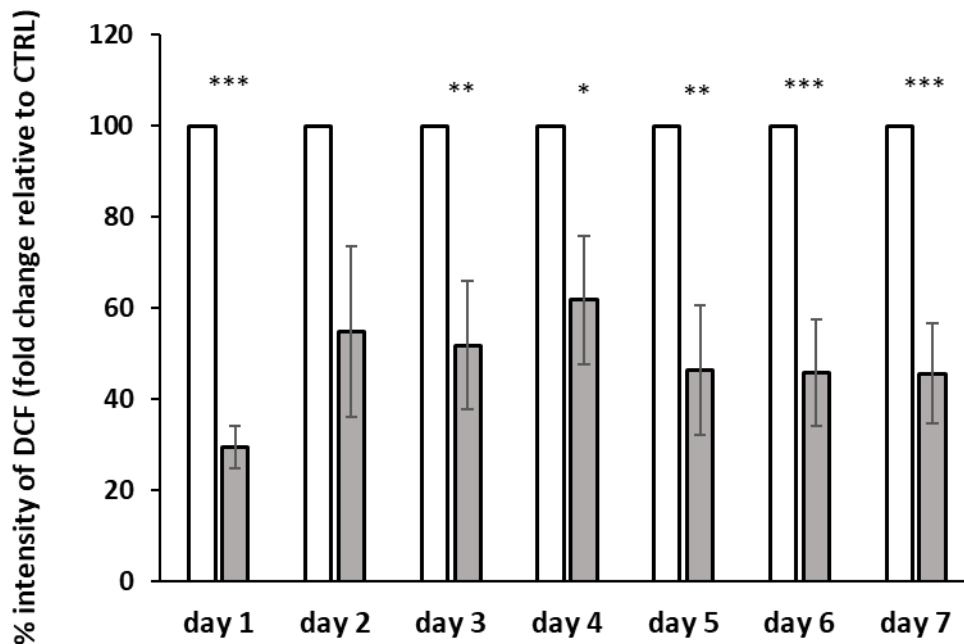


**Figure 16: hCG treatment decreases ROS levels**

Analysis of intracellular ROS production on gubernacular cells derived from pt #20 untreated (white histogram) and treated with hCG (grey histogram). ROS levels were analyzed every day up to 7 days after hCG treatment. Values are presented as mean  $\pm$  SEM. Statistical legend:  $p < 0.05$  (\*),  $p < 0.01$  (\*\*), and  $p < 0.001$  (\*\*\*) for hCG-treated cells versus untreated cells.

To further confirm the antioxidant properties of hCG, we identified 7 proteins by mass spectrometry (**Table 5**) that regulate oxidative stress and that resulted significantly downregulated in hCG treated cells: 1) exonuclease 3'-5' domain-containing protein 2 (*EXD2*), the reduced levels of which increases ROS production<sup>150</sup>; 2) glutamate-cysteine ligase regulatory subunit (*GCLM*), which is the rate limiting enzyme of glutathione synthesis and is involved in the antioxidant response<sup>151</sup>; 3) cytoplasmic aconitate hydratase (*ACO1*), which is strictly connected with the iron-regulatory protein IRP1<sup>152</sup>, a protein that coordinates the cellular iron metabolism and that also functions as a ROS sensor<sup>153</sup>; 4) thioredoxin (*TXN*) and 5) thioredoxin domain-containing protein 17 (*TXNDC17*), which are known protectors against reactive oxygen stress<sup>154</sup>; 6) bis(5'-nucleosyl)-tetrphosphatase (*NUDT2*), which emerged as a protein involved in the anti-oxidant response by the Atlas genetic oncology research tool<sup>155</sup>; and 7) metalloredutase STEAP3 (*STEAP3*), whose knockdown has been shown to significantly increase ROS levels in renal cell carcinoma<sup>156</sup>. The massive down-regulation of the expression of proteins involved in the antioxidant response after hCG exposition supports that this hormone decreases total intracellular ROS levels and, consequently, cells decrease their antioxidant armory. In conclusion, we can assume that hCG targets oxidative phosphorylation, but not glycolysis, and that the conceivable slackening of electron transport chain could cause a decrease in ROS levels.

## Testicular torsion

### 6.8 *In vitro* culture of gubernacular cells derived from patients with testicular torsion

Gubernacular cells obtained after enzymatic digestion of tissue (**Figure 8**) were plated in a T25 primary cell culture flask. Interestingly, the lag period during which cells adapted to the *in vitro* condition was variable among patients. We considered the healthy state of the cells, based on cellular morphology, and the gain of about 80–90% of confluence as signs of exponentially growing cells. As reported in **Table 6**, it is evident that the temporal window within which cells started to exponentially grow was different among patients. Indeed, patient #4 derived gubernacular cells that quickly attached to the flask, that presented a healthy cellular state, and that started to exponentially grow 7 days after tissue processing (**Table 6**). Conversely, patient #15 derived gubernacular cells that were struggling to attach to the flask and only after 15 days presented a healthy cellular status and started to exponentially grow 30 days after tissue processing (**Table 6**). Finally, for patient #12, cells were never able to attach to the flask and grow (not applicable: N/A; **Table 6**). For patients #4 and #15, exponentially growing cells were harvested to perform experiments or were divided into two other flasks to amplify the cells. In both patients, cells were monitored during the culture period, which was about 120 days; after this period, cells entered a senescent status and slowed down their proliferation.

**Table 6:** Clinical and biological evaluations of the analyzed patients and patient derived cells.

Patient	Age	Clinical Evaluation	Biological Evaluation (Days Necessary for Cells to Exponentially Grow)
#4	12 yrs	Testicle torsion—preservation of testicle after derotation	7 days
#12	14 yrs	Testicle torsion—removal of testicle due to necrosis	N/A
#15	14 yrs	Morgagni hydatid torsion and epididymitis	30 days



As represented in **Figure 17**, the cellular morphology of gubernacular cells is composed of a mix of cell types, with some cells showing a fibroblast shape (white arrows) and other cells presenting a bigger size with some striae, typical of smooth and striated muscle cells containing actin (black arrows).

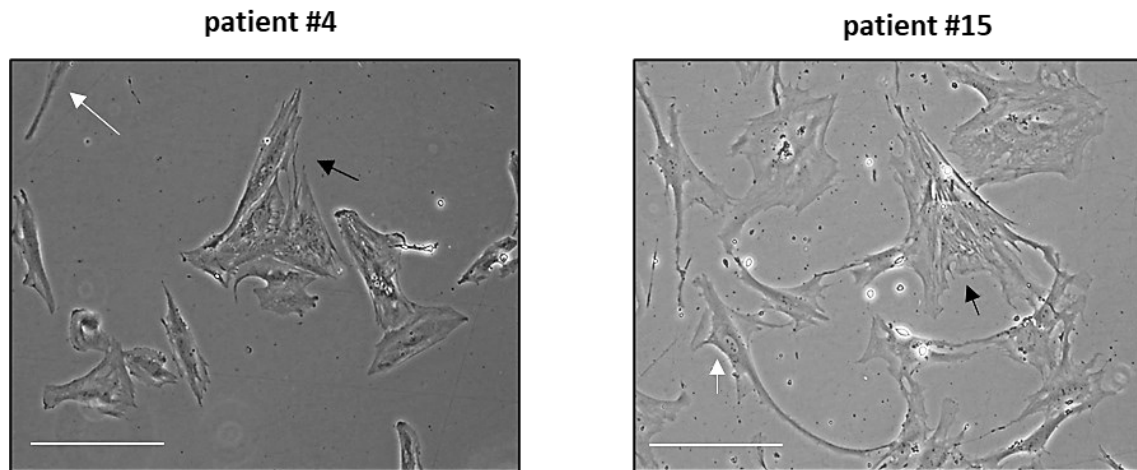


**Figure 17**

Representative, bright field images of gubernacular cells of patients #4 and #15. White arrows indicate cells with fibroblast features and black arrows indicate cells with smooth muscle features. Scale bar: 25  $\mu\text{m}$

## 6.9 Gubernacular Cells Express AR and LHCGR

The expression and role of the androgen receptor (AR) in gubernaculum testis have been deeply investigated during testicular descent alongside the demonstration that AR signaling in gubernacular cells is required for its eversion and outgrowth<sup>157</sup>. However, to our knowledge, there is no evidence about the expression of AR in the gubernaculum of patients affected by testicular torsion at pubertal age or either about the expression of another important receptor that has a key role in testicular function, i.e., the luteinizing hormone receptor (LHCGR). Thus, we quantitatively analyzed the mRNA levels of *AR* and *LHCGR* in gubernacular cells derived from the control patient (i.e., the patient affected by cryptorchidism, in confirmation of data of Figure 10A) and patients #4 and #15. We used a breast cancer cell line (MCF7) for the positive control cells and a pancreatic cancer cell line (PaCa44) for the negative control cells, whose values were undetectable, as previously described<sup>158</sup>. The data reported in **Figure 18A** show that *AR* expression was differentially expressed among the two patients. Indeed, patient #4 had a significantly higher *AR* mRNA expression relative to the control cells and to patient #15, whereas the latter showed an opposite trend. The control patient showed an *AR* mRNA expression similar to that of the control cell line. In regard to

LHCGR, patients #4 and #15 and the control patient showed a similar level of LHCGR mRNA induction in comparison to the control cells, bearing a significantly higher expression (**Figure 18B**).

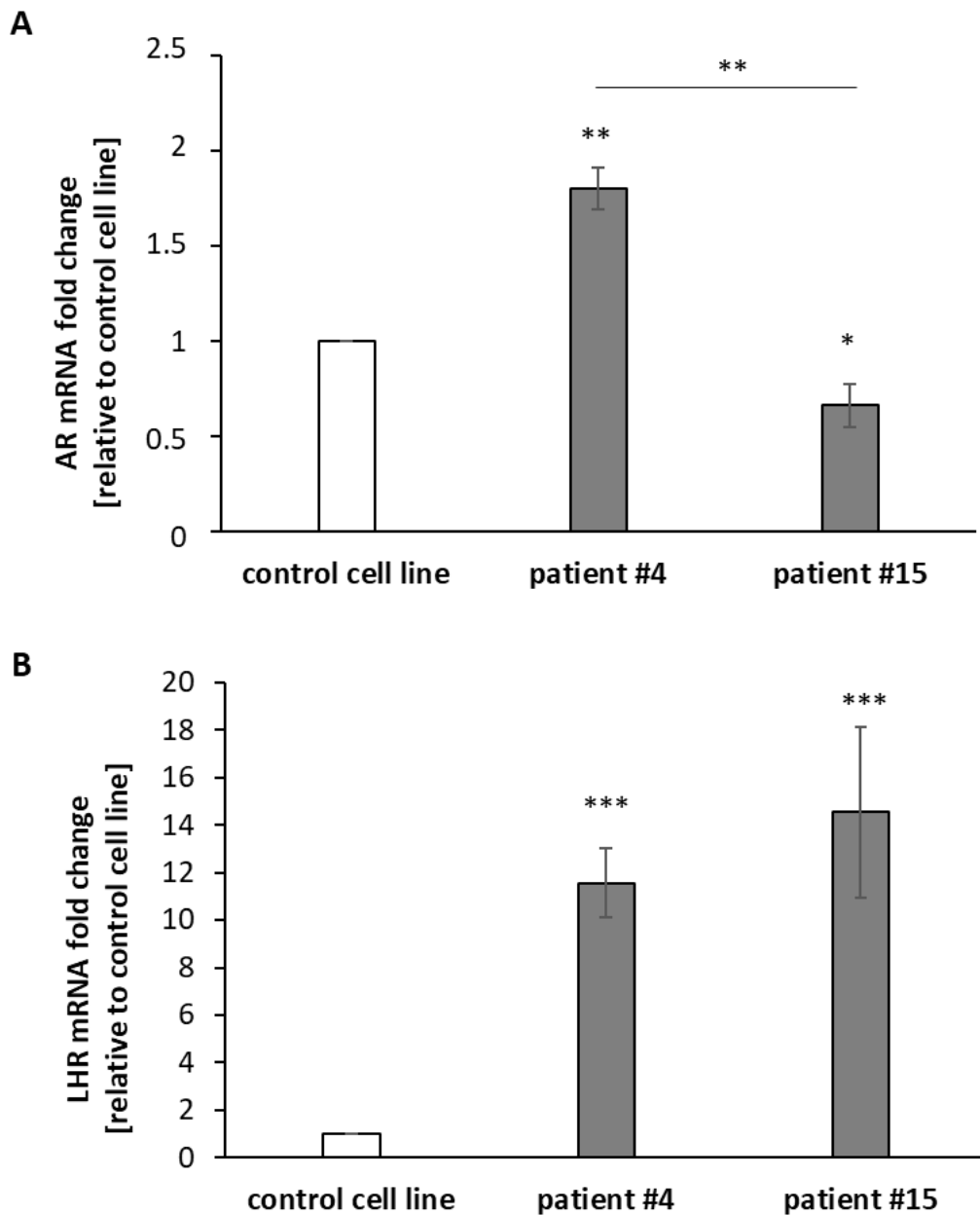


**Figure 18: mRNA expression levels of LHCGR and AR in gubernacular cells**

mRNA expression levels in gubernacular cells cultured *in vitro* of A) AR and B) LHR normalized on the housekeeping gene (RpLp0) expression and reported as fold change relative to the breast cancer cell line MCF7. PaCa44 cell line, used as negative control, has not been reported in the analysis since the expression of the two receptor was absent (undetermined). Values are the means ( $\pm$ SD) of two independent biological replicates. Statistical legend:  $p < 0.05$  (\*) and  $p < 0.01$  (\*\*) for gubernacular cells versus control cells (MCF7) or for patient #4 versus patient #15.

## 6.10 Gubernacular cell proliferation is stimulated by hCG treatment

As our data revealed that the gubernaculum also expresses LHCGR (**Figure 18B**), which is the receptor of LH and hCG, we tested the *in vitro* response of the gubernacular cells of patients #4 and #15 to hCG treatment by analyzing cell proliferation. As schematically represented in **Figure 11A**, we followed the same plan for treating the cells *in vitro* with 100 UI/mL hCG once a week for 4 weeks and then analyzed cell proliferation after the end of the 5th week. We chose this therapeutic scheme because it was very similar to the posology used in clinics for certain testicular pathologies. It is noteworthy that, as reported in the Materials and Methods, cells were treated and maintained in culture in a medium depleted with FBS, which included LH and FSH<sup>158</sup>, in order to evaluate the effect on cell proliferation determined only by hCG. As a control, we used gubernacular cells derived from a younger patient (2 years old) who had not been affected by testicular torsion but by cryptorchidism, here reported as the “control patient” (**Figure 19**). Our data showed that both patients #4 and #15, as well as the control patient, showed a significant increase in the percentage of cell proliferation when treated *in vitro* with hCG in comparison to the respective control cells, i.e., the same patient cells but untreated, thus corresponding to 100% of cell proliferation (**Figure 19**). In addition, the gubernacular cells of patient #15 treated with hCG showed a less proliferative capacity in comparison to both patient #4 and the control patient.

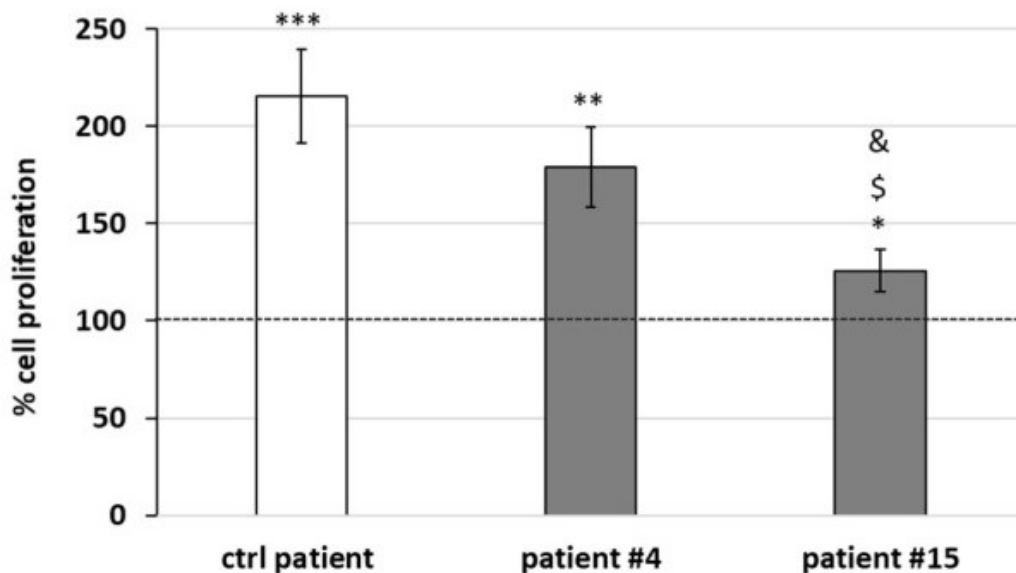


**Figure 19**

Cell proliferation of gubernacular cells cultured at 37 °C with 5% CO<sub>2</sub> in an FBS-deprived medium treated with 100 UI/mL hCG once a week for 4 weeks. Gubernacular cells derived from a 2-year-old patient affected by cryptorchidism were used as a control. The percentage of cell proliferation was evaluated by analyzing the data of hCG treated cells for a specific patient (corresponding to the histograms) with the data obtained for the same patient cells that were not treated whose proliferation corresponded to 100% (dashed line). Values are the means (±SD) of three independent biological replicates. Statistical legend:  $p < 0.5$  (\*),  $p < 0.01$  (\*\*), and  $p < 0.001$  (\*\*\*) for treated versus untreated cells of the same patient;  $p < 0.05$  (\$), (&) for hCG treated cells of patient #15 versus hCG treated cells of control patient and hCG treated cells of patient #4, respectively.

## 7. DISCUSSION

Over the world the incidence of andrological diseases is continuously increasing as is the interest in them, and thus the need for a therapeutic response is pressing. There are numerous efforts aimed to find a cure for infertility, which is the primary consequence of most of these pathologies, but there is still much to be investigated regarding therapeutic measures to counteract the impairment of reproductive function early and effectively within adolescence, or even earlier in childhood, when some of these diseases occur.

Among andrological dysfunctions affecting pediatric age there are cryptorchidism and testicular torsion, which are object of this work.

Cryptorchidism, which arises with the absence of one or both testicles into the scrotum, is the first andrological disease occurring in childhood that affects male fertility; therefore, our attention was first focused to it. Although there is quite clear knowledge about undescended testicles and their possible causes, the exact regulation events of testicular descent are not yet known; furthermore, the choice of the first line of treatment and the most advantageous moment to implement it are still subject of debate. While many suggest that surgery is the first line treatment, others still believe that hormone therapy gives results or it could be the combination of both, but it all depends on the position of the testicles. There is no denying that the only hormone therapy has its controversies. As previously reported by our collaborators, cryptorchid patients that underwent orchidopexy followed by subcutaneously administration of hCG show a significant increase in testicular volume and vascularization compared to untreated patients; therefore, this procedure results the most effective approach to treat cryptorchidism (2). However, despite this important clinical evidence about the effect of hCG, a portion of patients (about 40%) still do not respond to the therapy. Up to now, it is not known whether the reason of the non-response to hCG is linked to the unique posology given to different patient subtypes or to the presence of alterations in the signal cascade of this hormonal stimulation. With this study we aimed to perform the first step towards the complicate area of precision medicine by laying the basis of the generation of a personalized predictive model of therapeutic response for cryptorchid patients after orchidopexy. For this goal, we cultured *in vitro* primary tissue biopsies derived from a para-testicular component, i.e. gubernaculum testis, of cryptorchid patients who underwent surgery; afterwards we characterized the effect of hCG on these cells. We chose gubernaculum tissue since it is known to have a crucial role during testicular descent and both gubernacular anatomical positioning and development are linked to testicular one. From a clinical point of view, since cryptorchid patients generally exhibit a retained small testicle, which could present alterations in adult age, including fertility problems, hypogonadism, and tumor

development<sup>159</sup>, the biopsy and study of gubernaculum leads to maintain completely intact the testicle.

In this study, we considered four cryptorchid patients who respected the inclusion criteria. This pediatric patient set is heterogenous and, since surgery is generally performed between 6 and 18 months of age, we divided them into three age-categories: young patients (pt #3 and #20, who are 1 and 2 years old, respectively), middle-aged patient (pt #7, who is 5 years old), advance-aged patient (pt #2, who is 8 years old). Firstly, we optimized a protocol to digest the gubernacular tissue enzymatically and to culture and amplify gubernacular cells *in vitro*. For all the patients, gubernacular cells were able to grow in culture and were maintained for more than 3 months, thus permitting to perform many cellular and molecular analyses. In addition, all the samples were composed by mixed cellular populations, typical of gubernaculum. However, at a first glance, we noticed that the proliferation rate was different among the patients, with a slower doubling time for cells derived from the oldest patient (pt #2) in comparison to patient #20, who is representative of the young patient category. Then, we demonstrated that gubernacular cells share some similarities with testis, i.e. the expression of gonadotropin receptors (LHCGR and FSHR), representing a good candidate to study the response of testicular cells to hormonal stimulation. Additionally, as expected, androgen receptor is also expressed by gubernacular cells since it responds to the stimulation of testosterone during fetal period by favoring gubernaculum regression and the testicular descent into the scrotum<sup>160</sup>. Indeed, during the first 3–6 months after birth - also called “mini-puberty” - gonadotropin and testicular endocrine function remains active as well as testosterone production<sup>161</sup>.

The effect of hCG on cell proliferation clearly shows that cells derived from all the cryptorchid patients respond *in vitro* to the therapy by increasing their proliferation and that, interestingly, the strength of the effect is higher in younger patients in comparison with the oldest one. To further support this evidence, cells derived from control patients, who are pubertal or adult, show a significant less extent of cell proliferation in comparison with cryptorchid patients after hCG treatment. Finally, also the analysis of the capability of treated gubernacular cells to form and maintain during the time tubular structures, which resemble a vessel-like organization, supports the diverse response among patients with different ages. This result is noteworthy since gubernaculum contributes to increase the blood supply to the testicle<sup>162</sup>: here we show that hCG treatment could improve testicle functionality also by supporting gubernaculum and thus, from a clinical point of view, during orchidopexy it is recommendable to maintain the cranial part of the gubernaculum that may offer more functional support. In fact, after surgery, when the testis is fixed into the scrotum, the residual part of the gubernaculum may create a new network of blood vessels with the dissected

scrotum. In addition to the age of the patients, our data also highlight the importance of the expression levels of the short variant of LHCGR, which is reported in the literature to be related with a low effect of the receptor's ligands<sup>163</sup>. Altogether, this first set of data clearly show that gubernaculum shares key molecular features with the testis, among all the expression of LHCGR, rendering this tissue sensible to hormonal stimulations.

The second part of this study on cryptorchidism was aimed at the investigation of the metabolic alterations induced by hCG. Our results indicate that the oxygen consumption is partially inhibited by the hormone, suggesting that the oxidative metabolism is slowed by hCG treatment. On the other side, the analysis of glycolysis shows that this metabolic pathway is not affected after hCG exposition, as confirmed by ECAR assay and analysis of pyruvate kinase activity and lactate secretion. In support to this evidence, the analysis of regulated metabolic enzymes by mass spectrometry corroborates the inhibition of the oxidative metabolism by hCG treatment. Accordingly, a previous study performed on Leydig cells derived from mice showed that the stimulation of LHCGR increases the dependence on glycolysis and decreases the dependence on oxidative metabolism<sup>164</sup>. Nevertheless, to completely understand the metabolic arrangement of hCG-stimulated cells, future analyses are needed, for instance a metabolomic approach, to understand how cells compensate the alterations of the energetic metabolism and produce the ATP necessary to sustain the increased cellular proliferation by hCG.

Finally, in line with the decreased oxygen consumption, we show that hCG drops the levels of ROS together with a reduced expression of many antioxidant enzymes. This finding suggests that hCG decreases the cellular respiration by slowing the electron transport chain within a threshold that is tolerable by the cells, therefore there is a low ROS production together with a low expression of antioxidant enzymes. Furthermore, it is important to note that the *in vitro* antioxidant action of hCG is maintained for 7 days after the treatment, at which time the next treatment is administered, allowing the inference that the oxidative state can be kept low for all the duration of therapy.

Our gubernaculum-based *in vitro* model for cryptorchid patients is very promising; for this reason, further studies are needed to effectively validate this model to predict the response to hCG therapy in a personalized way, in particular i) implementing the number of patients, ii) performing a parallel study on the patient and on the cells derived from the same patient between our *in vitro* model and clinical evaluation of the effects of hCG, iii) testing a range of hCG doses and iv) analyzing the effects of other hormones, including FSH.

This work also extended to another pathological condition that typically occurs in the adolescent population, representing the most significant cause of testicular loss: testicular torsion. Testicular torsion is a disease that necessarily requires a prompt diagnosis and treatment alongside a surgeon's

decision on whether to preserve the testes or not. A negative long-term effect of a damaged testicle left in place could be an alteration of the fertility potential of the subject. At present, the only safe approach to treat testicular torsion is timely surgery, albeit no adjuvant therapeutic approach is currently considered in the post-operative phase. As chorionic gonadotropin is a treatment generally used to improve fertility potential in infertile men and increase testicular trophism in post-operative period of cryptorchid patients, we assumed that the administration of this treatment in patients with testicular torsion may improve testicle health status. Starting from this hypothesis, our study focused on the *in vitro* validation of these remarks in order to understand if this approach could also be applied in this therapeutic field. As with the study relating to cryptorchidism described above, our attention was also directed to the gubernaculum tissue, which is not only relevant during testicular descent but is also one of the major sources of testis vascularization. The mechanism of injury in testicular torsion consists of an ischemic event - at the same time the gubernaculum is also generally twisted and ischemic due to this pathological condition. Therefore, since gubernacular components become rich in vessels when treated with gonadotropin<sup>165</sup>, gubernaculum represents an important source to be exploited for analyzing both the viability of the testicle and the possible response to the treatment with chorionic gonadotropin. To achieve the aims of this study, we followed our optimized protocol for the tissue enzymatic digestion, for culturing and amplifying *in vitro* gubernacular cells. The potentiality to use gubernaculum for these *in vitro* studies was twofold: first, the testicle, which is suffering due to torsion, could be completely preserved and surgically untouched; second, from our previous data, the culture of gubernacular tissue provides a higher yield of *in vitro* growing cells in comparison to testicular cells, which propagate more slowly. Indeed, we demonstrate that viable primary cells – obtained from the digestion of a small portion of gubernacular tissue collected during surgery in pediatric patients – were able to grow in culture. However, as we also obtained tissue from a patient who underwent orchiectomy, here, we revealed that there was a good correlation between the clinical evaluation of testicle health and the ability of gubernacular cells to grow *in vitro*; indeed, the isolated cells derived from patient #12, whose testicle had been removed, were not able to grow *in vitro*, in line with the surgeon's decision to perform orchiectomy due to the presence of a necrotic testicle. Thus, this initial evidence suggests that the *in vitro* culture of the gubernaculum may be exploited as an evaluation of the state of the testicle, evidencing the viability of the organ and thereafter confirming to the surgeon whether there is a necessity or not to remove a testicle with a border-line health appearance. As we demonstrated, gubernacular cells express LHCGR and are capable of responding to hCG therapy. Therefore, we treated gubernacular cells derived from patients #4 and #15 with a treatment dosage and timing as close as possible to the posology and administration prescribed to patients. Indeed, we treated *in*

*in vitro* cultured cells with 100IU/mL of hCG every week for 4 weeks and we observed that gubernacular cells from both patients increased their proliferation after hormonal stimuli. Interestingly, when stimulated, cells from patient #4 showed significantly higher proliferation than cells of patient #15, confirming the different time windows within which the two cell types started to grow exponentially.

This study represents the first step toward a broader *in vitro* study and potential future clinical validations of an hCG-based therapeutic approach for patients affected by testicular torsion. However, some limits may be reported: (i) the number of patients would be implemented in the future to further corroborate the obtained results. However, as a preliminary study, our outcome was to evaluate the effectiveness of hormonal treatment on some representative cases, and it is necessary to take into account that *in vitro* evaluations can hardly be performed on a large set of patients. (ii) A surgical biopsy must be performed correctly; however, due to torsion, the difference between the gubernaculum, scrotal fat, etc., was not always clear, also considering the edema and the scrotal hematoma. (iii) In this study, we considered as a control patient a 2-year-old cryptorchid child whose tissue had been taken from our tissue collection and processed following the same protocol of the other patients; the response to the hCG treatment of the control patient was considered representative of a control group presenting a healthy testicle and having a good rate of response to hormonal stimulation. (iv) A future step would be to compare the *in vitro* response to the treatment with clinical information that would be obtained by analyzing testicular trophism and vascularization at the end of therapeutic treatment on the same patient. (v) It would be necessary to delineate a cut-off of therapy responder patients in order to propose orchiectomy after treatment. Clinically, to decide whether an injured testicle should be kept or removed during surgery, it will be fundamental to recognize the quality of the testicle to predict how it (and the gubernaculum) will respond to therapy. (vi) Finally, it is noteworthy that the data on *in vitro* proliferation analysis were obtained by treating the cells with a single standardized dosage. Therefore, a future goal would be to evaluate how the cells of each patient proliferate under different conditions of treatment with chorionic gonadotropin and to identify the dose and timing at which the gubernaculum of a given patient responds more. This information will permit proposing a tailored therapy for each patient.

During the period abroad at the Biology of the Testis Lab (BITE) in Brussels, I joined the project focused on testicular organoid, giving me the possibility to learn how to generate and characterize them. Testicular organoids have the advantage of manipulating testicular cells and microenvironmental conditions, to study testis architecture, and to assess *in vitro* spermatogenesis, making them a suitable system for the study of male infertility and the effect of potential therapies.



To date, however, unlike the success achieved in the animal model<sup>166</sup>, the benchmarks to determine the success of testicular organoids have not yet been fully achieved in the human model. The limits of this 3D culture system are essentially represented by the rarity and, when available, by the reduced size of the prepubertal testis tissue, which is the one that best adapts to the reorganization of the cells according to the correct architecture of the testicle. Therefore, the alternative that some groups encourage is the use of testicular tissue from transgender donors, which possesses properties similar to prepubertal tissue but, on the contrary, it is not scarce since orchidectomies are always complete.

## 8. CONCLUSION

Infertility is a prevalent condition that affects 48 million couples and 186 million people globally. Although several lifestyle choices, environmental and genetic factors are implicated in male infertility, understanding the prospective impact of these conditions is complicated due to the delays between diagnosis, treatment, and reproductive age. Undeniably, any condition affecting testicular function or causing testicular loss in childhood will affect fertility. Testicular dysfunction during fetal development may link infertility with common developmental and acquired disorders, such as testicular maldescent, torsion and even cancer.

In this study we propose a new *in vitro* model, represented by gubernaculum testis, for the study and therapeutic evaluation of andrological diseases affecting infertility, such as cryptorchidism and testicular torsion.

In our *in vitro* culture system, gubernaculum testis derived from cryptorchid patients responds *in vitro* to hCG treatment in a similar way as it has been clinically demonstrated for the testicle 6 months after therapy administration. Indeed, we show that also gubernacular cells express LHCGR, thus responding to hCG treatment through an increased cell proliferation and formation of vessel-like structures, together with a decrease of oxidative metabolism and reactive oxygen species. In addition, our data suggest that the effect of hCG is stronger in young patients in comparison to the oldest one, supporting that surgery as well as adjuvant administration of hCG should be performed as early as possible. Furthermore, from a surgical point of view, we also support the study of the gubernaculum for those undescended testes that require more surgical dissection, including intra-abdominal testes or higher into the inguinal channel. Certainly, the salvage of the gubernaculum or at least its cranial part, near the lower pole of the testes, may be associated with improvement of the testicular volume, function, and better response to hormonal therapy.

In this study, we also showed for the first time that a surgical biopsy of a small piece of the gubernaculum from pediatric patients affected by testicular torsion can grow in culture when the testis is not too damaged, paving the way for future experiments aimed at evaluating the *in vitro* health state of the testes and predicting in advance whether hormonal therapy with chorionic gonadotropin may improve the testicle condition and function in a personalized way.

Furthermore, studying the role of the different cell types composing testicular tissue by generating a three-dimensional human testicular organoid culture system has highlighted the intriguing potential of this system in the field of andrological diseases. However, all benchmarks for determining testicular organoid success have not yet been achieved in the human model. Of note, there are continuous and numerous efforts on multiple fronts to obtain the correct architecture of the testis

and *in vitro* spermatogenesis by this 3D culture system. These efforts are driven primarily by the search for an alternative tissue to the prepubertal one, which could allow the success of the testicular organoid but is a scarce and rare tissue. Therefore, to date, the most appropriate choice to pursue is that of cryopreservation of this precious testis tissue.

Final remarks: We observed that the gubernaculum originates from the gonads, it expresses some markers typical of the testicular cells, and again, its development and positioning are closely connected to that of the testicle; we demonstrated that it is possible to obtain a sufficient number of gubernacular cells starting even from a small biopsy. Therefore, the results of this thesis suggest that our *in vitro* model based on the gubernaculum testis – acting as a testicular sensor - could be indicated as a valid and promising alternative system to investigate the state of testicular health and define an effective and personalized therapeutic approach for cryptorchid and testicular torsion patient.

## 9. BIBLIOGRAPHY

1. Carson, S. A. & Kallen, A. N. Diagnosis and Management of Infertility: A Review. *JAMA* **326**, 65 (2021).
2. Leslie, S. W., Soon-Sutton, T. L. & Khan, M. A. Male Infertility. in *StatPearls* (StatPearls Publishing, Treasure Island (FL), 2024).
3. Sharma, A., Minhas, S., Dhillon, W. S. & Jayasena, C. N. Male infertility due to testicular disorders. *J. Clin. Endocrinol. Metab.* **106**, e442–e459 (2021).
4. Zampieri, N. Fertility Preservation in Pediatric Age: Future Perspective among Andrological Diseases. *Life* **13**, 1934 (2023).
5. Krausz, C. Male infertility: pathogenesis and clinical diagnosis. *Best Pract. Res. Clin. Endocrinol. Metab.* **25**, 271–285 (2011).
6. Leslie, S. W., Soon-Sutton, T. L. & Khan, M. A. Male Infertility. in *StatPearls* (StatPearls Publishing, Treasure Island (FL), 2024).
7. Pallotti, F. *et al.* The impact of male factors and their correct and early diagnosis in the infertile couple's pathway: 2021 perspectives. *J. Endocrinol. Invest.* **45**, 1807–1822 (2022).
8. Vasan, S. S. Semen analysis and sperm function tests: How much to test? *Indian J. Urol. IJU J. Urol. Soc. India* **27**, 41–48 (2011).
9. Wang, C., Mbizvo, M., Festin, M. P., Björndahl, L. & Toskin, I. Evolution of the WHO “Semen” processing manual from the first (1980) to the sixth edition (2021). *Fertil. Steril.* **117**, 237–245 (2022).
10. Fraietta, R., Zylberstejn, D. S. & Esteves, S. C. Hypogonadotropic Hypogonadism Revisited. *Clinics* **68**, 81–88 (2013).
11. Madbouly, K. *et al.* Clinical, endocrinological and histopathological patterns of infertile Saudi men subjected to testicular biopsy: A retrospective study from a single center. *Urol. Ann.* **4**, 166–171 (2012).
12. Hauser, R., Temple-Smith, P. D., Southwick, G. J. & de Kretser, D. Fertility in cases of hypergonadotropic azoospermia. *Fertil. Steril.* **63**, 631–636 (1995).

13. Andrade, D. L., Viana, M. C. & Esteves, S. C. Differential Diagnosis of Azoospermia in Men with Infertility. *J. Clin. Med.* **10**, 3144 (2021).
14. Lotti, F., Bertolotto, M. & Maggi, M. Historical trends for the standards in scrotal ultrasonography: What was, what is and what will be normal. *Andrology* **9**, 1331–1355 (2021).
15. Garolla, A. *et al.* Central role of ultrasound in the evaluation of testicular function and genital tract obstruction in infertile males. *Andrology* **9**, 1490–1498 (2021).
16. Abdel-Meguid, T. A. Predictors of sperm recovery and azoospermia relapse in men with nonobstructive azoospermia after varicocele repair. *J. Urol.* **187**, 222–226 (2012).
17. Ishikawa, T. Surgical recovery of sperm in non-obstructive azoospermia. *Asian J. Androl.* **14**, 109–115 (2012).
18. Vloeberghs, V. *et al.* How successful is TESE-ICSI in couples with non-obstructive azoospermia? *Hum. Reprod. Oxf. Engl.* **30**, (2015).
19. Errico, A. *et al.* Mitochondrial Dynamics as Potential Modulators of Hormonal Therapy Effectiveness in Males. *Biology* **12**, 547 (2023).
20. Zampieri, N., Patanè, S. & Camoglio, F. S. Twenty-year experience with macro-area school screening for andrological disease in paediatric age. *Andrologia* **53**, e14209 (2021).
21. Nassau, D. E., Chu, K. Y., Blachman-Braun, R., Castellan, M. & Ramasamy, R. The pediatric patient and future fertility: optimizing long-term male reproductive health outcomes. *Fertil. Steril.* **113**, 489–499 (2020).
22. Zampieri, N. Fertility Preservation in Pediatric Age: Future Perspective among Andrological Diseases. *Life* **13**, 1934 (2023).
23. Hutson, J. M. & Hasthorpe, S. Abnormalities of testicular descent. *Cell Tissue Res.* **322**, 155–158 (2005).
24. Hutson, J. M. *et al.* The Regulation of Testicular Descent and the Effects of Cryptorchidism. *Endocr. Rev.* **34**, 725–752 (2013).
25. Reny, S. E., Mukherjee, A. & Mol, P. M. The curious case of testicular descent: factors controlling testicular descent with a note on cryptorchidism. *Afr. J. Urol.* **29**, 12 (2023).

26. YAMAMOTO, A. *et al.* The mechanisms underlying the effects of AMH on Müllerian duct regression in male mice. *J. Vet. Med. Sci.* **80**, 557–567 (2018).
27. Lăptoiu, A.-R. *et al.* New Insights into the Role of INSL-3 in the Development of Cryptorchidism. *Children* **10**, 737 (2023).
28. Hughes, I. A. & Acerini, C. L. Factors controlling testis descent. *Eur. J. Endocrinol.* **159**, S75–S82 (2008).
29. Klonisch, T., Fowler, P. A. & Hombach-Klonisch, S. Molecular and genetic regulation of testis descent and external genitalia development. *Dev. Biol.* **270**, 1–18 (2004).
30. Hrabovszky, Z., Farmer, P. J. & Hutson, J. M. Undescended testis is accompanied by calcitonin gene related peptide accumulation within the sensory nucleus of the genitofemoral nerve in trans-scrotal rats. *J. Urol.* **165**, 1015–1018 (2001).
31. Skandhan, K. P. & Rajahariprasad, A. The process of spermatogenesis liberates significant heat and the scrotum has a role in body thermoregulation. *Med. Hypotheses* **68**, 303–307 (2007).
32. Gurney, J. K. *et al.* Risk factors for cryptorchidism. *Nat. Rev. Urol.* **14**, 534–548 (2017).
33. Shin, J. & Jeon, G. W. Comparison of diagnostic and treatment guidelines for undescended testis. *Clin. Exp. Pediatr.* **63**, 415–421 (2020).
34. Niedzielski, J. K., Oszukowska, E. & Słowikowska-Hilczer, J. Undescended testis – current trends and guidelines: a review of the literature. *Arch. Med. Sci. AMS* **12**, 667–677 (2016).
35. Ahn, C. & Jeung, E.-B. Endocrine-Disrupting Chemicals and Disease Endpoints. *Int. J. Mol. Sci.* **24**, 5342 (2023).
36. Hutson, J. M. & Hasthorpe, S. Testicular descent and cryptorchidism: the state of the art in 2004. *J. Pediatr. Surg.* **40**, 297–302 (2005).
37. Thorup, J. *et al.* The fate of germ cells in cryptorchid testis. *Front. Endocrinol.* **14**, 1305428 (2024).
38. Foresta, C., Zuccarello, D., Garolla, A. & Ferlin, A. Role of Hormones, Genes, and Environment in Human Cryptorchidism. *Endocr. Rev.* **29**, 560–580 (2008).
39. Lee, P. A. *et al.* Paternity after bilateral cryptorchidism. A controlled study. *Arch. Pediatr. Adolesc. Med.* **151**, 260–263 (1997).

40. Zhang, Y. *et al.* Benefits of orchidopexy on the fertility of adult men with bilateral cryptorchidism. *Asian J. Androl.* **20**, 632–633 (2018).
41. Gurney, J. K. *et al.* Risk factors for cryptorchidism. *Nat. Rev. Urol.* **14**, 534–548 (2017).
42. Viljoen, J. T., Zarrabi, A. & Van der Merwe, A. Management of cryptorchidism in adolescent and adult males. *Afr. J. Urol.* **26**, 40 (2020).
43. Giwercman, A., Hansen, L. L. & Skakkebaek, N. E. Initiation of sperm production after bilateral orchiopexy: clinical and biological implications. *J. Urol.* **163**, 1255–1256 (2000).
44. Zampieri, N., Murri, V. & Camoglio, F. S. Post-operative use of human chorionic gonadotrophin (u-hCG) inpatients treated for intrabdominal unilateral undescended testes. *Am. J. Clin. Exp. Urol.* **6**, 133–137 (2018).
45. Varela-Cives, R. *et al.* A cross-sectional study of cryptorchidism in children: testicular volume and hormonal function at 18 years of age. *Int. Braz. J. Urol. Off. J. Braz. Soc. Urol.* **41**, 57–66 (2015).
46. Kucharski, P. & Niedzielski, J. Neoadjuvant human Chorionic Gonadotropin (hCG) therapy may improve the position of undescended testis: a preliminary report. *Cent. Eur. J. Urol.* **66**, 224–228 (2013).
47. Peretti, M. *et al.* Mean Platelet Volume and Testicular Torsion: New Findings. *Urol. J.* **16**, 83–85 (2019).
48. Paola, A. S. & Khan, S. A. Clinical Evaluation of Scrotal Masses: An Overview. *Hosp. Pract.* **24**, 255–264 (1989).
49. Drlík, M. & Kočvara, R. Torsion of spermatic cord in children: A review. *J. Pediatr. Urol.* **9**, 259–266 (2013).
50. Pogorelič, Z., Anand, S., Artuković, L. & Krishnan, N. Comparison of the outcomes of testicular torsion among children presenting during the Coronavirus Disease 2019 (COVID-19) pandemic versus the pre-pandemic period: A systematic review and meta-analysis. *J. Pediatr. Urol.* **18**, 202–209 (2022).
51. Sharp, V. J., Kieran, K. & Arlen, A. M. Testicular torsion: diagnosis, evaluation, and management. *Am. Fam. Physician* **88**, 835–840 (2013).

52. Nassau, D. E., Chu, K. Y., Blachman-Braun, R., Castellan, M. & Ramasamy, R. The pediatric patient and future fertility: optimizing long-term male reproductive health outcomes. *Fertil. Steril.* **113**, 489–499 (2020).
53. Laher, A., Ragavan, S., Mehta, P. & Adam, A. Testicular Torsion in the Emergency Room: A Review of Detection and Management Strategies. *Open Access Emerg. Med. OAEM* **12**, 237–246 (2020).
54. Awad, N. *et al.* Degrees of Testicular Atrophy Following Orchidopexy for Testicular Torsion. *Cureus* **15**, (2023).
55. Kumar, V., Matai, P., Prabhu, S. P. & Sundeep, P. T. Testicular Loss in Children Due to Incorrect Early Diagnosis of Torsion. *Clin. Pediatr. (Phila.)* **59**, 436–438 (2020).
56. Dumitrescu, C. I. *et al.* Contrast enhanced ultrasound and magnetic resonance imaging in hepatocellular carcinoma diagnosis. *Med. Ultrason.* **15**, 261–267 (2013).
57. Jacobsen, F. M. *et al.* The Impact of Testicular Torsion on Testicular Function. *World J. Mens Health* **38**, 298–307 (2020).
58. Schick, M. A. & Sternard, B. T. Testicular Torsion. in *StatPearls* (StatPearls Publishing, Treasure Island (FL), 2024).
59. Garel, L. *et al.* Preoperative manual detorsion of the spermatic cord with Doppler ultrasound monitoring in patients with intravaginal acute testicular torsion. *Pediatr. Radiol.* **30**, 41–44 (2000).
60. Lent, V. & Stephani, A. Eversion of the tunica vaginalis for prophylaxis of testicular torsion recurrences. *J. Urol.* **150**, 1419–1421 (1993).
61. Park, K. & Choi, H. An Evolution of Orchiopexy: Historical Aspect. *Korean J. Urol.* **51**, 155–160 (2010).
62. Favorito, L. A., Costa, S. F., Julio Junior, H. R. & Sampaio, F. J. B. The importance of the gubernaculum in testicular migration during the human fetal period. *Int. Braz. J. Urol.* **40**, 722–729 (2014).
63. Johansen, T. E. & Blom, G. P. Histological studies of gubernaculum testis taken during orchiopexies. *Scand. J. Urol. Nephrol.* **22**, 107–108 (1988).
64. Costa, W. S., Sampaio, F. J. B., Favorito, L. A. & Cardoso, L. E. M. Testicular migration: remodeling of connective tissue and muscle cells in human gubernaculum testis. *J. Urol.* **167**, 2171–2176 (2002).



65. Johnson, K. J. *et al.* Insulin-Like 3 Exposure of the Fetal Rat Gubernaculum Modulates Expression of Genes Involved in Neural Pathways. *Biol. Reprod.* **83**, 774–782 (2010).
66. Huang, Z., Rivas, B. & Agoulnik, A. I. Insulin-like 3 signaling is important for testicular descent but dispensable for spermatogenesis and germ cell survival in adult mice. *Biol. Reprod.* **87**, 143 (2012).
67. Goh, D. W., Momose, Y., Middlesworth, W. & Hutson, J. M. The relationship among calcitonin gene-related peptide, androgens and gubernacular development in 3 animal models of cryptorchidism. *J. Urol.* **150**, 574–576 (1993).
68. Tanyel, F. C., Erdem, S., Büyükpamukçu, N. & Tan, E. Cremaster muscles obtained from boys with an undescended testis show significant neurological changes. *BJU Int.* **85**, 116–119 (2000).
69. Esteban-Lopez, M. & Agoulnik, A. I. Diverse Functions of Insulin-Like 3 Peptide. *J. Endocrinol.* **247**, R1–R12 (2020).
70. Costa, W. S., Sampaio, F. J. B., Favorito, L. A. & Cardoso, L. E. M. Testicular migration: remodeling of connective tissue and muscle cells in human gubernaculum testis. *J. Urol.* **167**, 2171–2176 (2002).
71. Viguera, R. M., Reyes, G., Moreno-Mendoza, N. & Merchant-Larios, H. Gubernacular fibroblasts express the androgen receptor during testis descent in cryptorchid rats treated with human chorionic gonadotrophin. *Urol. Res.* **32**, 386–390 (2004).
72. Cavalie, G. *et al.* Anatomy and histology of the scrotal ligament in adults: inconsistency and variability of the gubernaculum testis. *Surg. Radiol. Anat. SRA* **40**, 365–370 (2018).
73. Heinrich, A. & DeFalco, T. Essential Roles of Interstitial Cells in Testicular Development and Function. *Andrology* **8**, 903–914 (2020).
74. O'Donnell, L., Stanton, P. & de Kretser, D. M. Endocrinology of the Male Reproductive System and Spermatogenesis. in *Endotext* (eds. Feingold, K. R. *et al.*) (MDText.com, Inc., South Dartmouth (MA), 2000).
75. Tsutsumi, R. & Webster, N. J. G. GnRH Pulsatility, the Pituitary Response and Reproductive Dysfunction. *Endocr. J.* **56**, 729–737 (2009).

76. Shah, W. *et al.* The Molecular Mechanism of Sex Hormones on Sertoli Cell Development and Proliferation. *Front. Endocrinol.* **12**, 648141 (2021).
77. Gromoll, J. *et al.* A New Subclass of the Luteinizing Hormone/Chorionic Gonadotropin Receptor Lacking Exon 10 Messenger RNA in the New World Monkey (Platyrrhini) Lineage. *Biol. Reprod.* **69**, 75–80 (2003).
78. Ascoli, M., Fanelli, F. & Segaloff, D. L. The lutropin/choriogonadotropin receptor, a 2002 perspective. *Endocr. Rev.* **23**, 141–174 (2002).
79. Jonas, K. C. *et al.* Temporal reprogramming of calcium signalling via crosstalk of gonadotrophin receptors that associate as functionally asymmetric heteromers. *Sci. Rep.* **8**, 2239 (2018).
80. Zhang, M., Guan, R. & Segaloff, D. L. Revisiting and questioning functional rescue between dimerized LH receptor mutants. *Mol. Endocrinol. Baltim. Md* **26**, 655–668 (2012).
81. Jeoung, M., Lee, C., Ji, I. & Ji, T. H. Trans-activation, cis-activation and signal selection of gonadotropin receptors. *Mol. Cell. Endocrinol.* **260–262**, 137–143 (2007).
82. Tao, Y.-X., Johnson, N. B. & Segaloff, D. L. Constitutive and agonist-dependent self-association of the cell surface human lutropin receptor. *J. Biol. Chem.* **279**, 5904–5914 (2004).
83. Kossack, N., Simoni, M., Richter-Unruh, A., Themmen, A. P. N. & Gromoll, J. Mutations in a novel, cryptic exon of the luteinizing hormone/chorionic gonadotropin receptor gene cause male pseudohermaphroditism. *PLoS Med.* **5**, e88 (2008).
84. Troppmann, B., Kleinau, G., Krause, G. & Gromoll, J. Structural and functional plasticity of the luteinizing hormone/choriogonadotrophin receptor. *Hum. Reprod. Update* **19**, 583–602 (2013).
85. Liu, W. *et al.* Polymorphism in the Alternative Donor Site of the Cryptic Exon of LHCGR: Functional Consequences and Associations with Testosterone Level. *Sci. Rep.* **7**, 45699 (2017).
86. Kara, E., Dupuy, L., Bouillon, C., Casteret, S. & Maurel, M.-C. Modulation of Gonadotropins Activity by Antibodies. *Front. Endocrinol.* **10**, 15 (2019).
87. Nedresky, D. & Singh, G. Physiology, Luteinizing Hormone. in *StatPearls* (StatPearls Publishing, Treasure Island (FL), 2024).

88. Rosenberg, D. *et al.* Role of the PKA-regulated transcription factor CREB in development and tumorigenesis of endocrine tissues. *Ann. N. Y. Acad. Sci.* **968**, 65–74 (2002).
89. Gonçalves, C. I., Carriço, J., Bastos, M. & Lemos, M. C. Disorder of Sex Development Due to 17-Beta-Hydroxysteroid Dehydrogenase Type 3 Deficiency: A Case Report and Review of 70 Different HSD17B3 Mutations Reported in 239 Patients. *Int. J. Mol. Sci.* **23**, 10026 (2022).
90. Rey, R. A. Biomarkers of male hypogonadism in childhood and adolescence. *Adv. Lab. Med. Av. En Med. Lab.* **1**, (2020).
91. Bjerner, J., Biernat, D., Fosså, S. D. & Bjørro, T. Reference intervals for serum testosterone, SHBG, LH and FSH in males from the NORIP project. *Scand. J. Clin. Lab. Invest.* **69**, 873–879 (2009).
92. Lanciotti, L., Cofini, M., Leonardi, A., Penta, L. & Esposito, S. Up-To-Date Review About Minipuberty and Overview on Hypothalamic-Pituitary-Gonadal Axis Activation in Fetal and Neonatal Life. *Front. Endocrinol.* **9**, 410 (2018).
93. Fowler, P. A., Bhattacharya, S., Gromoll, J., Monteiro, A. & O’Shaughnessy, P. J. Maternal smoking and developmental changes in luteinizing hormone (LH) and the LH receptor in the fetal testis. *J. Clin. Endocrinol. Metab.* **94**, 4688–4695 (2009).
94. Bergadá, I. *et al.* Time Course of the Serum Gonadotropin Surge, Inhibins, and Anti-Müllerian Hormone in Normal Newborn Males during the First Month of Life. *J. Clin. Endocrinol. Metab.* **91**, 4092–4098 (2006).
95. Rey, R. A. Biomarkers of male hypogonadism in childhood and adolescence. *Adv. Lab. Med. Av. En Med. Lab.* **1**, (2020).
96. Howard, S. R. Interpretation of reproductive hormones before, during and after the pubertal transition- Identifying health and disordered puberty. *Clin. Endocrinol. (Oxf.)* **95**, 702–715 (2021).
97. Nwabuobi, C. *et al.* hCG: Biological Functions and Clinical Applications. *Int. J. Mol. Sci.* **18**, 2037 (2017).
98. Gridelet, V. *et al.* Human Chorionic Gonadotrophin: New Pleiotropic Functions for an “Old” Hormone During Pregnancy. *Front. Immunol.* **11**, (2020).

99. Chambers, A. E., Nayini, K. P., Mills, W. E., Lockwood, G. M. & Banerjee, S. Circulating LH/hCG receptor (LHCGR) may identify pre-treatment IVF patients at risk of OHSS and poor implantation. *Reprod. Biol. Endocrinol.* **9**, 161 (2011).
100. Cole, L. A. Biological functions of hCG and hCG-related molecules. *Reprod. Biol. Endocrinol.* **8**, 102 (2010).
101. Stenman, U.-H., Alfthan, H. & Hotakainen, K. Human chorionic gonadotropin in cancer. *Clin. Biochem.* **37**, 549–561 (2004).
102. Riccetti, L. *et al.* Human LH and hCG stimulate differently the early signalling pathways but result in equal testosterone synthesis in mouse Leydig cells in vitro. *Reprod. Biol. Endocrinol. RBE* **15**, 2 (2017).
103. Wang, Y., Chen, F., Ye, L., Zirkin, B. & Chen, H. Steroidogenesis in Leydig Cells: Effects of Aging and Environmental Factors. *Reproduction* **154**, REP-17 (2017).
104. Riccetti, L. *et al.* Human Luteinizing Hormone and Chorionic Gonadotropin Display Biased Agonism at the LH and LH/CG Receptors. *Sci. Rep.* **7**, 940 (2017).
105. Rajfer, J. *et al.* Hormonal therapy of cryptorchidism. A randomized, double-blind study comparing human chorionic gonadotropin and gonadotropin-releasing hormone. *N. Engl. J. Med.* **314**, 466–470 (1986).
106. Matthews, L. A., Abdul-Karim, F. W. & Elder, J. S. Effect of preoperative human chorionic gonadotropin on intra-abdominal rat testes undergoing standard and Fowler-Stephens orchiopexy. *J. Urol.* **157**, 2315–2317 (1997).
107. Leslie, S. W., Sajjad, H. & Villanueva, C. A. Cryptorchidism. in *StatPearls* (StatPearls Publishing, Treasure Island (FL), 2024).
108. Hildorf, S. E. Clinical aspects of histological and hormonal parameters in boys with cryptorchidism. *Apmis* **130**, 1–58 (2022).
109. Lee, J. A. & Ramasamy, R. Indications for the use of human chorionic gonadotropic hormone for the management of infertility in hypogonadal men. *Transl. Androl. Urol.* **7**, S348–S352 (2018).

110. Laursen, R. J. *et al.* Recombinant gonadotropin therapy to improve spermatogenesis in nonobstructive azoospermic patients – A proof of concept study. *Int. Braz. J. Urol. Off. J. Braz. Soc. Urol.* **48**, 471–481 (2022).
111. Sato, T. *et al.* Single Lgr5 stem cells build crypt-villus structures in vitro without a mesenchymal niche. *Nature* **459**, 262–265 (2009).
112. Spence, J. R. *et al.* Directed differentiation of human pluripotent stem cells into intestinal tissue in vitro. *Nature* **470**, 105–109 (2011).
113. Hu, H. *et al.* Long-Term Expansion of Functional Mouse and Human Hepatocytes as 3D Organoids. *Cell* **175**, 1591-1606.e19 (2018).
114. Greggio, C. *et al.* Artificial three-dimensional niches deconstruct pancreas development in vitro. *Dev. Camb. Engl.* **140**, 4452–4462 (2013).
115. Ishii, K. Reconstruction of dissociated chick brain cells in rotation-mediated culture. *Cytologia (Tokyo)* **31**, 89–98 (1966).
116. Nakagawa, S., Takada, S., Takada, R. & Takeichi, M. Identification of the laminar-inducing factor: Wnt-signal from the anterior rim induces correct laminar formation of the neural retina in vitro. *Dev. Biol.* **260**, 414–425 (2003).
117. Baert, Y. *et al.* Primary Human Testicular Cells Self-Organize into Organoids with Testicular Properties. *Stem Cell Rep.* **8**, 30–38 (2017).
118. Alves-Lopes, J. P., Söder, O. & Stukenborg, J.-B. Testicular organoid generation by a novel in vitro three-layer gradient system. *Biomaterials* **130**, 76–89 (2017).
119. Oliver, E. *et al.* Self-organising human gonads generated by a Matrigel-based gradient system. *BMC Biol.* **19**, 212 (2021).
120. Vermeulen, M. *et al.* Generation of Organized Porcine Testicular Organoids in Solubilized Hydrogels from Decellularized Extracellular Matrix. *Int. J. Mol. Sci.* **20**, 5476 (2019).

121. Pendergraft, S. S., Sadri-Ardekani, H., Atala, A. & Bishop, C. E. Three-dimensional testicular organoid: a novel tool for the study of human spermatogenesis and gonadotoxicity in vitro. *Biol. Reprod.* **96**, 720–732 (2017).
122. Rezaei Topraggaleh, T., Valojerdi, M., Montazeri, L. & Baharvand, H. Testis-derived macroporous 3D scaffold as a platform for the generation of mouse testicular organoids. *Biomater. Sci.* **7**, (2019).
123. Sakib, S. *et al.* Formation of organotypic testicular organoids in microwell culture. *Biol. Reprod.* **100**, (2019).
124. Edmonds, M. E. & Woodruff, T. K. Testicular organoid formation is a property of immature somatic cells, which self-assemble and exhibit long-term hormone-responsive endocrine function. *Biofabrication* **12**, 045002 (2020).
125. Rore, H., Owen, N., Piña-Aguilar, R. E., Docherty, K. & Sekido, R. Testicular somatic cell-like cells derived from embryonic stem cells induce differentiation of epiblasts into germ cells. *Commun. Biol.* **4**, 802 (2021).
126. Pryzhkova, M. V. & Jordan, P. W. Adaptation of Human Testicular Niche Cells for Pluripotent Stem Cell and Testis Development Research. *Tissue Eng. Regen. Med.* **17**, 223–235 (2020).
127. Alves-Lopes, J. P. & Stukenborg, J.-B. Testicular organoids: a new model to study the testicular microenvironment in vitro? *Hum. Reprod. Update* **24**, 176–191 (2018).
128. Dando, I., Carmona-Carmona, C. A. & Zampieri, N. Human Chorionic Gonadotropin-Mediated Induction of Breast Cancer Cell Proliferation and Differentiation. *Cells* **10**, 264 (2021).
129. Carpentier, G. *et al.* Angiogenesis Analyzer for ImageJ — A comparative morphometric analysis of “Endothelial Tube Formation Assay” and “Fibrin Bead Assay”. *Sci. Rep.* **10**, 11568 (2020).
130. Bifari, F. *et al.* Complete neural stem cell (NSC) neuronal differentiation requires a branched chain amino acids-induced persistent metabolic shift towards energy metabolism. *Pharmacol. Res.* **158**, 104863 (2020).
131. Dando, I. *et al.* Cannabinoids inhibit energetic metabolism and induce AMPK-dependent autophagy in pancreatic cancer cells. *Cell Death Dis.* **4**, e664 (2013).

132. Morgan, J. T. *et al.* Regional Variation in Androgen Receptor Expression and Biomechanical Properties May Contribute to Cryptorchidism Susceptibility in the LE/orl Rat. *Front. Endocrinol.* **9**, 738 (2018).
133. Zirkin, B. R. & Papadopoulos, V. Leydig cells: formation, function, and regulation. *Biol. Reprod.* **99**, 101–111 (2018).
134. Zampieri, N., Murri, V. & Camoglio, F. S. Post-operative use of human chorionic gonadotrophin (u-hCG) inpatients treated for intrabdominal unilateral undescended testes. *Am. J. Clin. Exp. Urol.* **6**, 133–137 (2018).
135. Errico, A. *et al.* Mitochondrial Dynamics as Potential Modulators of Hormonal Therapy Effectiveness in Males. *Biology* **12**, 547 (2023).
136. Liu, W. *et al.* Polymorphism in the Alternative Donor Site of the Cryptic Exon of LHCGR: Functional Consequences and Associations with Testosterone Level. *Sci. Rep.* **7**, 45699 (2017).
137. Gromoll, J. *et al.* A New Subclass of the Luteinizing Hormone/Chorionic Gonadotropin Receptor Lacking Exon 10 Messenger RNA in the New World Monkey (Platyrrhini) Lineage<sup>1</sup>. *Biol. Reprod.* **69**, 75–80 (2003).
138. Fu, D. *et al.* HMGB2 is associated with malignancy and regulates Warburg effect by targeting LDHB and FBP1 in breast cancer. *Cell Commun. Signal. CCS* **16**, 8 (2018).
139. Zhang, L. & Han, J. Branched-chain amino acid transaminase 1 (BCAT1) promotes the growth of breast cancer cells through improving mTOR-mediated mitochondrial biogenesis and function. *Biochem. Biophys. Res. Commun.* **486**, 224–231 (2017).
140. Fu, D. *et al.* HMGB2 is associated with malignancy and regulates Warburg effect by targeting LDHB and FBP1 in breast cancer. *Cell Commun. Signal. CCS* **16**, 8 (2018).
141. Zhang, L. & Han, J. Branched-chain amino acid transaminase 1 (BCAT1) promotes the growth of breast cancer cells through improving mTOR-mediated mitochondrial biogenesis and function. *Biochem. Biophys. Res. Commun.* **486**, 224–231 (2017).

142. Stracker, T. H. EXD2: A new regulator of mitochondrial translation and potential target for cancer therapy. *Mol. Cell. Oncol.* **5**, e1445943 (2018).
143. Lu, S. C. Glutathione synthesis. *Biochim. Biophys. Acta* **1830**, 3143–3153 (2013).
144. Lushchak, O. V., Piroddi, M., Galli, F. & Lushchak, V. I. Aconitase post-translational modification as a key in linkage between Krebs cycle, iron homeostasis, redox signaling, and metabolism of reactive oxygen species. *Redox Rep. Commun. Free Radic. Res.* **19**, 8–15 (2014).
145. Mueller, S. Iron regulatory protein 1 as a sensor of reactive oxygen species. *BioFactors Oxf. Engl.* **24**, 171–181 (2005).
146. Ahsan, M. K., Lekli, I., Ray, D., Yodoi, J. & Das, D. K. Redox regulation of cell survival by the thioredoxin superfamily: an implication of redox gene therapy in the heart. *Antioxid. Redox Signal.* **11**, 2741–2758 (2009).
147. NUDT2 (nudix hydrolase 2). [https://atlasgeneticsoncology.org/gene/41592/nudt2-\(nudix-hydrolase-2\)](https://atlasgeneticsoncology.org/gene/41592/nudt2-(nudix-hydrolase-2)).
148. Ye, C. L. *et al.* STEAP3 Affects Ferroptosis and Progression of Renal Cell Carcinoma Through the p53/xCT Pathway. *Technol. Cancer Res. Treat.* **21**, 15330338221078728 (2022).
149. Tirichen, H. *et al.* Mitochondrial Reactive Oxygen Species and Their Contribution in Chronic Kidney Disease Progression Through Oxidative Stress. *Front. Physiol.* **12**, (2021).
150. Stracker, T. H. EXD2: A new regulator of mitochondrial translation and potential target for cancer therapy. *Mol. Cell. Oncol.* **5**, e1445943 (2018).
151. Lu, S. C. Glutathione synthesis. *Biochim. Biophys. Acta* **1830**, 3143–3153 (2013).
152. Lushchak, O. V., Piroddi, M., Galli, F. & Lushchak, V. I. Aconitase post-translational modification as a key in linkage between Krebs cycle, iron homeostasis, redox signaling, and metabolism of reactive oxygen species. *Redox Rep. Commun. Free Radic. Res.* **19**, 8–15 (2014).
153. Mueller, S. Iron regulatory protein 1 as a sensor of reactive oxygen species. *BioFactors Oxf. Engl.* **24**, 171–181 (2005).



154. Ahsan, M. K., Lekli, I., Ray, D., Yodoi, J. & Das, D. K. Redox regulation of cell survival by the thioredoxin superfamily: an implication of redox gene therapy in the heart. *Antioxid. Redox Signal.* **11**, 2741–2758 (2009).
155. NUDT2 (nudix hydrolase 2). [https://atlasgeneticsoncology.org/gene/41592/nudt2-\(nudix-hydrolase-2\)](https://atlasgeneticsoncology.org/gene/41592/nudt2-(nudix-hydrolase-2)).
156. Ye, C. L. *et al.* STEAP3 Affects Ferroptosis and Progression of Renal Cell Carcinoma Through the p53/xCT Pathway. *Technol. Cancer Res. Treat.* **21**, 15330338221078728 (2022).
157. Kaftanovskaya, E. M. *et al.* Cryptorchidism in mice with an androgen receptor ablation in gubernaculum testis. *Mol. Endocrinol. Baltim. Md* **26**, 598–607 (2012).
158. Dando, I., Carmona-Carmona, C. A. & Zampieri, N. Human Chorionic Gonadotropin-Mediated Induction of Breast Cancer Cell Proliferation and Differentiation. *Cells* **10**, 264 (2021).
159. Rodprasert, W., Virtanen, H. E., Mäkelä, J.-A. & Toppari, J. Hypogonadism and Cryptorchidism. *Front. Endocrinol.* **10**, 906 (2019).
160. Barthold, J. *et al.* Transcriptome Analysis of the Dihydrotestosterone-Exposed Fetal Rat Gubernaculum Identifies Common Androgen and Insulin-Like 3 Targets. *Biol. Reprod.* **89**, (2013).
161. Rey, R. A. & Grinspon, R. P. Androgen Treatment in Adolescent Males With Hypogonadism. *Am. J. Mens Health* **14**, 1557988320922443 (2020).
162. Althobaiti, E., Badr, H., Aloqalaa, M., Alsharif, R. & Alqarni, N. Gubernaculum Sparing Laparoscopic Orchiopexy in Cryptorchidism with Ipsilateral Congenital Absence of the Vas Deferens: Unique Outcome. *Case Rep. Urol.* **2019**, 7408412 (2019).
163. Liu, W. *et al.* Polymorphism in the Alternative Donor Site of the Cryptic Exon of LHCGR: Functional Consequences and Associations with Testosterone Level. *Sci. Rep.* **7**, 45699 (2017).
164. Medar, M. L. J. *et al.* Dependence of Leydig Cell's Mitochondrial Physiology on Luteinizing Hormone Signaling. *Life Basel Switz.* **11**, 19 (2020).

165. El Zoghbi, C. S., Favorito, L. A., Costa, W. S. & Sampaio, F. J. B. Structural analysis of gubernaculum testis in cryptorchid patients submitted to treatment with human chorionic gonadotrophin. *Int. Braz J Urol Off. J. Braz. Soc. Urol.* **33**, 223–229; discussion 230 (2007).
166. Richer, G., Hobbs, R. M., Loveland, K. L., Goossens, E. & Baert, Y. Long-Term Maintenance and Meiotic Entry of Early Germ Cells in Murine Testicular Organoids Functionalized by 3D Printed Scaffolds and Air-Medium Interface Cultivation. *Front. Physiol.* **12**, 757565 (2021).